



U.S. Department  
of Transportation

**Federal Highway  
Administration**

Publication No. FHWA-RD-90-008

May 1990

---

# **Brittle-Ductile Transition of Bridge Steels**

## **Volume I: Final Report**

---

Research, Development, and Technology  
Turner-Fairbank Highway Research Center  
6300 Georgetown Pike  
McLean, Virginia 22101-2296

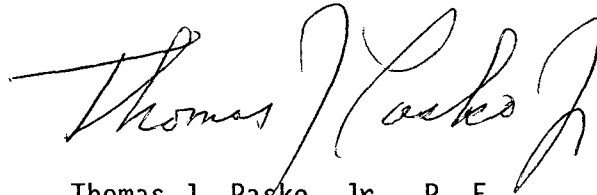
## FOREWORD

This report is volume I of a three-part research and development report titled "Brittle-Ductile Transition of Bridge Steels" performed by Materials Research Laboratories, Inc., for the Federal Highway Administration (FHWA), Office of Engineering and Highway Operations Research and Development under contract number DTFH61-86-C-00028.

An important feature of the mechanical behavior of structural steel is the occurrence of a brittle-ductile (B-D) transition temperature. This project was carried out to investigate the theory behind the transition and measure the toughness behavior of structural steels in the transition region.

Copies of this report are being given a type I distribution by an FHWA transmittal memorandum to all regional and division field offices. A limited number of copies for official use are available from the RD&T Report Center, 6300 Georgetown Pike, McLean, Virginia 22101-2296.

Additional copies may be obtained from the National Technical Information Service, 5285 Port Royal Road, Springfield, Virginia 22161.



Thomas J. Pasko, Jr., P. E.  
Director, Office of Engineering and  
Highway Operations Research and Development

## NOTICE

This document is disseminated under the sponsorship of the Department of Transportation in the interest of information exchange. The United States Government assumes no liability for its contents or use thereof.

The contents of this report reflect the views of the author who is responsible for the facts and the accuracy of the data presented herein. The contents do not necessarily reflect the policy of the Department of Transportation.

This report does not constitute a standard, specification, or regulation. The United States Government does not endorse products or manufacturers. Trade or manufacturers' names appear herein only because they are considered essential to the objective of this document.

TECHNICAL REFERENCE CENTER

Turner-Fairbank Hwy Res Cntr

FHWA, Room A200

Technical Report Documentation Page

1. Report No. FHWA-RD-90-008		2. 6300 Georgetown Pike McLean, VA 22201		3. Recipient's Catalog No.										
4. Title and Subtitle BRITTLE-DUCTILE TRANSITION OF BRIDGE STEELS, Volume I: Final Report				5. Report Date May 1990										
				6. Performing Organization Code										
7. Author(s) E. J. Ripling; P. B. Crosley and R. W. Armstrong				8. Performing Organization Report No. 7048										
9. Performing Organization Name and Address Materials Research Laboratory, Inc. One Science Road Glenwood, Illinois 60425				10. Work Unit No. (TRAIS) 3D1B2032										
				11. Contract or Grant No. DTFH61-86-C-00028										
12. Sponsoring Agency Name and Address Office of Engineering and Highway Operations R & D Federal Highway Administration 6300 Georgetown Pike McLean, Virginia 22101-2296				13. Type of Report and Period Covered Final Report June 1986 - August 1989										
				14. Sponsoring Agency Code										
15. Supplementary Notes COTR - William Wright (HNR-10)														
16. Abstract <p>The transition behavior of bridge steels and weldments largely determines their toughness under service loading rates and temperatures. Two aspects of the transition were investigated in this project: The first was to develop a better understanding of the micro-mechanics of fracture of bridge steels and welds. This study showed that the AASHTO yield strength dependent relationship between loading rate and test temperature should be expected.</p> <p>The second larger study consisted of measuring the fracture toughness of A572, A588, A852 and A514 plates, and Submerged Arc Weldments, at bridge loading rates using CTOD specimens. The latter are analyzed by elastic-plastic techniques so that testing could be extended into the transition region.</p> <p>The tests supported an earlier FHWA study and showed that the AASHTO CVI specifications for 1- and 2-in (25 and 51 mm) thick A572 and A588 and 1-in (25 mm) thick A852 and A514 are satisfactory. However, the Guide Specifications were found to be nonconservative for thick, heat-treated plates. This may be a result of the fact that Charpy specimens are sampled at the plate quarter-thickness while cracks initiate on the plate midplane. If further research supports this observation, it would be advisable to sample CVI near the midplane of plates for all plates.</p> <p style="text-align: center;">This volume is the first in a series. The others in the series are:</p> <table border="1" style="margin-left: auto; margin-right: auto;"> <thead> <tr> <th style="text-align: center;">FHWA No.</th> <th style="text-align: center;">Vol. No.</th> <th style="text-align: center;">Short Title</th> </tr> </thead> <tbody> <tr> <td style="text-align: center;">RD-90-009</td> <td style="text-align: center;">II</td> <td style="text-align: center;">Microstructural Aspects</td> </tr> <tr> <td style="text-align: center;">RD-90-010</td> <td style="text-align: center;">III</td> <td style="text-align: center;">Executive Summary</td> </tr> </tbody> </table>						FHWA No.	Vol. No.	Short Title	RD-90-009	II	Microstructural Aspects	RD-90-010	III	Executive Summary
FHWA No.	Vol. No.	Short Title												
RD-90-009	II	Microstructural Aspects												
RD-90-010	III	Executive Summary												
17. Key Words AASHTO, bridge steels and weldments, A572, A588, A852, A514, non-redundant, fracture critical, fracture, fracture control, fracture toughness, $K_{Ic}$ , CTOD Charpy Impact test, temperature shift			18. Distribution Statement No restrictions. This document is available to the public through the National Technical Information Service, Springfield, Virginia 22161											
19. Security Classif. (of this report) Unclassified		20. Security Classif. (of this page) Unclassified		21. No. of Pages 115	22. Price									

## UNITS

Throughout this report all properties are defined in both British and SI units. The conversion factors that were used are shown below:

<u>To Convert From</u>	<u>To</u>	<u>Multiply By</u>
Foot-pounds-force	joule (J)	1.356
inch	meter (m)	$2.54 \times 10^{-2}$
kips/inch <sup>2</sup> (ksi)	pascal (Pa)	$6.895 \times 10^6$
ksi-in <sup>1/2</sup>	MPa-m <sup>1/2</sup>	1.098

To convert degree Fahrenheit (F) to degree Celsius (C):  
 $C = 5(F-32)/9$

### NOTE:

$K_{Ic}$  is the designation for plane-strain fracture toughness measurements made according to ASTM Test Method E399. Both  $K_{Ic}$  and CTOD imply data collected at slow loading rates. The data  $K_{Ic}$  in this report, however, were all collected at a loading rate of 1-sec.

VOLUME I  
TABLE OF CONTENTS

<u>Section</u>	<u>Page No.</u>
1	INTRODUCTION ..... 1
	1.1 Linear Elastic Specimen Analysis ..... 3
	1.2 Elastic-Plastic Behaviors ..... 6
	1.3 The Use of CTOD in Fracture Control and the Correlation of CTOD Values With CVI Toughness ... 6
	1.4 Effect of Plate Thickness ..... 11
	1.5 Miscellaneous Topics Regarding CTOD Testing ..... 12
2	TEST RESULTS, BASE PLATES ..... 13
	2.1 Materials ..... 13
	2.2 Characterization Tests ..... 13
	2.3 $K_{Ic}$ and CTOD Test Results ..... 19
	2.4 Data Analysis ..... 36
	2.5 Evaluation of the Barsom-Rolfe Steel Selection Criterion ..... 54
	2.6 Comparison of $K_{Ic}$ From CVI and CTOD ..... 60
	2.7 Critical Crack Sizes at LPST ..... 61
3	TEST RESULTS, WELDMENTS ..... 64
	3.1 Material ..... 64
	3.2 Test Results ..... 65
	3.3 Analysis of Weldment Data ..... 65
4	DISCUSSION ..... 80
5	RECOMMENDATIONS ..... 83
	APPENDIX A - Analysis on Which CTOD is Based and Description of CTOD Test Method ..... 84
	APPENDIX B - Analytical Basis for Converting CTOD Data to $K_{Ic}$ ..... 92
	APPENDIX C - Calculation of Dynamic Yield Strengths ..... 99
	REFERENCES ..... 101

VOLUME I  
LIST OF FIGURES

<u>Fig. No.</u>		<u>Page No.</u>
1	Schematic showing crack in girder flange (top) and enlarged view of crack and plastic zone (bottom).....	2
2	$K_{IC}$ , CVN, CTOD and J correlations. Specimen size 1 <sup>c</sup> by 2 by 8 in (25 by 51 by 203 mm). Lower-bound values. Top: A516 steel. Bottom: A131 steel.....	9
3	Charpy impact energy vs test temperature (1-in (25 mm) thick A572-82, grade 50, plate C).....	24
4	Charpy impact energy vs test temperature (2-in (51 mm) thick A572-82, grade 50, plate D).....	24
5	Charpy impact energy vs test temperature (1-in (25 mm) thick A588-82, grade B, plate E).....	25
6	Charpy impact energy vs test temperature (2-in (51 mm) thick A588-82, grade B, plate F).....	25
7	Charpy impact energy vs test temperature (1-in (25 mm) thick A514, grade B, plate A).....	26
8	Charpy impact energy vs test temperature (2-in (51 mm) thick A514-85A, plate B).....	26
9	Charpy impact energy vs test temperature (1-in (25 mm) thick A852-85, plate H).....	27
10	Charpy impact energy vs test temperature (2-in (51 mm) thick A852-85, plate L).....	27
11	Charpy impact energy vs test temperature (3-in (76 mm) thick A852-85, plate M).....	28
12	Hyperbolic tangent best-fit curve.....	28
13	CTOD vs test temperature. (1-in (25 mm) thick A572-82, grade 50, plate C).....	30
14	CTOD vs test temperature. (2-in (51 mm) thick A572-82, grade 50, plate D).....	30

VOLUME I  
LIST OF FIGURES (CONTINUED)

<u>Fig. No.</u>		<u>Page No.</u>
15	CTOD vs test temperature. (1-in (25 mm) thick A588-82, grade B, plate E).....	31
16	CTOD vs test temperature. (2-in (51 mm) thick A588-82, grade B, plate F).....	31
17	CTOD vs test temperature. (1-in (25 mm) thick A514, grade B, plate A).....	32
18	CTOD vs test temperature. (2-in (51 mm) thick A514-85A, plate B).....	32
19	CTOD vs test temperature. (1-in (25 mm) thick A852-85, plate H).....	33
20	CTOD vs test temperature. (2-in (51 mm) thick A852-85, plate L).....	33
21	CTOD vs test temperature. (3-in (76 mm) thick A852-85, plate M).....	34
22	Test temperature, CTOD value in mils, and letter indication low (L), middle (M) or high (H) values of CTOD. Letter "S" indicates lower shelf values.....	35
23	Comparison of CVI values obtained on CTOD specimens 9CD2 and 9CD13 (1-in (25 mm) thick A572-82, grade 50, steel plate, plate C).....	37
24	Comparison of data shown in figure 23 with CVI values originally obtained on plate.....	37
25	Definition of LPST.....	39
26	$K_c$ ( $K_{Tc}$ ) calculated from CVI (Barsom-Rolfe correlation) and hyperbolic tangent fit to data (1-in (25 mm) thick A572-82, grade 50, plate C).....	42
27	$K_c$ ( $K_{Tc}$ ) calculated from CVI (Barsom-Rolfe correlation) and hyperbolic tangent fit to data (2-in (51 mm) thick A572-82, grade 50, plate D).....	42

VOLUME I  
LIST OF FIGURES (CONTINUED)

<u>Fig. No.</u>		<u>Page No.</u>
28	$K_c$ ( $K_{IC}$ ) calculated from CVI (Barsom-Rolfe correlation) and hyperbolic tangent fit to data (1-in (25 mm) thick A588-82, grade B, plate E).....	43
29	$K_c$ ( $K_{IC}$ ) calculated from CVI (Barsom-Rolfe correlation) and hyperbolic tangent fit to data (2-in (51 mm) thick A588-82, grade B, plate F).....	43
30	$K_c$ ( $K_{IC}$ ) calculated from CVI (Barsom-Rolfe correlation) and hyperbolic tangent fit to data (1-in (25 mm) thick A514, grade B, plate A).....	44
31	$K_c$ ( $K_{IC}$ ) calculated from CVI (Barsom-Rolfe correlation) and hyperbolic tangent fit to data (2-in (51 mm) thick A514-85A, plate B).....	44
32	$K_c$ ( $K_{IC}$ ) calculated from CVI (Barsom-Rolfe correlation) and hyperbolic tangent fit to data (1-in (25 mm) thick A852-85, plate H).....	45
33	$K_c$ ( $K_{IC}$ ) calculated from CVI (Barsom-Rolfe correlation) and hyperbolic tangent fit to data (2-in (51 mm) thick A852-85, plate L).....	45
34	$K_c$ ( $K_{IC}$ ) calculated from CVI (Barsom-Rolfe correlation) and hyperbolic tangent fit to data (3-in (76 mm) thick A852-85, plate M).....	46
35	Comparison of $K_c$ ( $K_{IC}$ ) obtained from CTOD and CVI. (1-in (25 mm) thick A572-82, grade 50, plate C).....	49
36	Comparison of $K_c$ ( $K_{IC}$ ) obtained from CTOD and CVI. (2-in (51 mm) thick A572-82, grade 50, plate D).....	49
37	Comparison of $K_c$ ( $K_{IC}$ ) obtained from CTOD and CVI. (1-in (25 mm) thick A588-82, grade B, plate E).....	50
38	Comparison of $K_c$ ( $K_{IC}$ ) obtained from CTOD and CVI. (2-in (51 mm) thick A588-82, grade B, plate F).....	50
39	Comparison of $K_c$ ( $K_{IC}$ ) obtained from CTOD and CVI. (1-in (25 mm) thick A514, grade B, plate A).....	51
40	Comparison of $K_c$ ( $K_{IC}$ ) obtained from CTOD and CVI. (2-in (51 mm) thick A514-85A, plate B).....	51



VOLUME I  
LIST OF FIGURES (CONTINUED)

<u>Fig. No.</u>		<u>Page No.</u>
41	Comparison of $K_{IC}$ ( $K_{IC}$ ) obtained from CTOD and CVI. (1-in (25 mm) thick A852-85, plate H).....	52
42	Comparison of $K_{IC}$ ( $K_{IC}$ ) obtained from CTOD and CVI. (2-in (51 mm) thick A852-85, plate L).....	52
43	Comparison of $K_{IC}$ ( $K_{IC}$ ) obtained from CTOD and CVI. (3-in (76 mm) thick A852-85, plate M).....	53
44	$K_{IC}$ (1s) measurements and $K_{IC}$ (1s) values derived from $K_{IC}$ (static) and $K_{IC}$ (dynamic) measurements plotted against temperature measured relative to the LPST. A36 steel, all plates.....	56
45	$K_{IC}$ (1s) measurements and $K_{IC}$ (1s) values derived from $K_{IC}$ (static) and $K_{IC}$ (dynamic) measurements plotted against temperature measured relative to the LPST. A588 steel, all plates for which 25 or 30 ft-lb (34 or 41 J) temperature (as appropriate) as definable.....	57
46	$K_{IC}$ (1s) measurements and $K_{IC}$ (1s) values derived from $K_{IC}$ (static) and $K_{IC}$ (dynamic) measurements plotted against temperature measured relative to the LPST. A514 steel, all plates with definable 35 ft-lb (47 J) transition temperature.....	58
47	$K_{IC}$ values derived from $K_{IC}$ (static) measurements plotted against temperature measured relative to the LPST. A517 steel, all plates with definable 35 ft-lb (47 J) transition temperature.....	59
48	Charpy impact energy vs test temperature (1-in (25 mm) thick A572-82, grade 50, plate C, weld metal).....	69
49	Charpy impact energy vs test temperature (1-in (25 mm) thick A572-82, grade 50, plate C, HAZ).....	69
50	Charpy impact energy vs test temperature (2-in (51 mm) thick A572-82, grade 50, plate D, weld metal).....	70

VOLUME I  
LIST OF FIGURES (CONTINUED)

<u>Fig. No.</u>		<u>Page No.</u>
51	Charpy impact energy vs test temperature (2-in (51 mm) thick A572-82, grade 50, plate D, HAZ).....	70
52	Charpy impact energy vs test temperature (1-in (25 mm) thick A588-82, grade B, plate E, weld metal).....	71
53	Charpy impact energy vs test temperature (1-in (25 mm) thick A588-82, grade B, plate E, HAZ).....	71
54	Charpy impact energy vs test temperature (1-in (25 mm) thick A514, grade B, plate A, weld metal)....	72
55	Charpy impact energy vs test temperature (1-in (25 mm) thick A514, grade B, plate A, HAZ).....	72
56	Charpy impact energy vs test temperature (1-in (25 mm) thick A852-85, plate H, weld metal).....	73
57	Charpy impact energy vs test temperature (1-in (25 mm) thick A852-85, plate H, HAZ).....	73
58	Comparison of base plate, weld metal and heat-affected zone Charpy impact energy vs test temperature (1-in (25 mm) thick A572-82, grade 50, plate C).....	75
59	Comparison of base plate, weld metal and heat-affected zone Charpy impact energy vs test temperature (1-in (25 mm) thick A588-82, grade B, plate E).....	75
60	Comparison of base plate, weld metal and heat-affected zone Charpy impact energy vs test temperature (1-in (25 mm) thick A514, grade B, plate A).....	76
61	Comparison of base plate, weld metal and heat-affected zone Charpy impact energy vs test temperature (1-in (25 mm) thick A852-85, plate H)....	76
62	Comparison of base plate, weld metal and heat-affected zone Charpy impact energy vs test temperature (2-in (51 mm) thick A572-82, grade 50, (plate D).....	77

VOLUME I  
LIST OF FIGURES (CONTINUED)

<u>Fig. No.</u>		<u>Page No.</u>
63	CTOD values as a function of test temperature for the 2-in (51 mm) thick A572-82, grade 50 steel plate (plate D).....	78
64	CTOD values as a function of test temperature for the 1-in (25 mm) thick A588-82, grade B steel plate (plate E).....	78
65	CTOD values as a function of test temperature for the 2-in (51 mm) thick A588-82, grade B steel plate (plate F).....	79
66	CTOD values as a function of test temperature for the 1-in (25 mm) thick A852-85 steel plate (plate H).....	79
67	Dugdale strip yield model.....	86
68	Schematic load-clip gauge displacement showing plastic ( $V_p$ ) and elastic component of total displacement ( $V_u$ ).....	86
69	Types of load (P) vs clip gauge displacement (V) records.....	89
70	Schematic load-displacement curve for a specimen exhibiting measurable plastic deformation prior to fracture.....	93
71	Non-dimensional load-displacement curve for a 3-point bend specimen with $a_0/W = 0.5$ based on small-scale plasticity model.....	97
72	1-sec loading time tensile properties vs test temperature.....	100

VOLUME I  
LIST OF TABLES

<u>Table No.</u>		<u>Page No.</u>
1	Maximum $K_{Ic}$ that can be measured in bridge steel plates.....	4
2	Current base metal Charpy V-Notch requirements for fracture critical members.....	14
3	Chemical composition of plates A572-82, grade 50.....	15
4	Chemical composition of plates A588-82, grade B.....	16
5	Chemical composition of plates A514.....	17
6	Chemical composition of plates A852-85.....	18
7	Room temperature tensile properties of A572, grade 50 steel plate. Longitudinal direction.....	20
8	Room temperature tensile properties of A588, grade B steel plate. Longitudinal direction.....	21
9	Room temperature tensile properties of A514 steel plate. Longitudinal direction.....	22
10	Room temperature tensile properties of A852-85 steel plate. Longitudinal direction.....	23
11	LPST for test plates.....	40
12	Critical crack sizes at LPST for plates for design stress equal to one-half the yield strength.....	63
13	Plate preparation and welding requirements.....	66
14	Subcontractor's welding procedure qualification form.....	67
15	Room temperature tensile properties of weld metal. Longitudinal direction.....	68

VOLUME II  
TABLE OF CONTENTS

<u>Section</u>	<u>Page No.</u>
1 INTRODUCTION .....	1
2 THE DUCTILE-BRITTLE (D-B) TRANSITION .....	2
3 DISLOCATION MECHANICS BASED CONSTITUTIVE RELATIONS .....	8
4 THE BARSOM-ROLFE TRANSITION TEMPERATURE SHIFT .....	17
5 REFERENCES .....	20

VOLUME II  
LIST OF FIGURES

<u>Fig. No.</u>	<u>Page No.</u>
1 Proposal of Ludwik suggesting that cleavage fracture occurs at a point, F, where flow stress and fracture stress vs strain curves intersect.....	3
2 Relative positions of flow stress, cleavage fracture stress, and shear fracture stress vs strain curves to produce: (a) ductile shear failure (b) ductile cleavage failure (c) brittle shear failure (d) brittle cleavage failure.....	5
3 Stress-strain curves at a variety of temperatures showing the fracture changes from shear to cleavage.....	7
4 Schematic diagrams of stress dependence on (a) temperature, (b) strain rate, (c) strain and (d) polycrystal grain diameter.....	9
5 Crack growth by coalescence of cavities.....	12
6 Microvoid coalescent fracture surface appearance.....	12

VOLUME II  
LIST OF FIGURES (CONTINUED)

<u>Fig. No.</u>		<u>Page No.</u>
7	Pre-yield deformation needed to form a cleavage crack.....	14
8	Three-dimensional view of pre-yield deformation needed to form a cleavage crack.....	14
9	Dependence of cleavage stress, $\sigma_C$ , on grain size, $\lambda$ . Cleavage stress is lowered when grain boundary carbide plates ( $t_1$ and $t_2$ ) are cracked by dislocation pile-ups.....	15
10	Cleavage fracture surface appearance.....	15

VOLUME III  
TABLE OF CONTENTS

<u>Section</u>		<u>Page No.</u>
1	INTRODUCTION .....	1
2	THEORETICAL ASPECTS OF THE BRITTLE-DUCTILE (B-D) TRANSITION .....	2
3	SMALL SPECIMEN MODELING OF BRIDGE FRACTURES .....	3
4	TEST RESULTS, BASE PLATES .....	5
	4.1 Materials .....	5
	4.2 Types of Tests .....	5
	4.3 Data Analysis .....	5
	4.4 Evaluation of the Barsom-Rolfe Steel Selection Criterion .....	7
	4.5 Comparison of $K_{IC}$ From CVI and CTOD .....	8
	4.6 Critical Crack Sizes at LPST .....	8
5	TEST RESULTS, WELDMENTS .....	12
	5.1 Material .....	12
	5.2 Test Results .....	12
	5.3 Analysis of Weldment Data .....	13

VOLUME III  
TABLE OF CONTENTS (CONTINUED)

<u>Section</u>	<u>Page No.</u>
6 DISCUSSION .....	19
7 RECOMMENDATIONS .....	21
REFERENCES .....	22

VOLUME III  
LIST OF FIGURES

<u>Fig. No.</u>	<u>Page No.</u>
1 Toughness comparison of A572-82, grade 50 steel plate in 1- and 2-in (25 and 51 mm) thicknesses; points converted from CTOD, curves from CVI values...	9
2 Toughness comparison of A588-82, grade B steel plate in 1- and 2-in (25 and 51 mm) thicknesses; points converted from CTOD, curves from CVI values...	9
3 Toughness comparison of A514, grade B steel plate in 1- and 2-in (25 and 51 mm) thicknesses; points converted from CTOD, curves from CVI values.....	10
4 Toughness comparison of A852-85 steel plate in 1- 2- and 3-in (25, 51 and 76 mm) thicknesses; points converted from CTOD, curves from CVI values.....	10
5 Comparison of base plate, weld metal and heat-affected zone Charpy impact energy vs test temperature (1-in (25 mm) thick A572-82, grade 50, plate C).....	14
6 Comparison of base plate, weld metal and heat-affected zone Charpy impact energy vs test temperature (2-in (51 mm) thick A572-82, grade 50, plate D).....	14
7 Comparison of base plate, weld metal and heat-affected zone Charpy impact energy vs test temperature (1-in (25 mm) thick A588-82, grade B, plate E).....	15

VOLUME III  
LIST OF FIGURES (CONTINUED)

<u>Fig. No.</u>		<u>Page No.</u>
8	Comparison of base plate, weld metal and heat-affected zone Charpy impact energy vs test temperature (1-in (25 mm) thick A514, grade B, plate A).....	15
9	Comparison of base plate, weld metal and heat-affected zone Charpy impact energy vs test temperature (1-in (25 mm) thick A852-85, plate H)....	16
10	CTOD values as a function of test temperature for the 2-in (51 mm) thick A572-82, grade 50 steel plate (plate D).....	17
11	CTOD values as a function of test temperature for the 1-in (25 mm) thick A588-82, grade B steel plate (plate E).....	17
12	CTOD values as a function of test temperature for the 2-in (51 mm) thick A588-82, grade B steel plate (plate F).....	18
13	CTOD values as a function of test temperature for the 1-in (25 mm) thick A852-85 steel plate (plate H).....	18

VOLUME III  
LIST OF TABLES

<u>Table No.</u>		<u>Page No.</u>
1	Current base metal Charpy V-notch requirements zone 2: minimum service temperature from -1°F to -30°F.....	6
2	Critical crack sizes at LPST for plates for design stress equal to one-half the yield stress.....	11



## CHAPTER 1: INTRODUCTION

Bridge members are generally large compared to the size of cracks or defects that they may contain. An example of this is a crack that may occur on the flame-cut edge of a girder flange, figure 1 (top). When a load is applied to such a member, the metal near the crack tip flows, forming a plastic zone, figure 1 (bottom). Since the plastic zone, like the crack, cannot resist stresses acting across it, it is customary to consider the "effective crack" length as the sum of the lengths of the actual crack and calculated radius of the plastic zone. Even this effective crack length is so small compared to the bridge element that the plastic zone is completely surrounded by material that deforms in a linear-elastic fashion. It is because the stresses and strains within this surrounding material are linearly related that a linear-elastic analysis of bridge elements can be made. A fracture mechanics analyses of the structure, however, requires the use of a critical value of fracture toughness, and the test specimen most commonly used for measuring this value (ASTM E399) is too small to contain the crack and its plastic zone in elastically deformed metal at temperatures well into the transition range. The limitation imposed by the need for a linear-elastic analysis can be avoided, however, by using an elastic-plastic analysis as is done for crack tip opening displacement (CTOD) specimens.

The purpose of the project described in this volume is to evaluate fracture toughness by using CTOD specimens and to use this information to evaluate the relationship between measured fracture toughness values and those implied by Charpy V-notch Impact tests in the vicinity of the "lowest anticipated service temperature" (LAST).

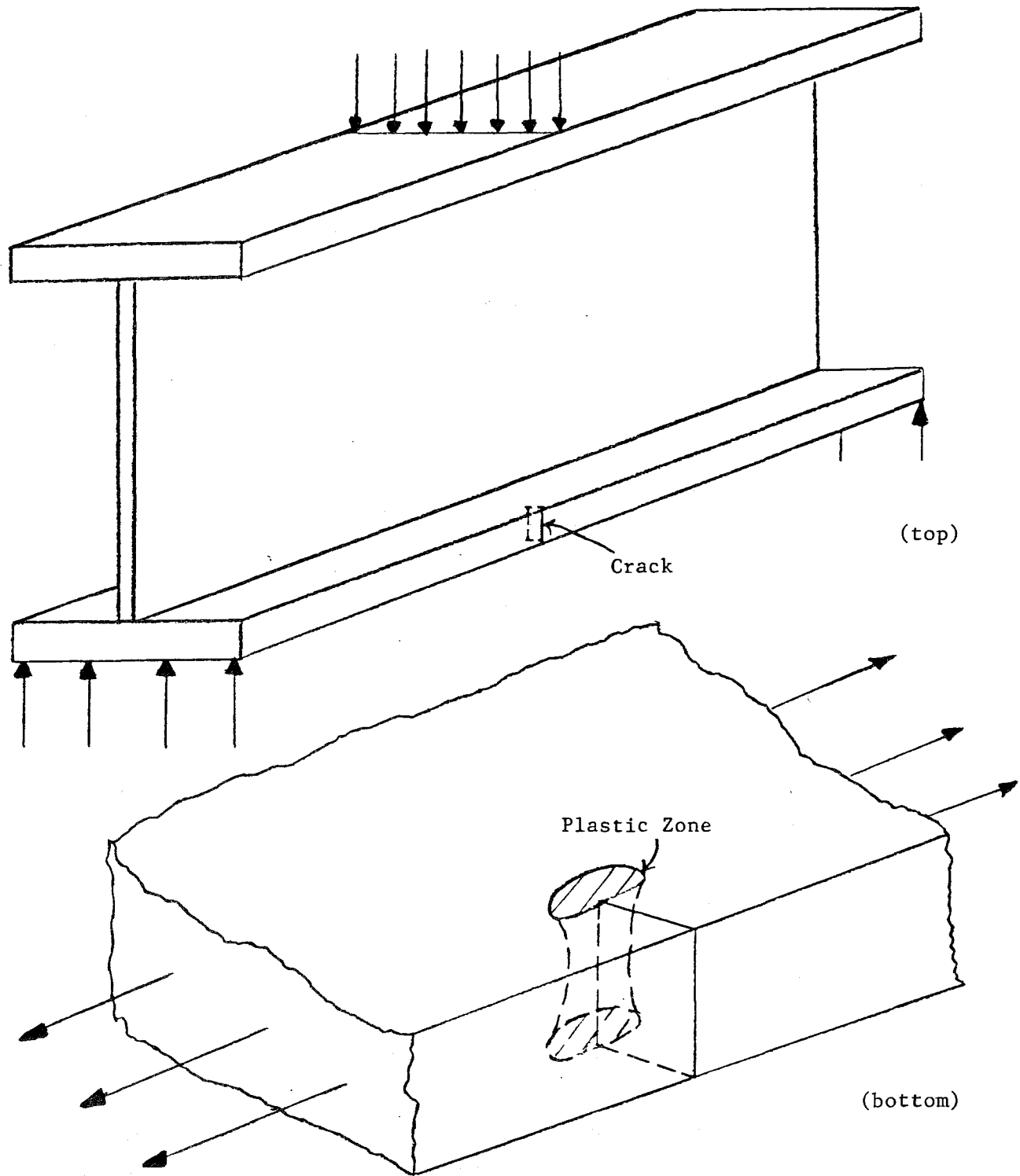


Figure 1. Schematic showing crack in girder flange (top) and enlarged view of crack and plastic zone (bottom).

## 1.1 Linear Elastic Specimen Analysis

Actually, fracture toughness specimens, either elastic or elastic-plastic, are seldom used for directly evaluating bridge steels. The size, ease of testing, and cost of Charpy V-notched Impact (CVI) specimens makes the use of this type of test an obvious choice for quality assurance and post mortem analyses of bridge members. The problem is one of using a CVI specimen to imply a value of fracture toughness for different steel types, temperature zones, and plate thicknesses. The AASHTO Guide Specifications for CVI are based on the Barsom-Rolfe correlation of CVI with the plane strain fracture toughness ( $K_{Ic}$ ). The use of  $K_{Ic}$  has the obvious advantage that it makes it possible to relate the flaw sizes and stresses that are needed to cause fast cracks to initiate. It has two serious limitations, however: First, the test only yields valid data for plane strain cracking, and since the Guide Specifications were designed to avoid this type of cracking, the toughness of the steels cannot be measured in the temperature range where they are used. Second,  $K_{Ic}$  measurements cannot be used to evaluate the effect of plate thickness on crack resistance.

The dimension that most commonly causes tests to be invalid is the specimen thickness, B. It is required that:

$$B \geq 2.5(K_Q/\sigma_{ys})^2 \quad (1)$$

where  $K_Q$  = the measured stress-intensity-factor

and  $\sigma_{ys}$  = the material yield strength.

The maximum specimen thickness obviously is the plate thickness; hence the maximum valid  $K_{Ic}$  that can be measured for the common bridge steel plates can be calculated, on the basis of their minimum allowable yield strengths, as shown in table 1.

Table 1.

Maximum  $K_{Ic}$  that can be measured  
in bridge steel plates.

Steel:	M-183	M-233	M-222	M-244
AASHTO	A36	A572 Gr50	A588 A852	A514/A517
ASTM				
Yield strength (ksi)	36	50	50	100
Max $K_{Ic}$ (ksi/in)				
in 1.0-in plate	23	32	32	63
in 2.0-in plate	32	45	45	89
in 2.5-in plate	36	**	50	100
in 4.0-in plate	46	**	63	***

\*\* Not used in welded structures.

\*\*\* Not permitted in welded structures in Zone 3.

Conversion Factor: 1 in = 25.4 mm; 1 ksi = 6.895 MPa;  
1 ksi/in = 1.098 MPa-m<sup>1/2</sup>

Note that for 2.5-in (64 mm) thick plates, the maximum measurable  $K_{Ic}$  value is numerically equal to the metals yield strength. For thinner plates, the measuring capability is less, and for thicker plates it is more.

In addition to the  $K_{Ic}$  specimen having a limited measuring capability, the requirement for plane strain cracking makes the test independent of specimen thickness. Hence, the important variable of thickness can not be evaluated by this test. The variation in toughness requirements for different plate thicknesses in the present AASHTO Guide Specifications is based on experience. CTOD tests can be conducted on specimens of any thickness, and this is an important reason for using this kind of specimen. This topic is discussed in more detail in section 1.4.

The AASHTO Charpy V-notch requirements for fracture critical members, based on correlations of Charpy V-notch and  $K_{Ic}$  test results, are intended to ensure that bridges cannot fail by plane strain fracturing. An exhaustive study by the contractor has shown that this objective is generally achieved.<sup>[1]</sup> But what level of fracture safety does this provide? The only inference that can be drawn is that when the AASHTO requirements are met, the fracture toughness of the bridge steels should exceed the values given in the above table when temperatures are at or above the LAST. Since there is no standard linear elastic fracture mechanics test method to evaluate higher levels of toughness, the increased margin of toughness cannot be quantitatively specified. Sometimes it is stated that the AASHTO requirements ensure that fractures in bridges will be "elastic-plastic," rather than "elastic"; but, in effect, such a statement merely defines "elastic-plastic" to be synonymous with failure to meet the ASTM E399 thickness requirement.

Linear-elastic fracture mechanics is not inherently limited to crack extension under plane strain conditions. In ASTM Standard E561, the crack tip stress state is far from plane strain; but the resistance to crack growth is nonetheless measured in terms of the linear-elastic parameter,  $K$ , the stress intensity factor. This approach is viable as long as the crack tip plastic zone is small compared to the in-plane dimensions of the specimen, regardless of thickness. Hence, the limits of a linear-elastic analysis can be extended by increasing the in-plane dimensions and ignoring the plane strain requirement.

Some tests were run on this project using compact ASTM E399 specimens with large in-plane dimensions, but this type of test was discontinued when it was found that the data that were needed could be obtained by using a  $K$  calculation for CTOD specimens that was developed in the course of this project.

## 1.2 Elastic-Plastic Behaviors

Characterization of the crack tip stress field by the stress intensity factor,  $K$ , relies on the fact that linear elastic stress fields exhibit a singularity at the crack tip. Elastic-plastic analyses indicate that plastic strains also show a singularity at the crack tip. It should be possible, therefore, to devise a crack tip characterization parameter which applies within the plastic zone and, consequently, is not affected by whether or not the plastic zone is embedded in a linear elastic region. Two elastic plastic parameters are the basis of standard test procedures, the J-integral and the crack tip opening displacement, CTOD. The second parameter, CTOD, is the one selected for study in this program.

Physically, the CTOD is the finite opening displacement or "stretch" which develops at the leading edge of a crack when a cracked structure or specimen is loaded; the fracture toughness of a material is the critical value of CTOD, the value attained just prior to the onset of crack extension. Early work on CTOD included attempts to measure CTOD with probes reaching to the leading edge of the crack; but for practical purposes the definition had to be analytically based. A description of the analysis on which CTOD is based is given in appendix A.

## 1.3 The Use of CTOD in Fracture Control and the Correlation of CTOD Values With CVI Toughness

The purpose for using CTOD tests for measuring the fracture toughness of bridge steels is to extend the measurements to values higher than those that can be made with  $K_{Ic}$  tests as well as to be able to evaluate the effect of plate thickness. As stated earlier, this does not imply the use of CTOD testing as a requirement in the AASHTO Guide Specifications. Charpy V-notch Impact toughness

requirements will continue to be cited by AASHTO so that one important determination to be made by this project is how well CTOD values can be implied from CVI tests. If this can be done, then CVI values will be able to be used to estimate CTOD values above the LAST, much as CVI can now be used to estimate  $K_{Ic}$  below the LAST.

Whether CTOD is evaluated directly or by means of a CVI-to-CTOD correlation, a method for applying CTOD data to fracture control and analysis of bridge elements is still needed. A number of techniques have been developed to use CTOD for fracture control, and these are discussed below. Use of CTOD for fracture control and analysis and a CVI-to-CTOD correlation are related topics.

#### Correlation of CTOD values with Charpy V-notch Impact toughness

The success at relating  $K_{Ic}$  values to Charpy V-notch toughness by using the Barsom/Rolfe two-step procedure suggests that the best way for relating CTOD to CVI might be to convert CTOD to critical K values, and then follow the Barsom/Rolfe procedure.

A method for converting CTOD to  $K_c$  is to use the expression for the elastic contribution to CTOD given by British Standard BS5723-1979 (see appendix A):

$$\delta = [K^2(1-\nu^2)]/[\sigma_Y E] \quad (2)$$

where

- $\delta$  = CTOD
- K = Stress Intensity Factor
- $\nu$  = Poisson's Ratio
- $\sigma_Y$  = Flow Stress
- E = Elastic Modulus

The problem is one of defining the flow stress. In the British Standard, the flow stress is defined as two times the yield strength. Wellman and Rolfe carried out a study in which they used four pressure vessel steels and one ship steel to find correlations of CTOD, J-integral, and CVI to  $K_{Ic}$ .<sup>[2]</sup> On the basis of their data they selected for  $\sigma_Y$  a value of 1.61 times the average of the dynamic yield and tensile strength. The correlations they presented for one pressure vessel and one ship steel is shown in figure 2. They also compared one and two-step correlations of CVI to CTOD to  $K_{Ic}$ , and as found earlier, the two-step procedure was better than a one-step one. Hence, only a two-step procedure was considered in this project.

#### Data analysis

The basis for correlating  $K_{Ic}$  or CTOD with CVI is the Barsom-Rolfe criterion. Bridges experience a loading rate of about 1-sec. Hence,  $K_{Ic}$  or CTOD tests, when used to model bridge behavior, are loaded to failure in 1-sec. CVI specimens are loaded much faster than this so that a temperature shift is part of the B-R criterion. The temperature shift in the AASHTO Guide Specifications is the difference between the LAST and the specified CVI test temperature for each plate material and thickness (see table 2).

The Guide Specifications do not relate CVI test temperatures to zones for weld metal, rather a fixed ft-lb requirement and temperature is specified for all zones. This prohibits the use of a temperature shift for weldments. Hence although the base plates are analyzed by use of a B-R type criterion, the weldments can only be analyzed by comparing the weld metal and heat-affected CVI and CTOD values to those obtained on the plate used in the weldment.



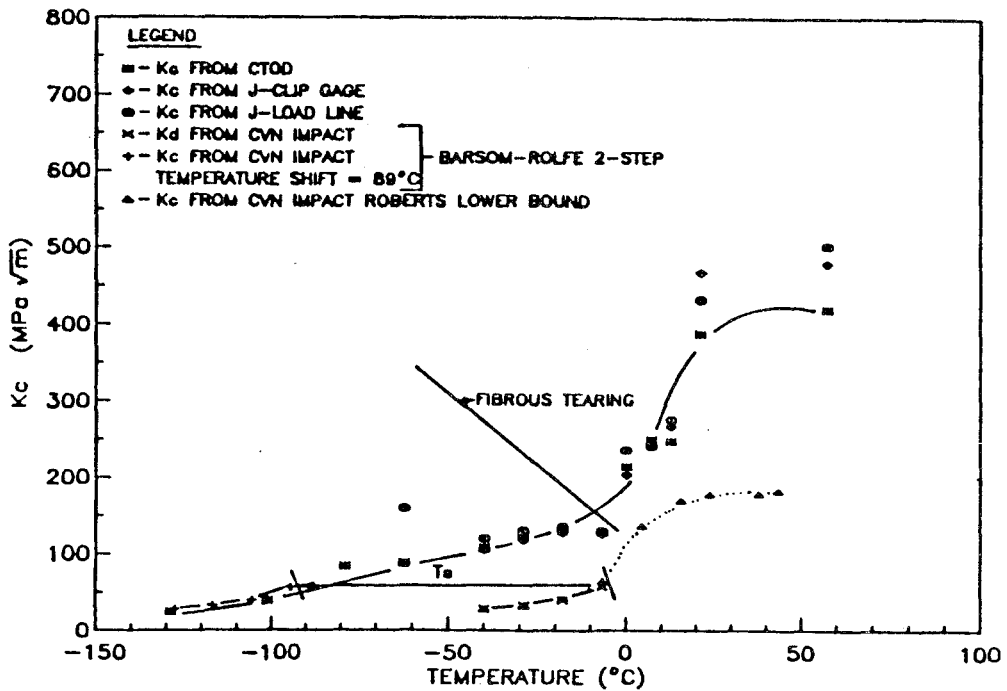
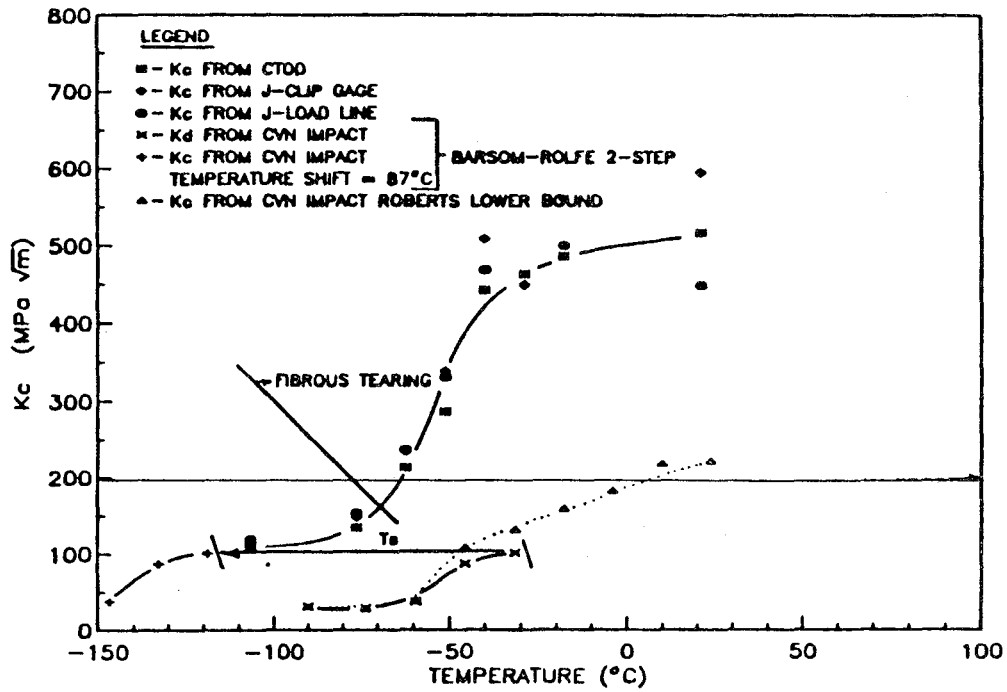


Figure 2.  $K_c$ , CVN, CTOD and J correlations.  
 Specimen size 1 by 2 by 8 in (25 by 51 by 203 mm).  
 Lower-bound values. Top: A516 steel.  
 Bottom: A131 steel.[2]

## Use of CTOD test results in fracture control and analysis

One way to use CTOD test results for fracture control and analysis is to use CTOD- $K_{Ic}$  correlations to estimate  $K_{Ic}$ . Having the latter value, well established fracture mechanics procedures can be used to relate critical crack sizes and stresses. In spite of this, other methods have been suggested for using CTOD directly in fracture control, particularly for metals tougher than those used for bridges, and these are briefly reviewed below.

Burdekin and Dawes have developed a CTOD based design curve which makes it possible to use CTOD directly without the intermediate step of converting to  $K_{Ic}$ .<sup>[3]</sup> This approach is most useful for structures that might experience large strains, even well in excess of the yield strain ( $\epsilon_{ys}$ ). The design curve was developed primarily for pressure vessels and has a built-in factor of safety ranging from 1 to about 5, with an average value of about 2.5. Their method does not appear to be as useful for bridge elements as the CTOD- $K_{Ic}$  correlations since AASHTO will continue to use CVI for quality control and quality assurance.

A third method has been suggested by Barsom and Rolfe: "Use finite element analysis techniques to model the specific structural geometry being analyzed. Develop stress, load, pressure, and so on versus CTOD curves for the specific flaw geometry assumed to be present in the structure. Conduct CTOD tests on the materials of interest to determine the critical CTOD and the critical load directly from the load-CTOD curve."<sup>[4]</sup> The use of finite element techniques for  $K$  or CTOD analysis is obviously desirable but again does not address the problem of material selection and quality assurance as now done in the AASHTO Guide Specifications.

#### 1.4 Effect of Plate Thickness

An important consideration in material selection and fracture control is the fact that toughness varies with plate thickness. There are two sources of this toughness variation: one is metallurgical and the other mechanical. The metallurgical variation results because cast ingots are reduced more for thin plates than for thick ones, and cooling rates are faster for thin plates than for thick ones. The latter effect is most serious in heat-treated plates. Both A514/517 and A852 are not especially rich in alloy elements so that for thick plates, the center plane will tend to have coarser, higher temperature transformation products such as pearlite and coarse bainite while surface microstructure will tend toward martensite and finer bainite. For normalized or hot rolled products the slower cooling rate at the center will give larger grains than at the surface. These toughness differences become apparent when CVI tests are made at various depths in thick plates. Since the AASHTO Guide Specifications are based on CVI tests, these through-the-thickness variations would be accounted for if the CVI specimen locations and the thickness location where cracks initiate are the same.

The mechanical effect of thickness is due to the fact that differing amounts of thickness constraint occur during cracking. As thickness and/or yield strength are increased and/or test temperature is decreased, thickness constraint increases; higher constraint decreases toughness.

Because of the importance of thickness, all plate materials were tested in 1- and 2-in (25 and 51 mm) thickness in this project, and one material was tested in 3-in (76 mm) thickness as well.

## 1.5 Miscellaneous Topics Regarding CTOD Testing

It is helpful to have some information on the comparative costs of CTOD and  $K_{Ic}$  testing if the former is to be considered as a replacement for the latter. In the present project the CTOD specimens all had widths equal to twice their thickness, and this specimen is identical with the  $K_{Ic}$  bend specimen. Both specimens require the use of a fatigue crack as a crack starter so that CTOD and three-point bend  $K_{Ic}$  specimens are identical in both shape and testing procedures. Obviously this makes their machining and testing costs identical.

Fracture toughness testing of welds presents a problem for any specimen shape because of the varied microstructure associated with the weld and the presence of residual stresses. These cause problems in obtaining a straight front on the fatigue crack. The residual stress problem can be minimized by applying a small transverse compressive strain to the specimen prior to fatiguing, and is the method used in this project.

## CHAPTER 2: TEST RESULTS, BASE PLATES

### 2.1 Materials

Four compositions of bridge plate were used in the study: ASTM designation A572, Grade 50, A588, A514 and A852. (The corresponding AASHTO designations are: M233, M222, M244 and M270, Grade 70W, respectively.) The widely used low strength A36 was not a part of the program since its high ratio of toughness to yield strength greatly decreases the probability of failure by fast fracture in bridge elements. The first two of the selected steels have minimum yield strength of 50 ksi (345 MPa) and are used in the hot rolled or normalized condition so that their microstructures are ferrite-pearlite; the latter two have minimum yield strengths of 100 and 75 ksi (690 and 517 MPa), respectively, which are obtained by quenching and tempering; hence their microstructures should be bainite-martensite.

All plate compositions were tested in 1- and 2-in (25 and 51 mm) thicknesses. The A852 was also tested in 3-in (76 mm) thickness. The plates were ordered to a zone 2 requirement, and the plate thicknesses and their Charpy V-notch toughness requirements for zone 2 are shown in table 2.

Characterization tests were performed on all plates, and where possible these results were compared with ASTM values and those supplied by the mill.

### 2.2 Characterization Tests

Chemical Analysis, Tensile and Charpy Impact Tests were conducted on all plates. The compositions shown in tables 3 to 6, and

Table 2.

Current base metal Charpy V-Notch requirements  
for fracture critical members. <sup>(1)</sup>

<u>AASHTO</u>	<u>ASTM DESIGNATION</u>	<u>THICKNESS INCHES</u>	<u>ZONE 2</u> <sup>(2)</sup>
M233	A572, Grade 50	1 and 2	25 ft-lb @ 40°F
M22	A588	1 and 2	25 ft-lb @ 40°F
M244	A514	1 and 2	35 ft-lb @ 0°F
M270, Gr. 70W	A852	1, 2 and 3	30 ft-lb @ 20°F

Conversion factors: 1 in = 25.4 mm; 1 ft-lb = 1.356 J;  
1°F = 5(F-32)/9°C

- (1) The CVN-impact testing shall be "P" plate frequency testing in accordance with AASHTO T-243 (ASTM A673). Charpy impact tests are required on only one end of each plate. The Charpy test pieces shall be coded with respect to heat/plate number and that code shall be recorded on the mill-test report of the steel supplier with the test results. If requested by the engineer, the broken pieces from each test (three specimens, six halves) shall be packaged and forwarded to the Quality Assurance organization of the State. Use the average of three tests. If the energy value for more than one of three test specimens is below the minimum average requirements, or if the energy value for one of the three specimens is less than two-thirds of the specified minimum average requirements, a retest shall be made and the energy value obtained from each of the three retest specimens shall equal or exceed the specified minimum average requirements.
- (2) Zone 2: Minimum Service Temperature from -1°F to -30°F (-18°C to -34°C).

Table 3.

Chemical composition of plates A572-82, grade 50.

<u>C</u>	<u>Mn</u>	<u>P</u>	<u>S</u>	<u>Si</u>	<u>Cu</u>	<u>Ni</u>	<u>Cr</u>	<u>V</u>	<u>Al</u>	<u>Cb</u>
1-in (25 mm) thick (plate C) -										
<u>Supplied by Mill</u>										
.18	1.19	.017	.013	.246				.051	.044	
<u>ASTM Requirement</u>										
.23*	1.35*	.04*	.05*	.40*						*Maximum
<u>Plate Analysis</u>										
.18	1.26	.022	.015	.28				.05		<.01
2-in (51 mm) thick (plate D) -										
<u>Supplied by Mill</u>										
.18	1.10	.012	.021	.271				.051	.050	
<u>ASTM Requirement</u>										
.23*	1.35*	.04*	.05*	.15- .40						*Maximum
<u>Plate Analysis</u>										
.19	1.10	.014	.020	.27				.05		<.01

Table 4.

Chemical composition of plates A588-82, grade B.

<u>C</u>	<u>Mn</u>	<u>P</u>	<u>S</u>	<u>Si</u>	<u>Cu</u>	<u>Ni</u>	<u>Cr</u>	<u>V</u>	<u>Al</u>	<u>Cb</u>
1-in (25 mm) thick (plate E) -										
<u>Supplied by Mill</u>										
.18	1.00	.015	.011	.373	.262	.31	.56	.028		.042
<u>ASTM Requirement</u>										
.20*	0.75- 1.35	.04*	.05*	.15- .50	.20- .40	.50*	.40- .70	.01- .10	*Maximum	
<u>Plate Analysis</u>										
.14	1.02	.022	.012	.40	.29	.35	.57	.03		
2-in (51 mm) thick (plate F) -										
<u>Supplied by Mill</u>										
.12	1.06	.011	.017	.343	.312	.31	.60	.040	.035	
<u>ASTM Requirement</u>										
.20*	0.75- 1.35	.04*	.05*	.15- .50	.20- .40	.50*	.40- .70	.01- .10	*Maximum	
<u>Plate Analysis</u>										
.12	1.02	.014	.018	.30	.29	.56	.04			



Table 5.

Chemical composition of plates A514.

<u>C</u>	<u>Mn</u>	<u>P</u>	<u>S</u>	<u>Ti</u>	<u>Si</u>	<u>Ni</u>	<u>Cr</u>	<u>Mo</u>	<u>V</u>	<u>B</u>	
1-in (25 mm) thick A514, grade B (plate A) -											
<u>Supplied by Mill</u>											
.20	.95	.010	.014	.020	.31	--	.58	.20	.060	.0008	
<u>ASTM Requirement</u>											
.12- .21	.070- 1.00	.035 max	.04 max	.01- .03	.20- .35	--	.40- .65	.15- .25	.03- .08	.0005- .005	
<u>Plate Analysis</u>											
.18	.91	.010	.012	.01	.30	--	.54	.20	.04	.0020	
<u>C</u>	<u>Mn</u>	<u>P</u>	<u>S</u>	<u>Si</u>	<u>Cu</u>	<u>Ni</u>	<u>Cr</u>	<u>V</u>	<u>Al</u>	<u>Mo</u>	<u>B</u>
2-in (51 mm) thick A514-85A (plate B) -											
<u>Supplied by Mill</u>											
.17	0.64	.011	.010	.319	-	1.24	.98	-	-	.470	.0023
<u>ASTM Requirement</u>											
.12- .21	.070- 1.00	max	.035 max	.04 .03	.01- .35	.20- --	.65	.40- .25	.15- .08	.03- .005	.0005- .
<u>Plate Analysis</u>											
.19	0.65	.009	.013	.31	-	1.25	.96	-	-	.50	.0033

Table 6.

Chemical composition of plates A852-85.

<u>C</u>	<u>Mn</u>	<u>P</u>	<u>S</u>	<u>Si</u>	<u>Cu</u>	<u>Ni</u>	<u>Cr</u>	<u>V</u>	<u>Al</u>	<u>Mo</u>	<u>B</u>
1-in (25 mm) thick (plate H) -											
<u>Supplied by Mill</u>											
.12	1.06	.011	.017	.343	.312	.31	.60	.040	.035	-	-
<u>ASTM Requirement</u>											
(Not Available)											
<u>Plate Analysis</u>											
.12	1.04	.007	.016	.35	.30	.29	.58	.04	-	-	-
2-in (51 mm) thick (plate L) -											
<u>Supplied by Mill</u>											
.17	1.12	.023	.014	.371	.284	.28	.57	.062	.064	-	-
<u>ASTM Requirement</u>											
(Not Available)											
<u>Plate Analysis</u>											
.18	1.10	.021	.014	.35	.24	.27	.53	.06	-	-	-
3-in (76 mm) thick (plate M) -											
<u>Supplied by Mill</u>											
.18	1.19	.023	.012	.343	.263	.32	.60	.061	.056	-	-
<u>ASTM Requirement</u>											
(Not Available)											
<u>Plate Analysis</u>											
.17	1.14	.023	.011	.37	.26	.31	.58	.06	-	-	-

tensile results shown in tables 7 to 10 were all consistent with ASTM and AASHTO. The Charpy Impact toughnesses of all the plates, figures 3 to 11, were considerably higher than the zone 2 AASHTO requirements shown in table 2.

The curves drawn on the CVI Energy vs Test Temperature charts are hyperbolic tangent best fits to the data. These curves are defined by the expression in figure 12 and the three parameters that characterize the curve, the upper shelf (US), the transition temperature (TT), and the slope of the curve at the TT (slope), are also identified. The latter are also added to each plot in figures 3 to 11. The algorithm used for calculating the curves assumes that the lower shelf value is zero.

### 2.3 $K_{Ic}$ and CTOD Test Results

Three-point bend tests were conducted on all plates according to British Standard BS5762-79 except for the 3-in (76 mm) thick plate of A852. This was tested according to the tentative ASTM Standard Test Method using compact specimens since the bend specimen would have required too much material. The CTOD test can be interpreted over the complete range of material behaviors from linear elastic to general yielding. The validity requirements in this test are not associated with specimen size, but with the straightness and flatness of the precrack. Hence, valid data were obtained on all the specimens that were tested.

When the load-displacement record indicated that the test displayed only linear elastic deformation, a  $K_{Ic}$  calculation was also made by using ASTM Test Method E399. If the calculation showed the test to be valid, this was indicated in the figures.

Table 7.

Room temperature tensile properties of A572,  
grade 50 steel plate. Longitudinal direction.

<u>Tensile Strength ksi</u>	<u>Yield Strength ksi</u>	<u>Elong. (2-in G.L.) Percent</u>	<u>Red. in Area Percent</u>
a) 1-in (25 mm) thick (plate C) -			
<u>Supplied by Mill</u>			
79.9	58.7	26 (8 in.)	---
<u>ASTM Requirements</u>			
65 min.	50 min.	18 (8 in.) 21 (2 in.)	--- ---
<u>Measured on Plate</u>			
82.8	58.1	31	69.1
82.5	57.1	30	68.5
82.7	58.8	31	69.7
Average:			
82.7	58.0	30.7	69.1
b) 2-in (51 mm) thick (plate D) -			
<u>Supplied by Mill</u>			
82.7	53.9	22	---
<u>ASTM Requirements</u>			
65 min.	50 min.	18 (8 in.) 21 (2 in.)	--- ---
<u>Measured on Plate</u>			
75.4	49.7	33	69.5
75.8	49.1	32	65.8
77.7	51.5	32	68.8
Average:			
76.3	50.1	32.3	68.0

Conversion Factor: 1 in = 25.4 mm; 1 ksi = 6.895 MPa

Table 8.

Room temperature tensile properties of A588,  
grade B steel plate. Longitudinal direction.

<u>Tensile Strength ksi</u>	<u>Yield Strength ksi</u>	<u>Elong. (2-in G.L.) Percent</u>	<u>Red. in Area Percent</u>
a) 1-in (25 mm) thick (plate E) -			
<u>Supplied by Mill</u>			
78.0	56.5	23 (8 in.)	---
<u>ASTM Requirements</u>			
70 min.	50 min.	18 (8 in.) 21 (2 in.)	--- ---
<u>Measured on Plate</u>			
82.3	57.0	34	71.4
81.8	56.9	30	73.2
81.2	56.0	32	72.6
Average:			
81.8	56.6	32	72.4
b) 2-in (51 mm) thick (plate F) -			
<u>Supplied by Mill</u>			
80.6	54.4	30 (8 in.)	---
<u>ASTM Requirements</u>			
70 min.	50 min.	18 (8 in.) 21 (2 in.)	--- ---
<u>Measured on Plate</u>			
76.7	55.4	33	67.2
76.5	54.7	32	67.9
76.5	55.1	33	67.4
Average:			
76.5	55.1	32.7	67.5

Conversion Factor: 1 in = 25.4 mm; 1 ksi = 6.895 MPa

Table 9.

Room temperature tensile properties of A514  
steel plate. Longitudinal direction.

<u>Tensile Strength ksi</u>	<u>Yield Strength ksi</u>	<u>Elong. (2-in G.L.) Percent</u>	<u>Red. in Area Percent</u>
a) 1-in (25 mm) thick A514, grade B (plate A) -			
<u>Supplied by Mill</u>			
119	107	20	63
<u>ASTM Requirements</u>			
110-130	100	18 min.	50 min.
<u>Measured on Plate</u>			
117.7	107.3	19	66.8
117.9	107.3	19	65.0
112.8	102.8	20	64.2
Average:			
116.1	105.8	19.3	65.3
b) 2-in (51 mm) thick A514-85A (plate B) -			
<u>Supplied by Mill</u>			
127.9	111.7	20	53
129.4	115.4	20	57
Average:			
128.7	113.6	20	55
<u>ASTM Requirements</u>			
110-130	100 Min.	18 Min.	50 Min.
<u>Measured on Plate</u>			
136.7	126.7	21	67.3
138.1	128.2	21	66.1
136.9	126.8	21	67.8
Average:			
137.2	127.2	21	67.1

Conversion Factor: 1 in = 25.4 mm; 1 ksi = 6.895 MPa

Table 10.

Room temperature tensile properties of A852-85 steel plate. Longitudinal direction.

<u>Tensile Strength</u> ksi	<u>Yield Strength</u> ksi	<u>Elong. (2-in G.L.)</u> Percent	<u>Red. in Area</u> Percent
a) 1-in (25 mm) thick (plate H) -			
<u>Supplied by Mill</u>			
94.6	82.0	34.0	-
94.1	81.5	32.0	-
<u>ASTM Requirements</u>			
NOT SPECIFIED			
<u>Measured on Plate</u>			
92.5	78.3	27.0	73.0
93.5	78.4	27.0	73.1
92.9	78.1	28.0	74.4
Average:			
93.0	78.3	27.3	73.5
b) 2-in (51 mm) thick (plate L) -			
<u>Supplied by Mill</u>			
97.9	80.4	21.0	-
101.8	80.2	20.0	-
<u>ASTM Requirements (Transverse)</u>			
NOT SPECIFIED			
<u>Measured on Plate</u>			
100.3	82.9	26.0	70.0
100.6	83.3	25.0	69.4
100.3	82.6	26.0	69.4
Average:			
100.4	82.9	25.7	69.6
c) 3-in (76 mm) thick (plate M) -			
<u>Supplied by Mill</u>			
101.7	84.1	20.0	-
105.9	88.9	22.0	-
<u>ASTM Requirements (Transverse)</u>			
NOT SPECIFIED			
<u>Measured on Plate</u>			
93.4	76.3	27.0	71.7
95.5	79.1	26.0	71.8
94.6	75.1	27.0	70.0
Average:			
94.5	76.8	26.7	71.2

Conversion Factor: 1 in = 25.4 mm; 1 ksi = 6.895 MPa

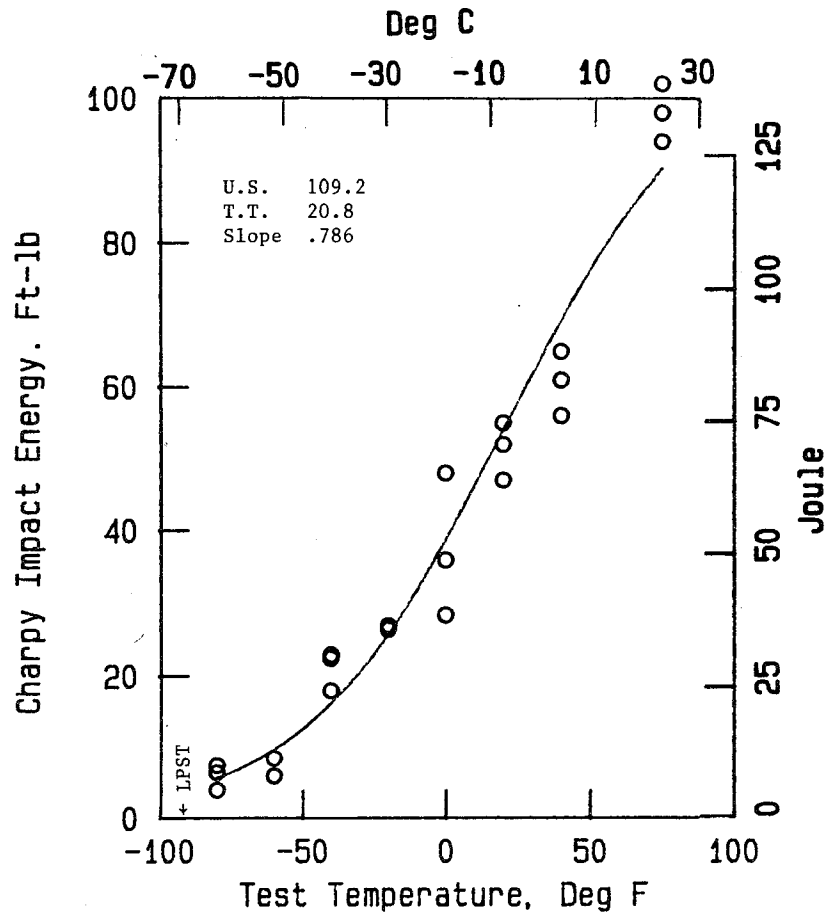


Figure 3. Charpy impact energy vs test temperature (1-in (25 mm) thick A572-82, grade 50, plate C).

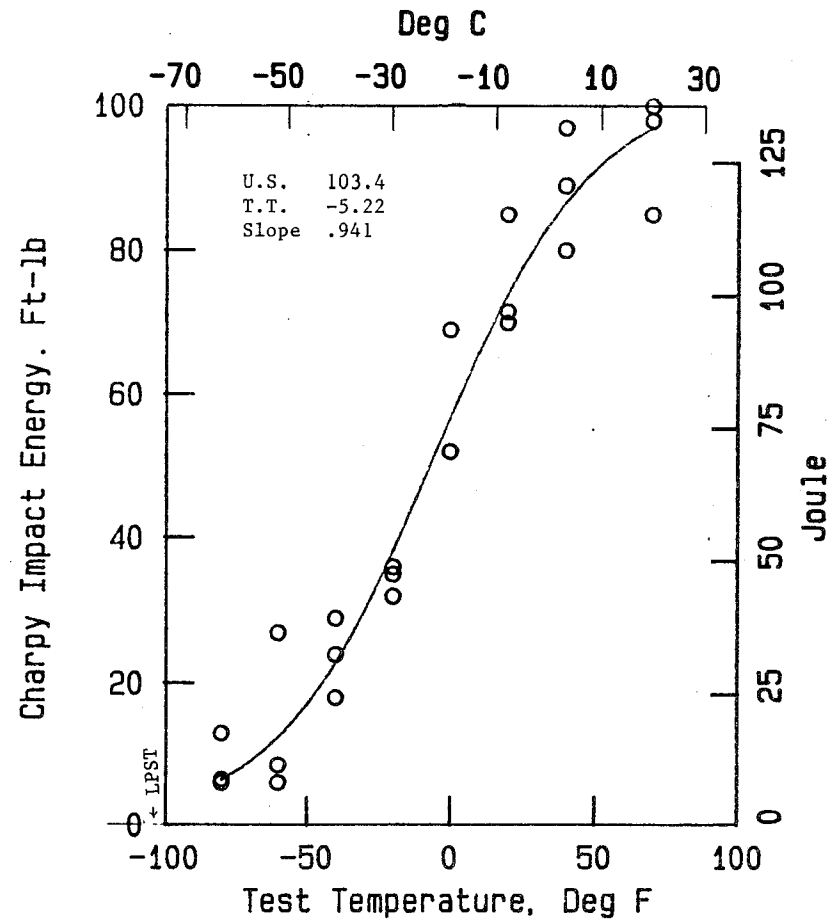


Figure 4. Charpy impact energy vs test temperature (2-in (51 mm) thick A572-82, grade 50, plate D).



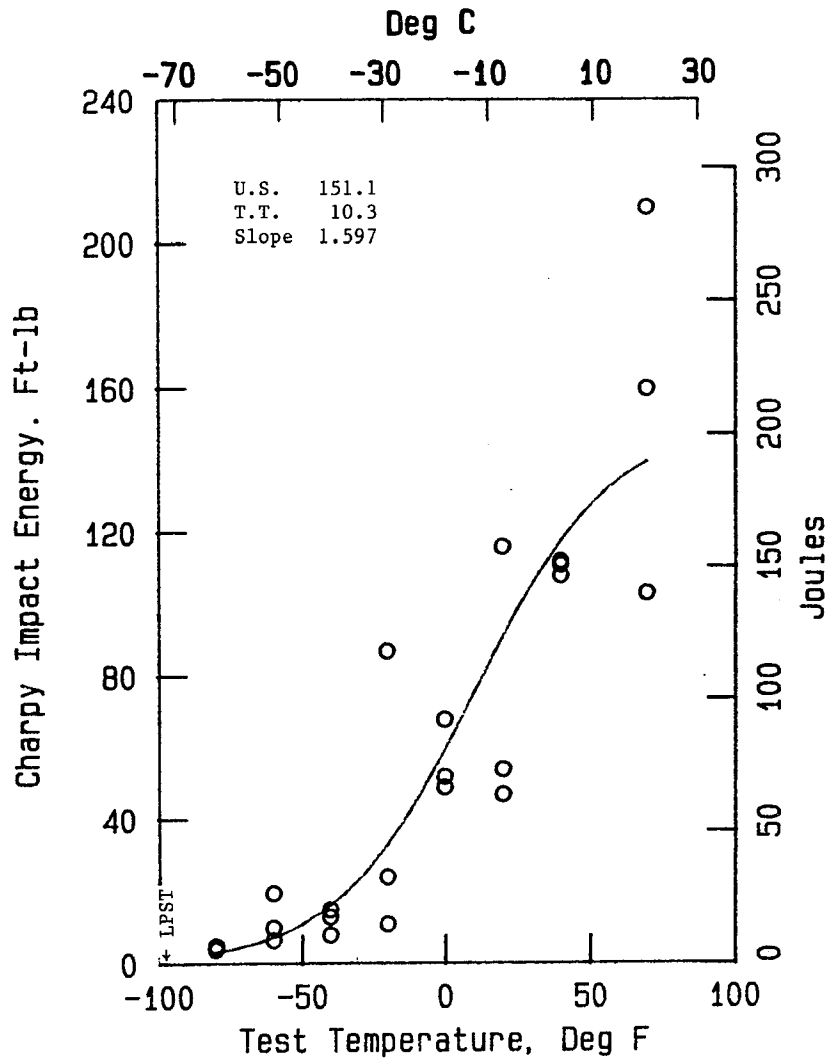


Figure 5. Charpy impact energy vs test temperature (1-in (25 mm) thick A588-82, grade B, plate E).

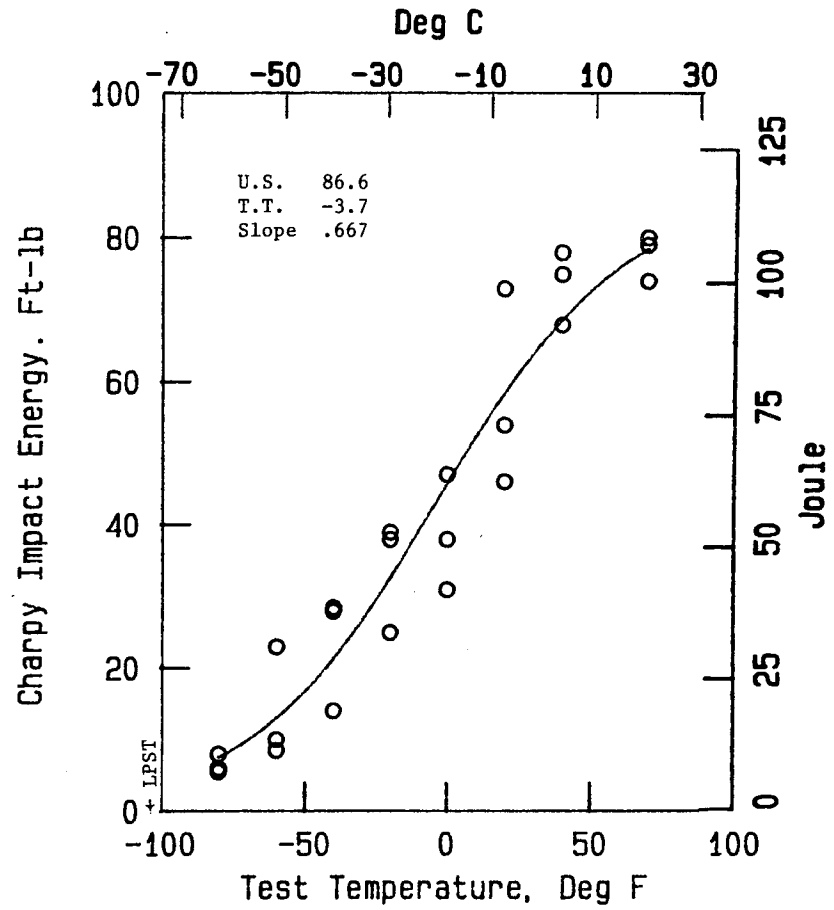


Figure 6. Charpy impact energy vs test temperature (2-in (51 mm) thick A588-82, grade B, plate F).

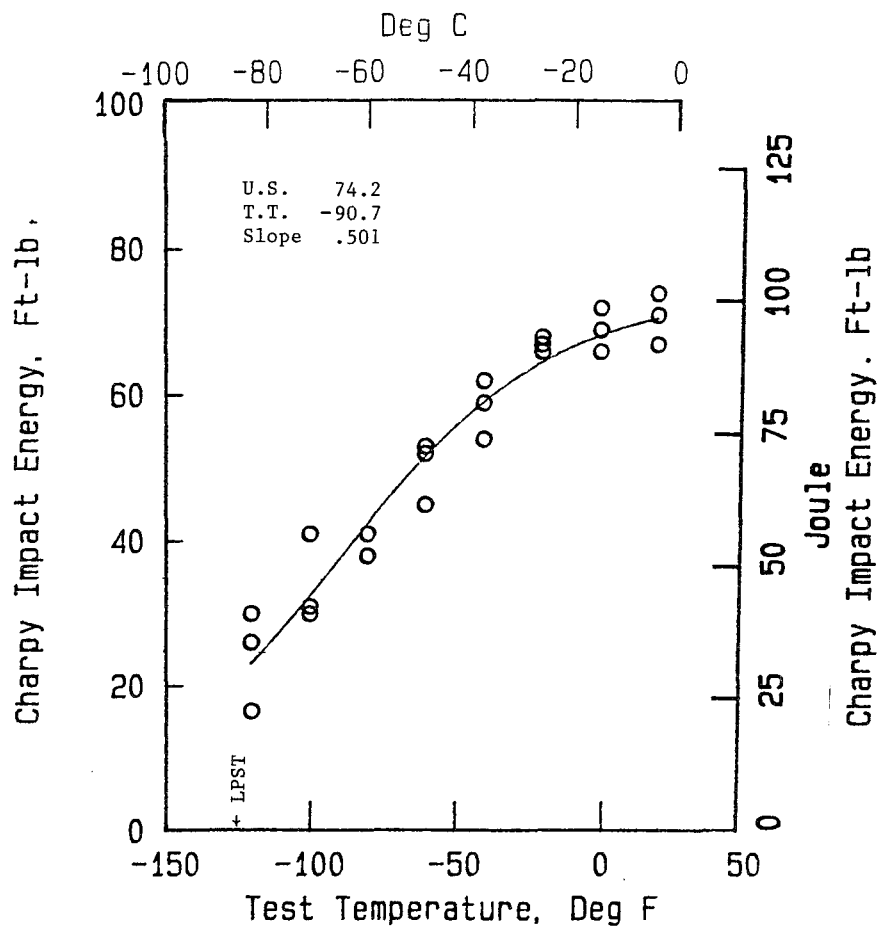


Figure 7. Charpy impact energy vs test temperature (1-in (25 mm) thick A514, grade B, plate A).

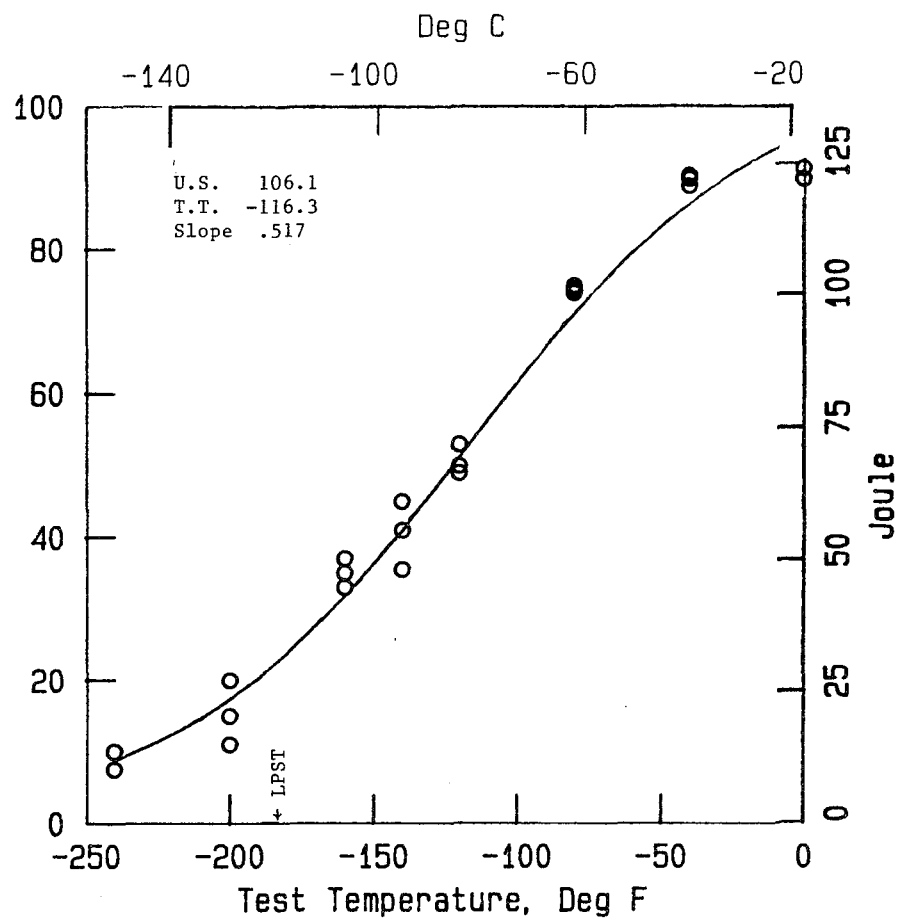


Figure 8. Charpy impact energy vs test temperature (2-in (51 mm) thick A514-85A, plate B).

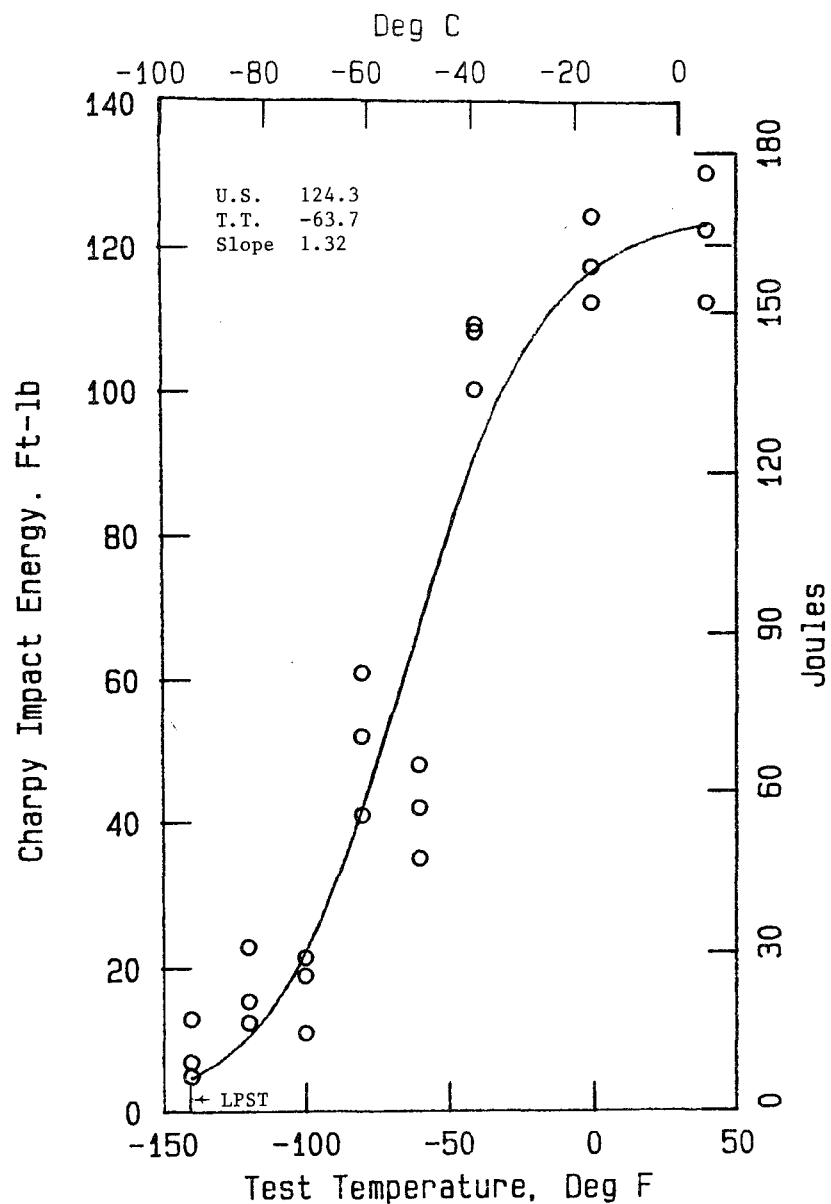


Figure 9. Charpy impact energy vs test temperature (1-in (25 mm) thick A852-85, plate H).

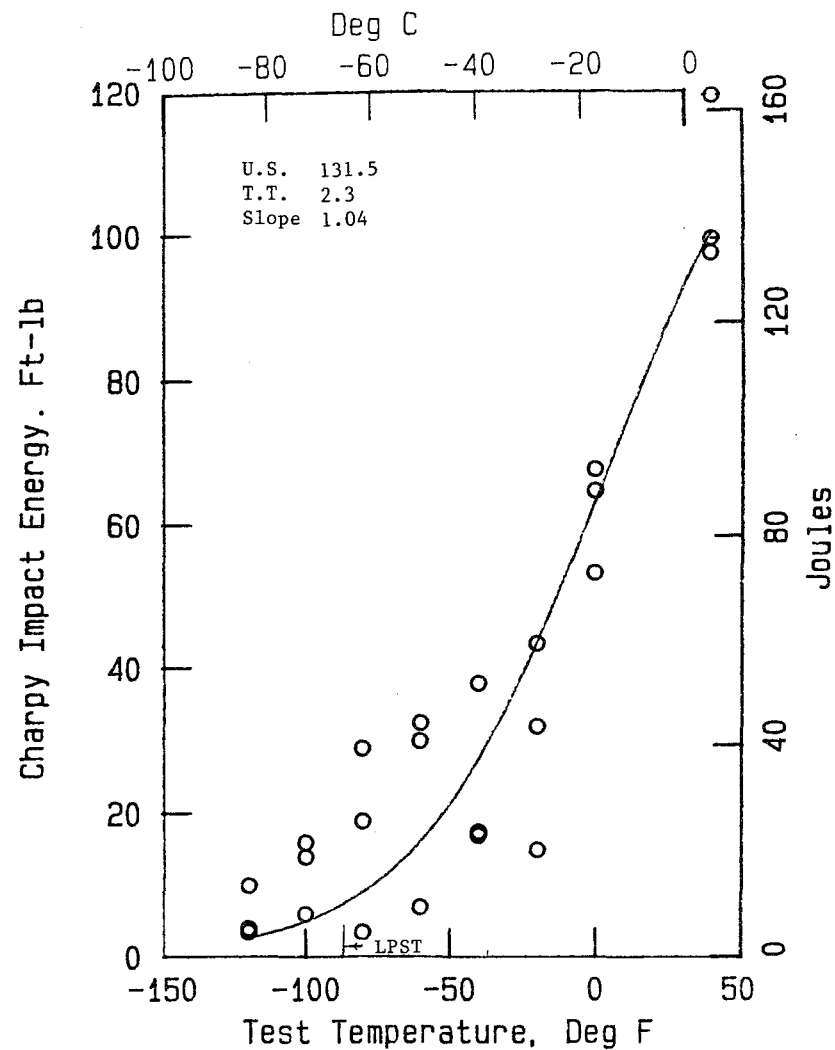


Figure 10. Charpy impact energy vs test temperature (2-in (51 mm) thick A852-85, plate L).

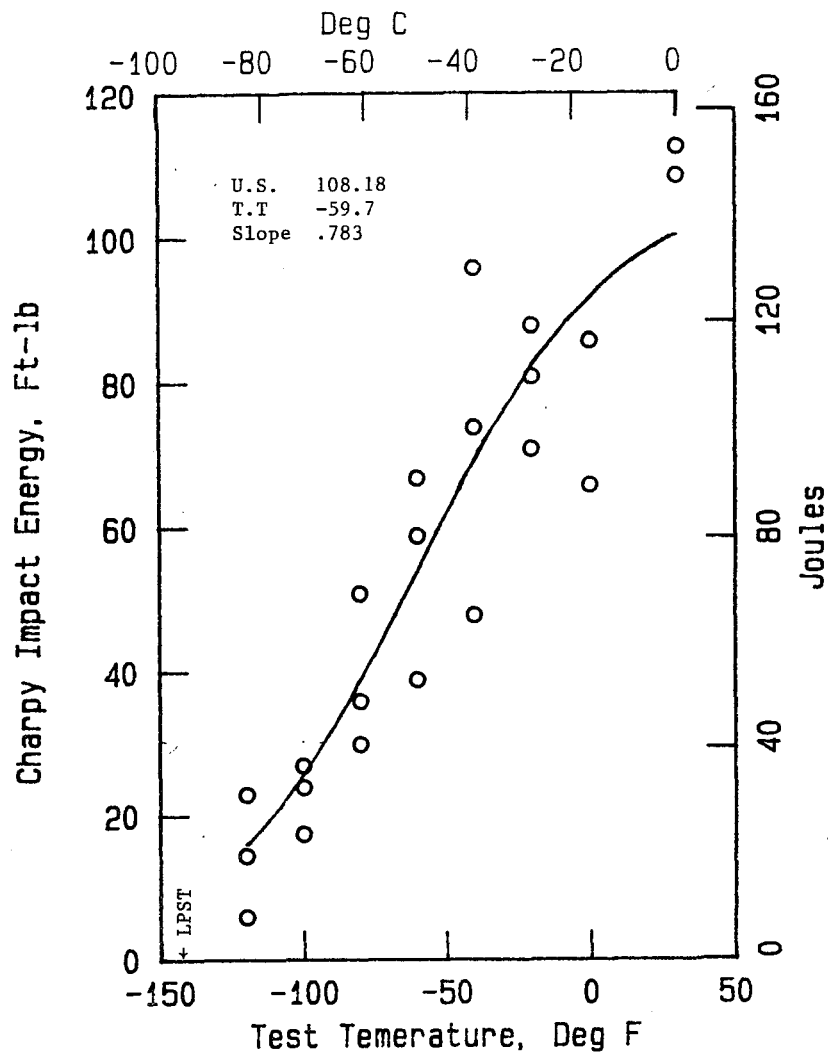
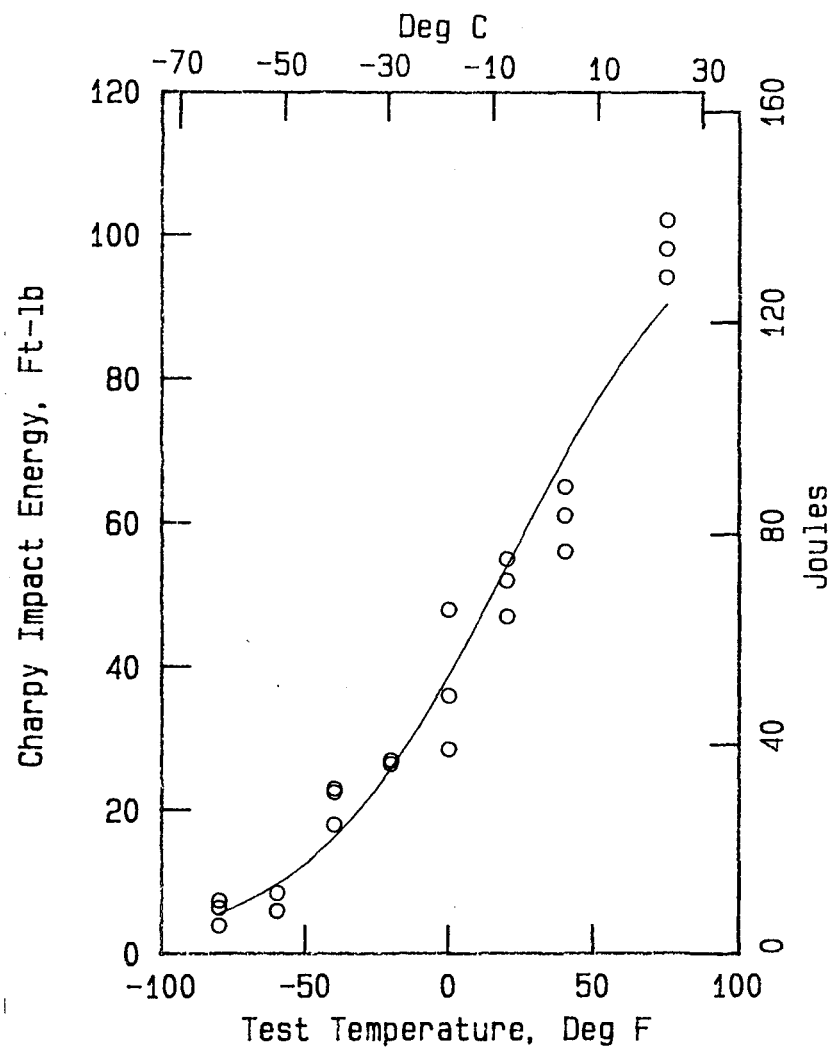


Figure 11. Charpy impact energy vs test temperature (3-in (76 mm) thick A852-85, plate M).



$$CVI = A (1 + \tanh (T - T_o)/B)$$

Upper Shelf = 2A

Transition Temperature =  $T_o$

Slope at Transition

Temperature =  $(1/2)A/B$

Figure 12. Hyperbolic tangent best-fit curve.

Six test temperatures were used for the three-point bend specimens of each test plate other than for the A852 steel where only five test temperatures were used; three specimens were tested at each temperature. An attempt was made to select the two temperatures at which valid  $K_{IC}$  values would be obtained. This was done by running the CVI specimens first, and using these data to estimate the highest temperature at which valid  $K_{IC}$  data should be obtained. Two sets of data were collected at test temperatures lower than the latter, and the rest above.

The CTOD test data are plotted in figures 13 to 21.

#### Comparison of CVI and CTOD data scatter

It is apparent that the scatter in the CTOD vs test temperature curves is greater than that in the CVI vs test temperature curves. An example of this is seen by comparing the CVI and CTOD plots for the 1-in (25 mm) thick plate of A572 (plate C), figures 3 and 13. It was thought that this might be a result of the fact that the CVI specimens were all taken out of a small volume of the plate while the CTOD specimens sampled a much larger volume. Indeed, an examination of the locations and values of the CTOD specimens within plate C, figure 22, suggested that the values did not scatter randomly with location but rather that some parts of the plate appeared to be tougher than other parts. In order to determine whether or not the plate actually did show this kind of behavior, CVI specimens were cut out of tested CTOD specimens at the quarter-thickness position so that the notches for the former were less than 2 1/2-in (64 mm) from the notch of the latter. The CTOD specimens selected for this purpose were those tested at -80°F (-62°C) since these showed a large amount of scatter.

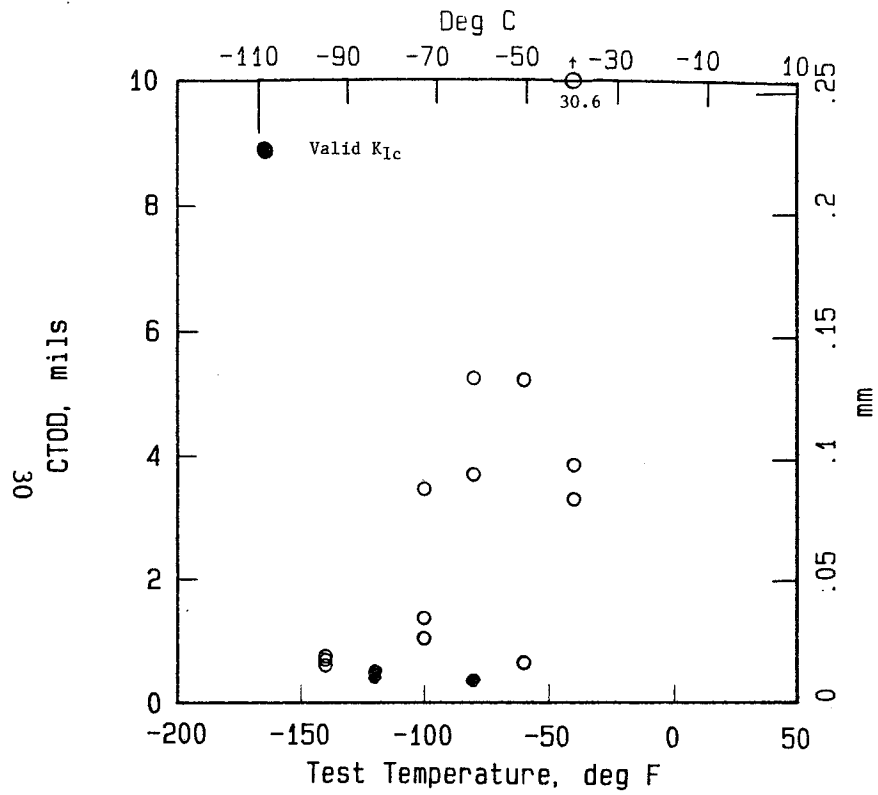


Figure 13. CTOD vs test temperature. (1-in (25 mm) thick A572-82, grade 50, plate C).

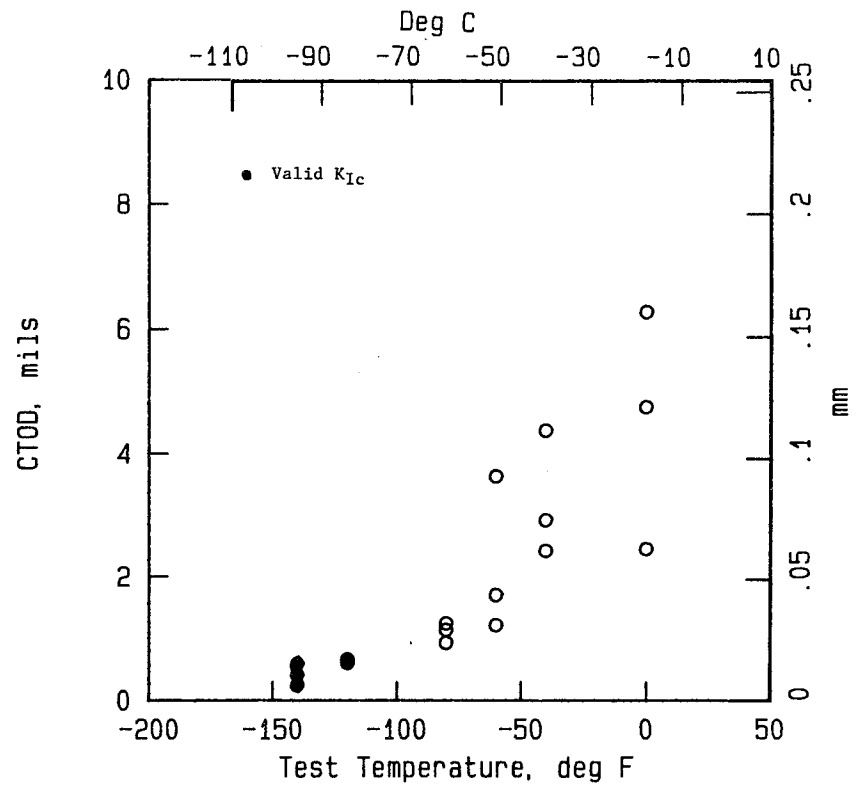


Figure 14. CTOD vs test temperature. (2-in (51 mm) thick A572-82, grade 50, plate D).

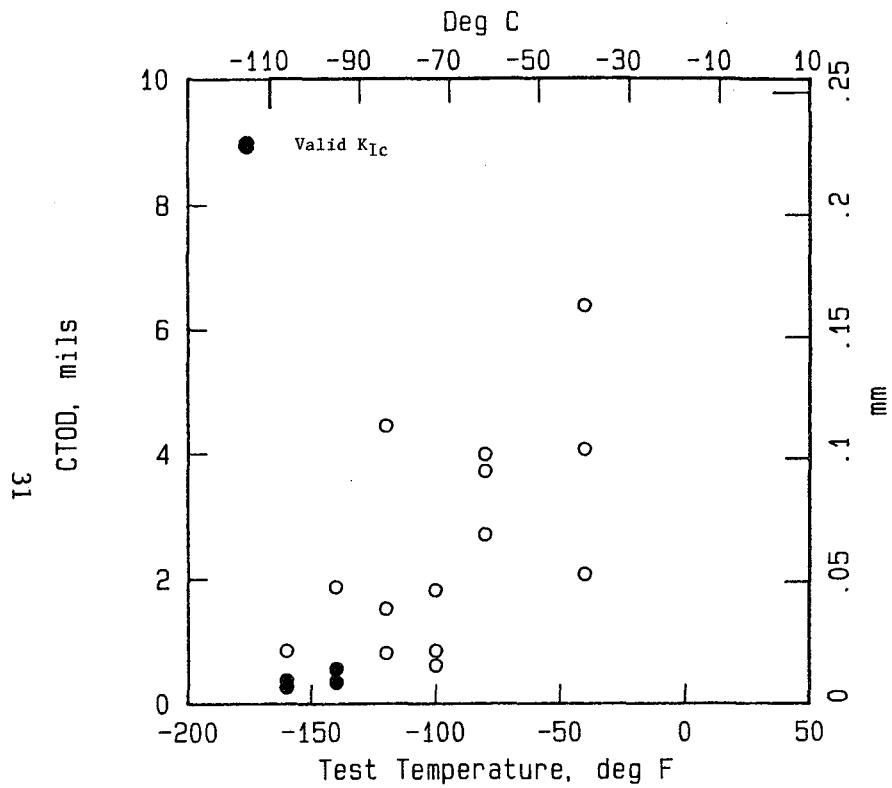


Figure 15. CTOD vs test temperature.  
 (1-in (25 mm) thick A588-82, grade B, plate E).

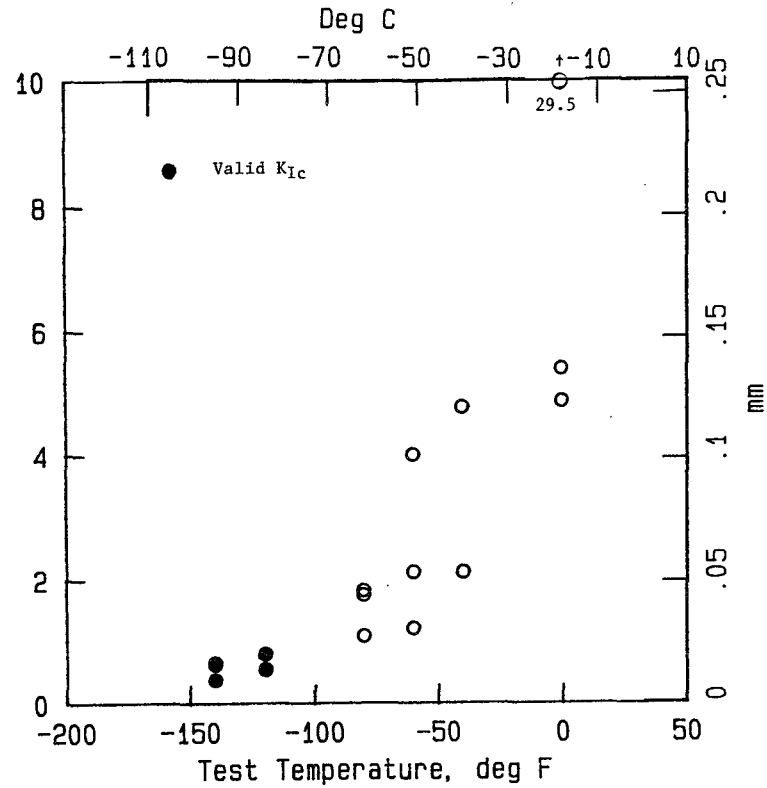


Figure 16. CTOD vs test temperature.  
 (2-in (51 mm) thick A588-82, grade B, plate F).

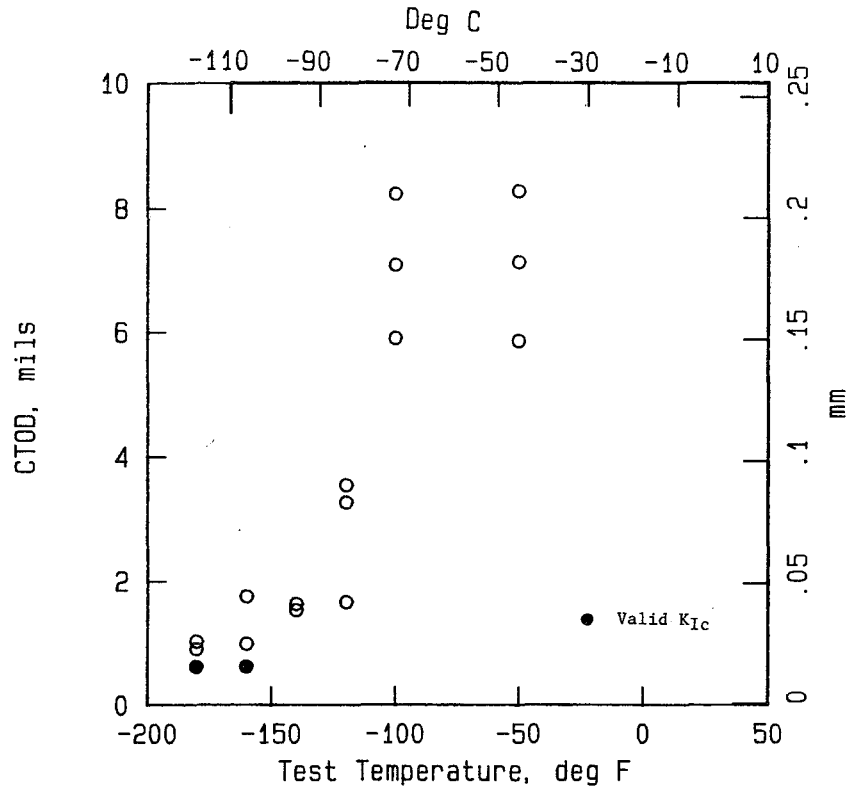


Figure 17. CTOD vs test temperature.  
(1-in (25 mm) thick A514, grade B, plate A).

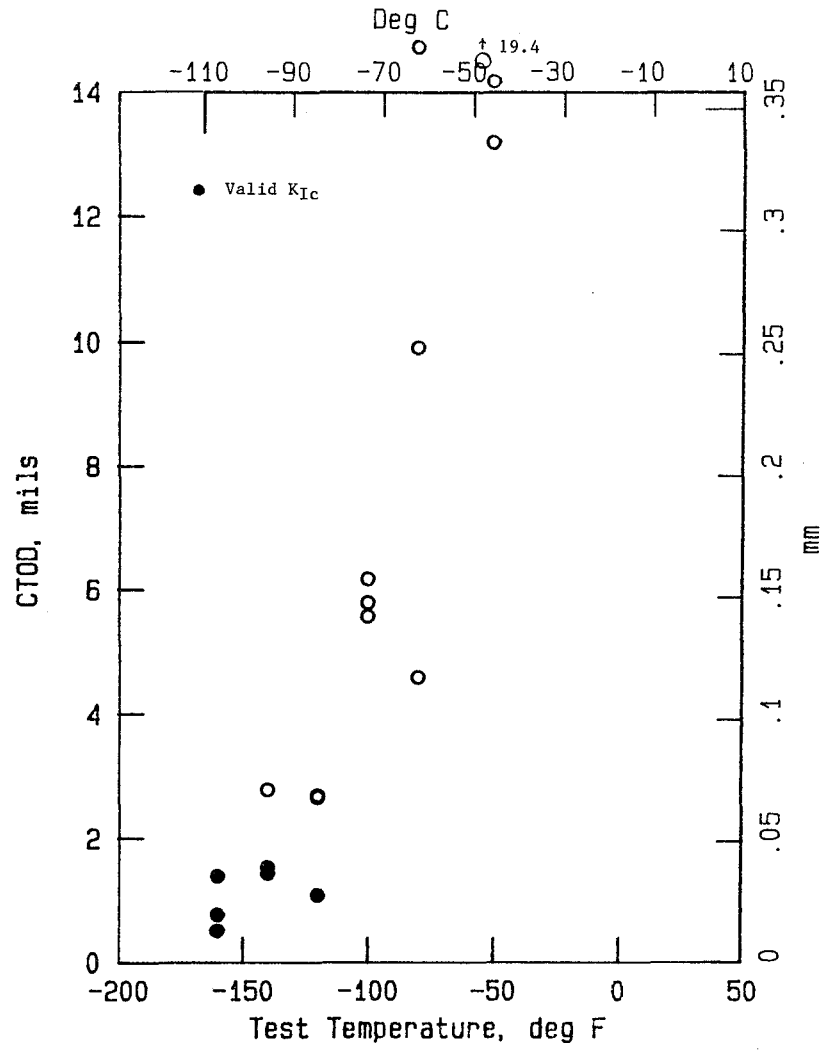


Figure 18. CTOD vs test temperature.  
(2-in (51 mm) thick A514-85A, plate B).



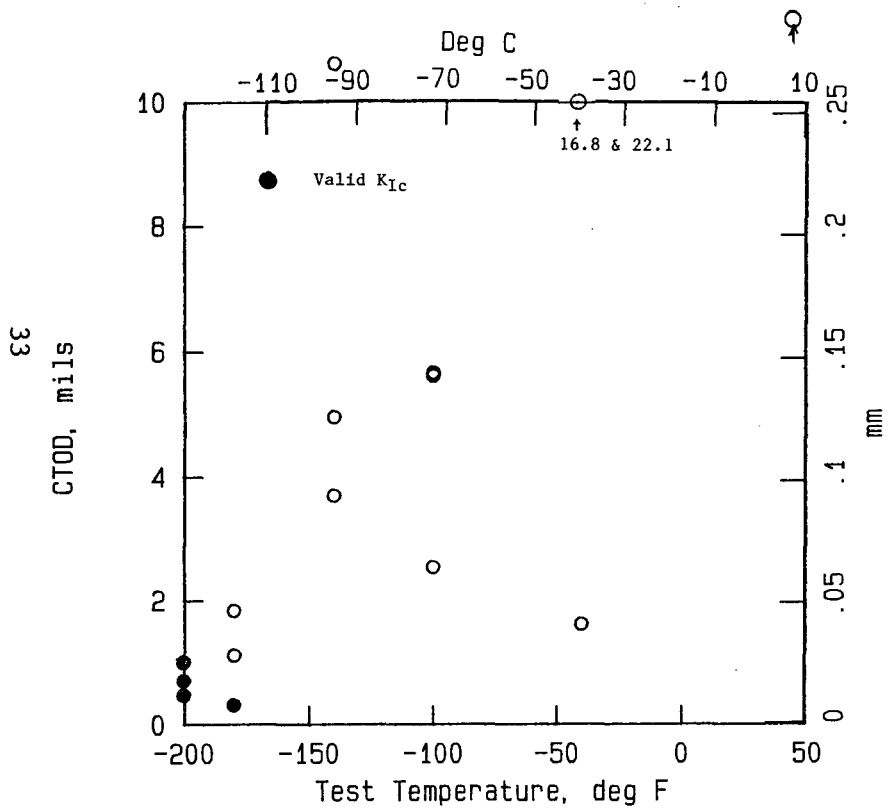


Figure 19. CTOD vs test temperature.  
(1-in (25 mm) thick A852-85, plate H).

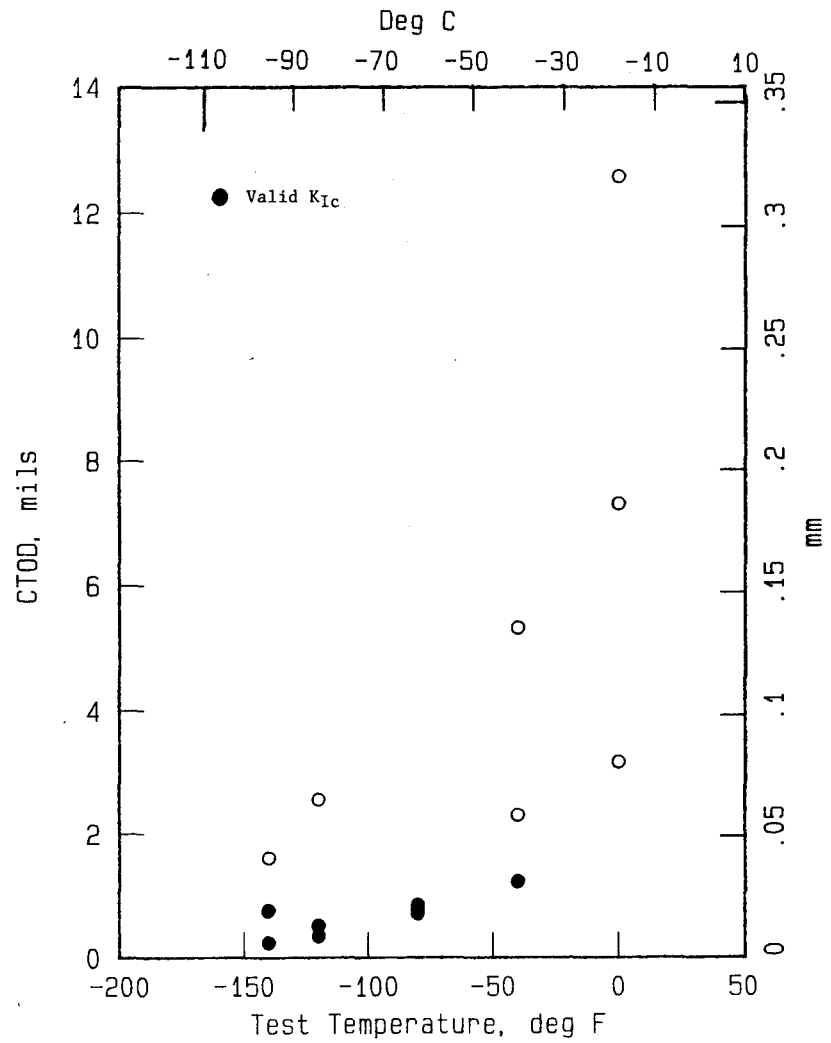


Figure 20. CTOD vs test temperature.  
(2-in (51 mm) thick A852-85, plate L).

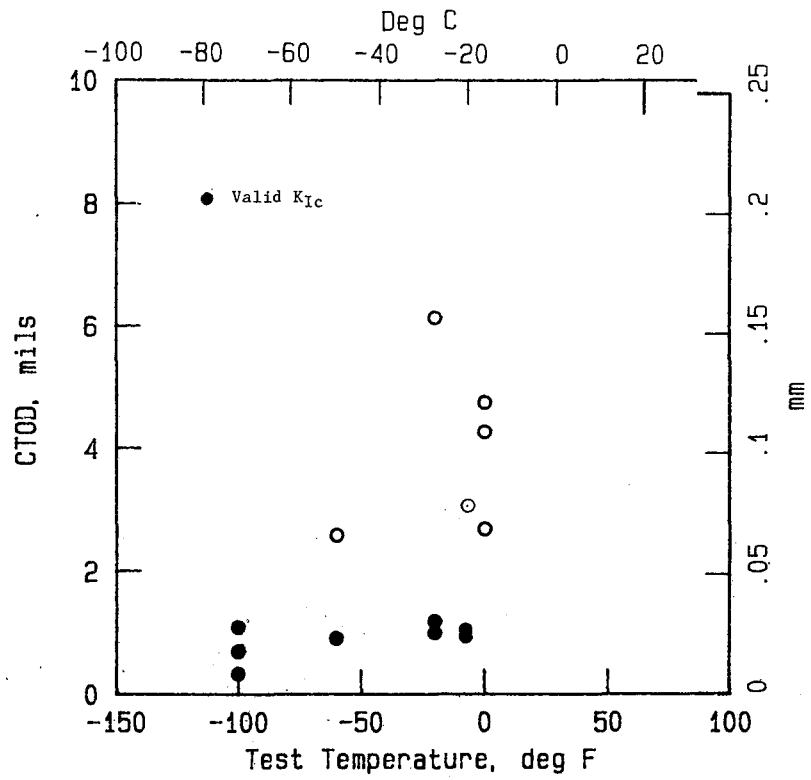


Figure 21. CTOD vs test temperature.  
(3-in (76 mm) thick A852-85, plate M).

		L	S	M	H	
	-100	1.13	-140 0.67	-40 4.02	-40 30.75	
		L	S	S	S	
	-80	0.35	-120 0.55	-120 0.53	-120 0.45	
		L	L	S	L	
	-60	0.72	-100 1.48	-140 0.76	-60 0.70	
		C N	M	H	L	
			-80 3.88	-100 3.64	-40 3.46	
			H	H	S	
			-60 5.40	-80 5.25	-140 0.82	

R D  
↔

Figure 22. Test temperature, CTOD value in mils, and letter indication low (L), middle (M) or high (H) values of CTOD. Letter "S" indicates lower shelf values.

(1-in (25 mm) thick A572-82, grade 50, plate C)

Three CTOD specimens, identified as 13, 7 and 2, had been tested at  $-80^{\circ}\text{F}$  ( $-62^{\circ}\text{C}$ ) and had CTOD values of 5.25, 3.70 and 0.35 mils (0.133, .094 and .0089 mm), respectively, where the latter was a valid  $K_{Ic}$  test. The CVI results of 16 specimens cut from specimens 13 and from 2, i.e., the CTOD specimens with the highest and lowest toughness, are compared in figure 23. It is apparent that although the CTOD value differed by a factor of more than 10 to 1, the CVI curves were almost identical. The data collected on the specimens cut from CTOD bars are compared with the original CVI data collected on the plate in figure 24; all three of these CVI-Temperature curves are similar. The difference in scatter between the two kinds of specimens is discussed in section 3.

#### 2.4 Data Analysis

##### CVI data (definition of Lowest Permissible Service Temperature [LPST])

The present AASHTO CVI requirements for the four steels being studied on this project are given in table 2. To evaluate the performance of the steels in the most straight-forward way, it would be necessary to have plates that just pass these requirements; viz., the plates should have exactly 25 ft-lb (34 J) at  $+40^{\circ}\text{F}$  ( $+4^{\circ}\text{C}$ ) for A572-50 and A588. If this were possible, 1-sec loading time fracture toughness could be measured on the plates at, and above the LAST (Lowest Anticipated Service Temperature), to determine what fracture toughness values are implied by these AASHTO requirements. Of course, it is generally not possible to obtain plates with these exact properties so that some method must be found to relate the properties actually measured on plates to the Guide Specification requirements. A method for doing this was introduced on an earlier FHWA project.<sup>[1]</sup> The method requires the use of a new parameter, the Lowest Permissible

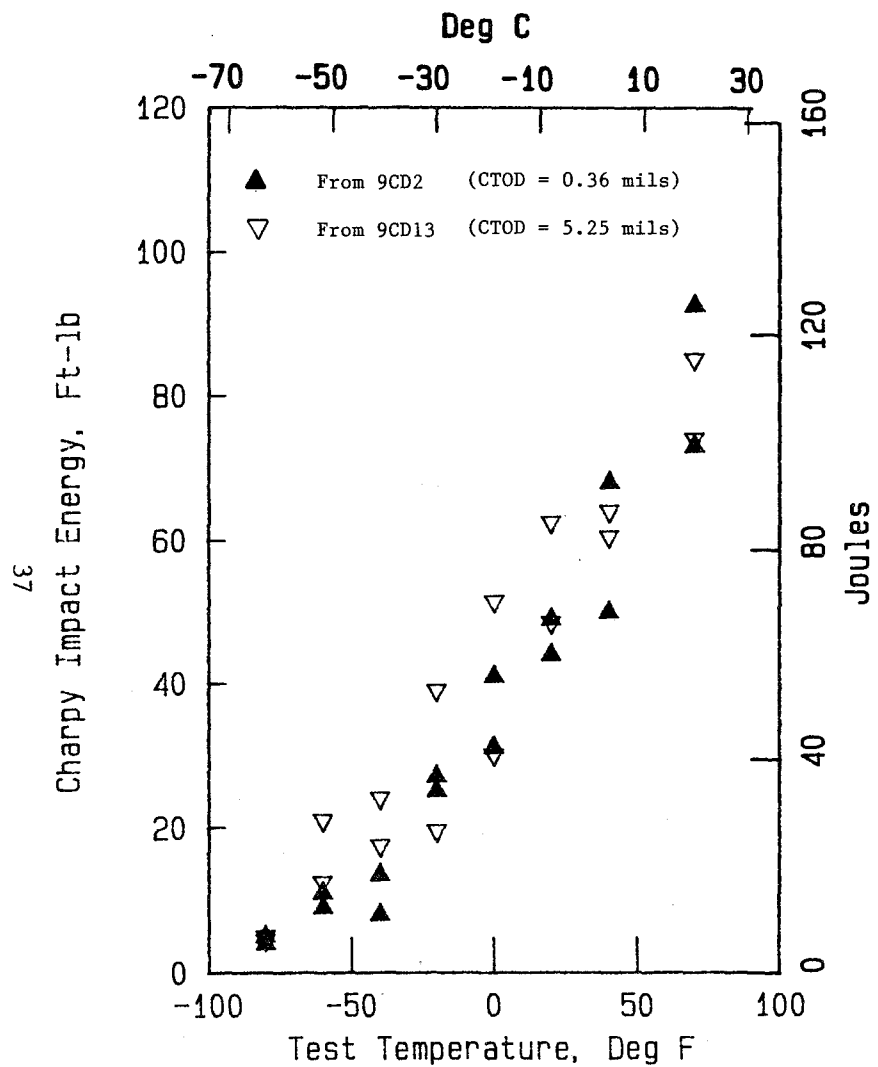


Figure 23. Comparison of CVI values obtained on CTOD specimens 9CD2 and 9CD13 (1-in (25 mm) thick A572-82, grade 50, steel plate, plate C).

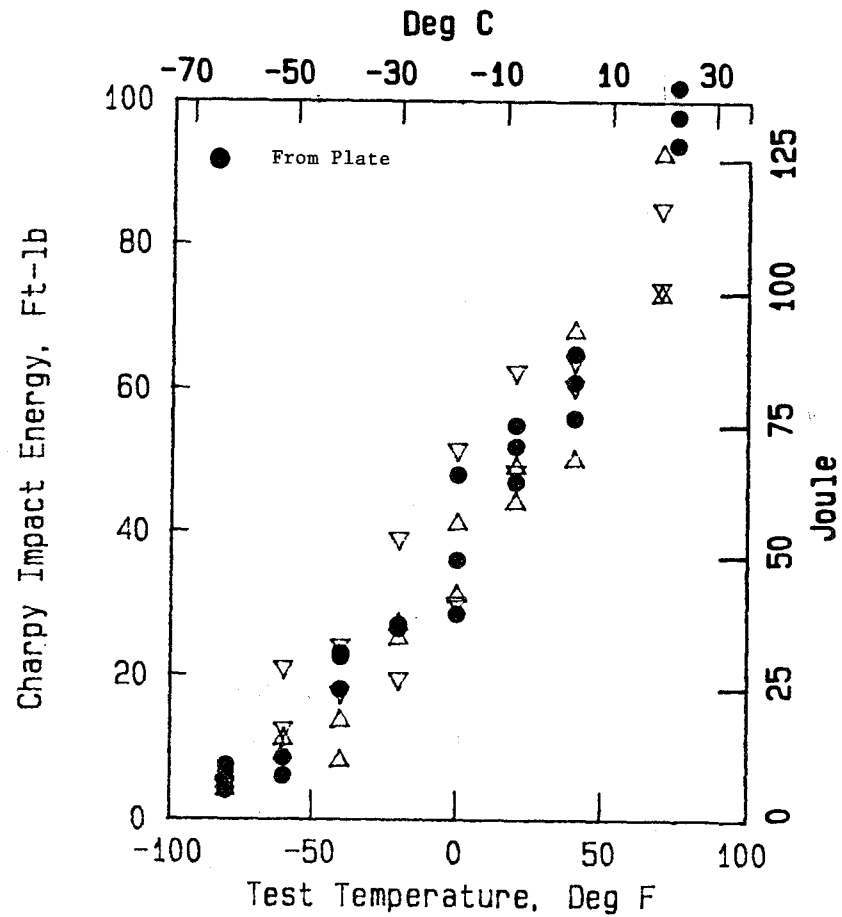


Figure 24. Comparison of data shown in figure 23 with CVI values originally obtained on plate.

Service Temperature, or LPST. Finding LPST is a two-step procedure: The first step consists of measuring the Charpy toughness on the test plate as a function of test temperature in order to find the temperature at which the plate has the toughness shown in table 2. For the ASTM A572-50 plate shown in figure 25, this required CVI toughness is 25 ft-lb (34 J). The temperature at which the 25 ft-lb (34 J) reference toughness occurs in the test plate (-22°F [-30°C] in this case) is used to calculate LPST in a second step. Again using Zone 2 as an example, it has a LAST of -30°F (-34°C) and for this LAST, a CVI reference toughness of 25 ft-lb (34 J) must be measured at +40°F (+4°C) i.e. there is a 70°F (39°C) temperature difference between the LAST and the temperature at which 25 ft-lb (34 J) must be measured. To find the LPST this temperature difference of 70°F (39°C) is subtracted from the temperature at which the test plate has a value of 25 ft-lb (34 J). For the plates used in this project, the values of LPST are shown in table 11. The LPST is a property of the plate, while the LAST is the lowest temperature expected within a particular zone.

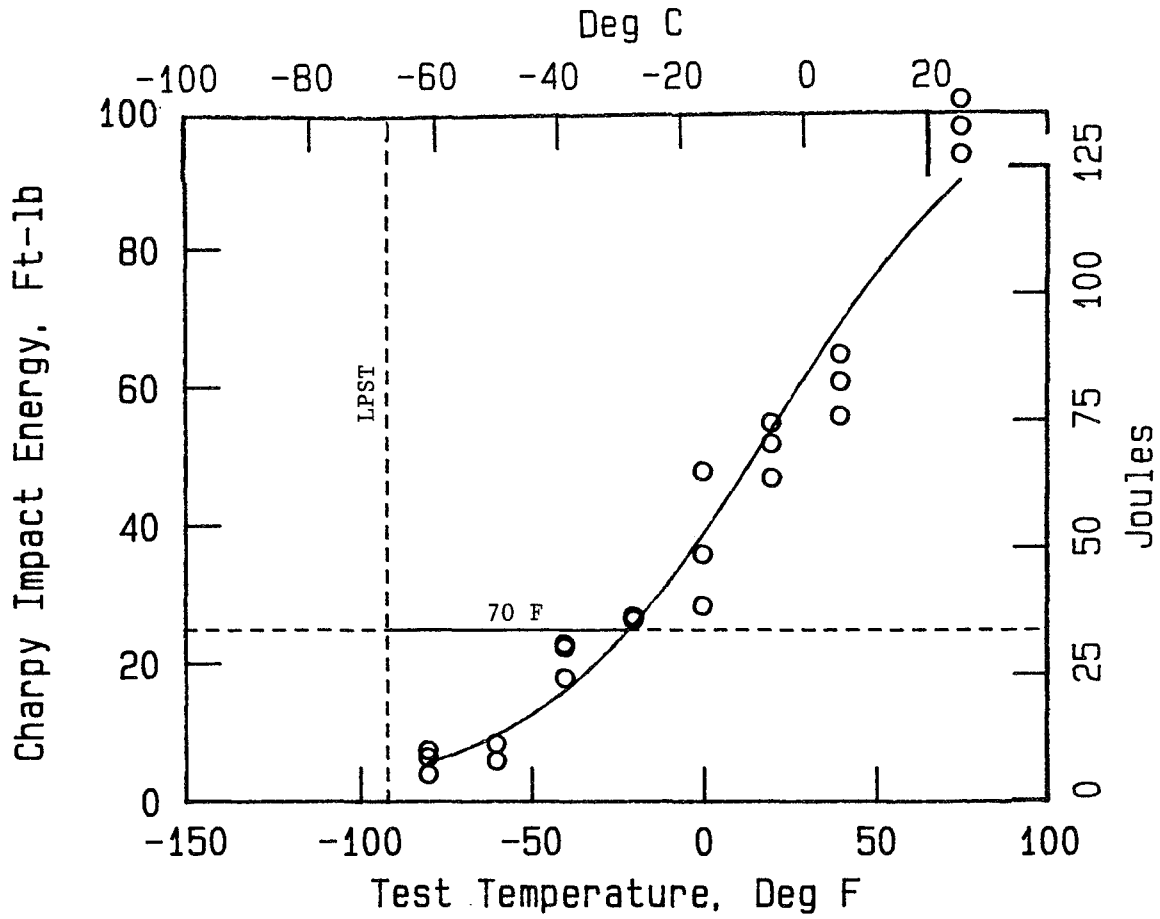
#### Comparison of CVI and CTOD toughness

##### Procedure for Converting CVI to K

In order to compare CVI and CTOD toughness, it is necessary that both of these parameters have the same units. CVI can be converted to K units by means of the Barsom-Rolfe (B-R) correlation so that K units were chosen for making the comparison. The Barsom-Rolfe relationship:

$$K_{Ic(d)} = \sqrt{5ECVI}, \quad (3)$$

where  $K_{Ic(d)}$  = dynamic toughness



-----  
 AASHTO, ZONE 2:

LAST = -30°F (-34°C)

25 ft-lb (34 J) @ 40°F (4°C) for service  
 at -30°F (-34°C)

-----

Figure 25. Definition of LPST.

Table 11.

LPST for test plates.

<u>Plate - ASTM Designation</u>	<u>Plate No.</u>	<u>Thickness</u>	<u>LPST</u>
A572-82, grade 50	C	1 in (25 mm)	-92°F (-69°C)
	D	2 in (51 mm)	-102°F (-74°C)
A588-82, grade B	E	1 in (25 mm)	-98°F (-72°C)
	F	2 in (51 mm)	-107°F (-77°C)
A514, grade B	A	1 in (25 mm)	-127°F (-88°C)
A514-85A, grade B	B	2 in (51 mm)	-185°F (-121°C)
A852-85	H	1 in (25 mm)	-142°F (-97°C)
	L	2 in (51 mm)	-87°F (-66°C)
	M	3 in (76 mm)	-143°F (-98°C)



is meant to apply only into the lower end of the transition range. Nevertheless, it can be applied formally to CVI values outside this range to facilitate comparison of CVI and  $K_c$  data. As will be shown in the following, the B-R correlation in this project was chosen to be limited not by the test temperature relative to the transition temperature, but by the ratio of  $K$  to  $\sigma_{yd}$ , where the latter is the dynamic yield strength. Since this establishes the maximum temperature over which  $K$  can be calculated from CTOD, it is also used for establishing the limit above which the Barsom-Rolfe correlation cannot be used. For the two non-heat-treated steels, A572 and A588, the  $K/\sigma_{yd}$  limit is about the same as the Barsom-Rolfe limit. For the two heat-treated steels, A852 and A514, the limit extends further into the transition range than it does in the B-R case.

Equation 3 would apply to  $K_{Ic}$  made at the same temperature as the CVI test only if the  $K_{Ic}$  test were made at the equivalent dynamic strain rate. The  $K_{Ic}$  of interest in this project is the value obtained with a 1-sec loading time. A key feature of the Barsom-Rolfe correlation is to account for the strain rate difference by means of a temperature shift. Thus, CVI measured at a temperature,  $T$ , would correlate with  $K_{Ic}$  (1-sec) measured at  $T - \Delta T$  where  $\Delta T$  is given by

$$\Delta T = 3/4(215 - 1.5 \sigma_{ys}) \quad (4)$$

where  $\sigma_{ys}$  is the steel's yield strength.

The CVI energy values plotted vs test temperature were all converted to  $K_c$  ( $K_{Ic}$ ) values, and these are plotted in figures 26 to 34. Hyperbolic tangent fits to the data are added to these curves, and it is these curves that will be compared with the  $K_c$  - Test Temperature data derived from 1-sec CTOD tests.

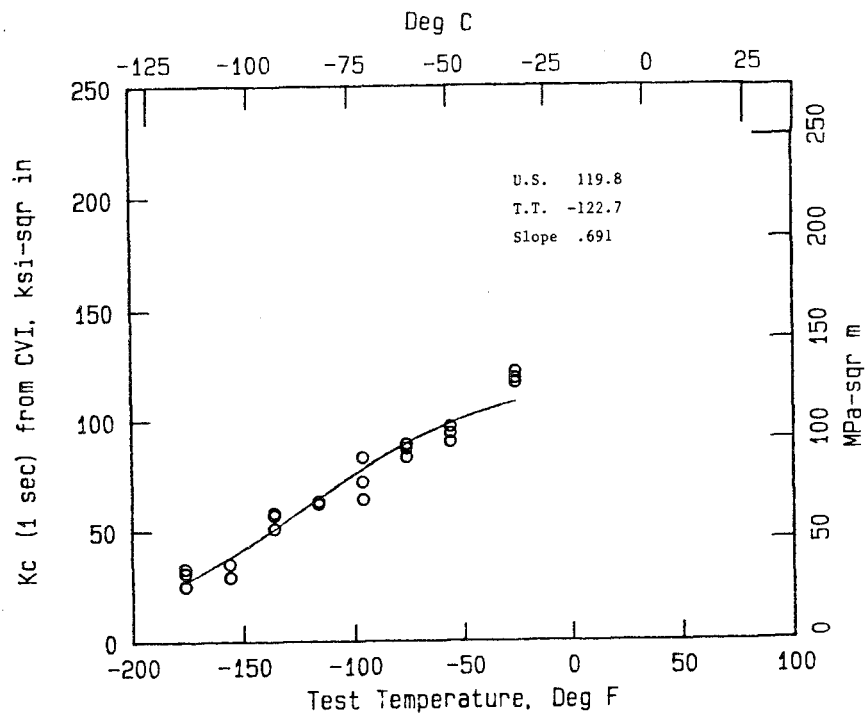


Figure 26.  $K_c$  ( $K_{Ic}$ ) calculated from CVI (Barsom-Rolfe correlation) and hyperbolic tangent fit to data (1-in (25 mm) thick A572-82, grade 50, plate C).

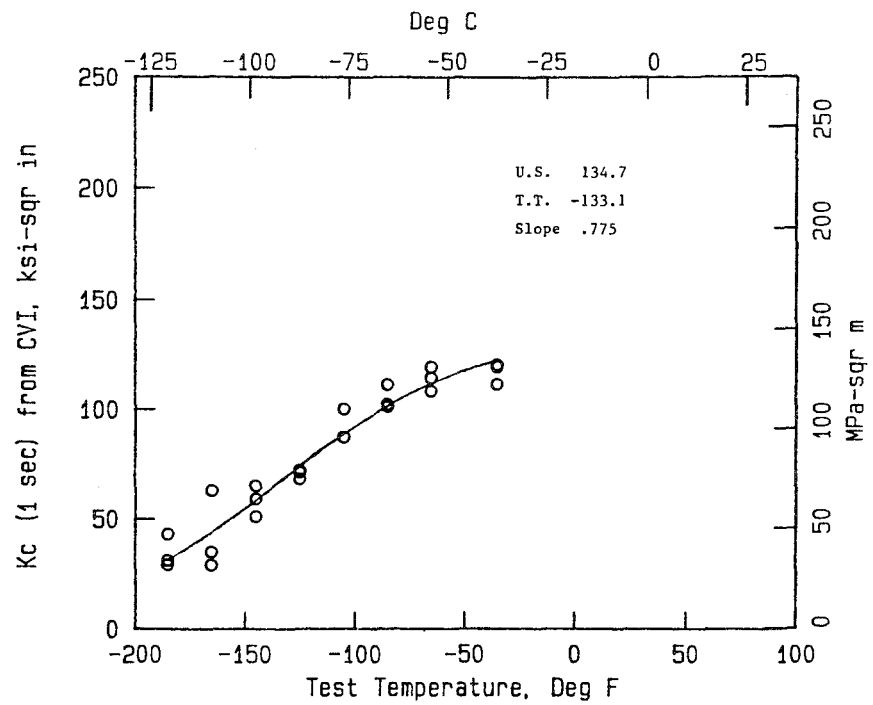


Figure 27.  $K_c$  ( $K_{Ic}$ ) calculated from CVI (Barsom-Rolfe correlation) and hyperbolic tangent fit to data (2-in (51 mm) thick A572-82, grade 50, plate D).

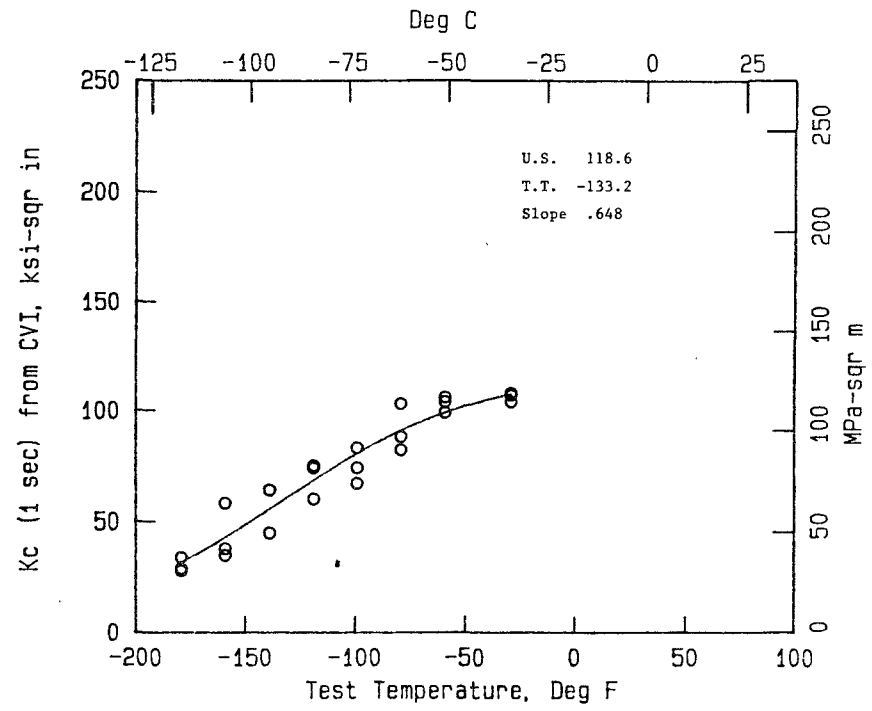
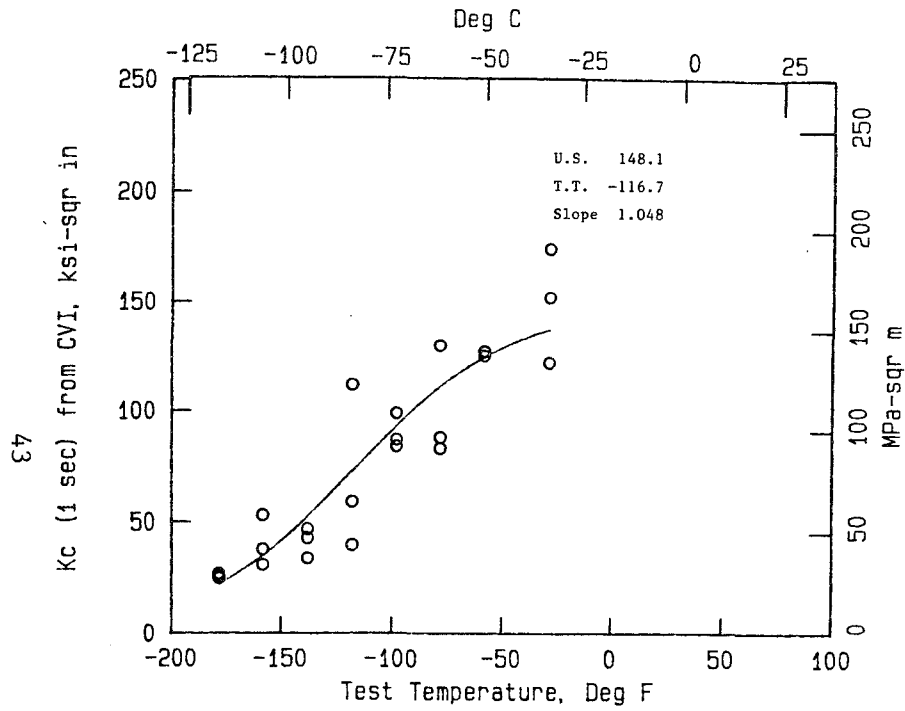


Figure 28.  $K_C$  ( $K_{Ic}$ ) calculated from CVI (Barsom-Rolfe correlation) and hyperbolic tangent fit to data (1-in (25 mm) thick A588-82, grade B, plate E).

Figure 29.  $K_C$  ( $K_{Ic}$ ) calculated from CVI (Barsom-Rolfe correlation) and hyperbolic tangent fit to data (2-in (51 mm) thick A588-82, grade B, plate F).

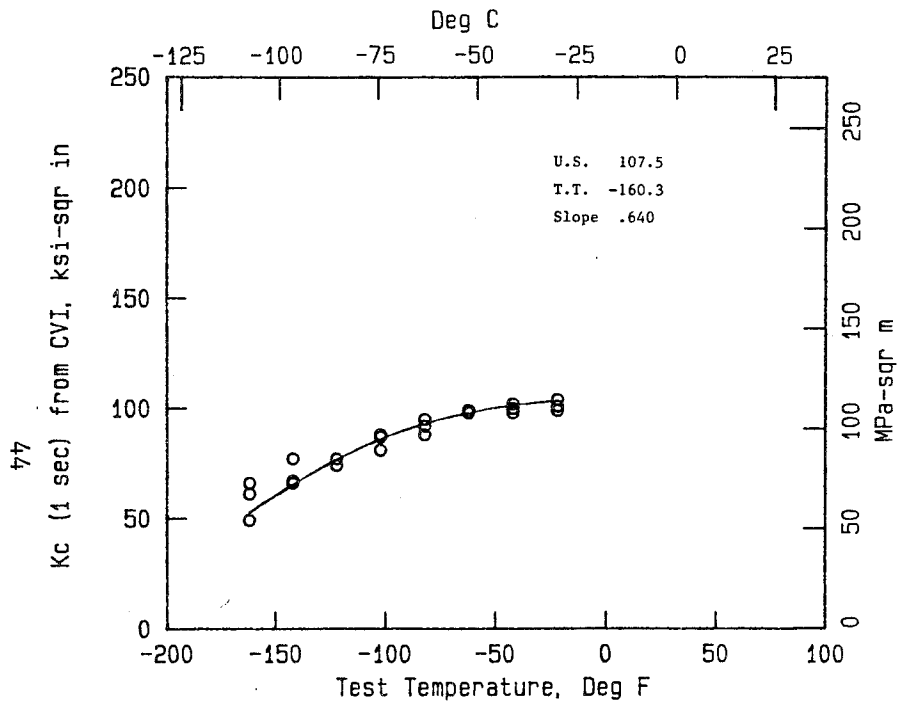


Figure 30.  $K_C$  ( $K_{Ic}$ ) calculated from CVI (Barsom-Rolfe correlation) and hyperbolic tangent fit to data (1-in (25 mm) thick A514, grade B, plate A).

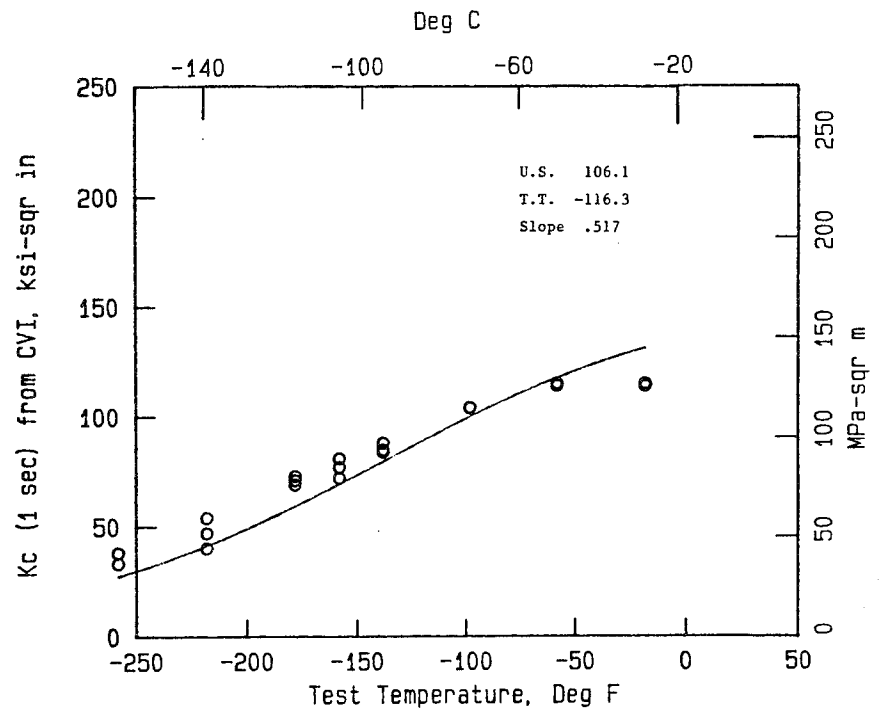


Figure 31.  $K_C$  ( $K_{Ic}$ ) calculated from CVI (Barsom-Rolfe correlation) and hyperbolic tangent fit to data (2-in (51 mm) thick A514-85A, plate B).

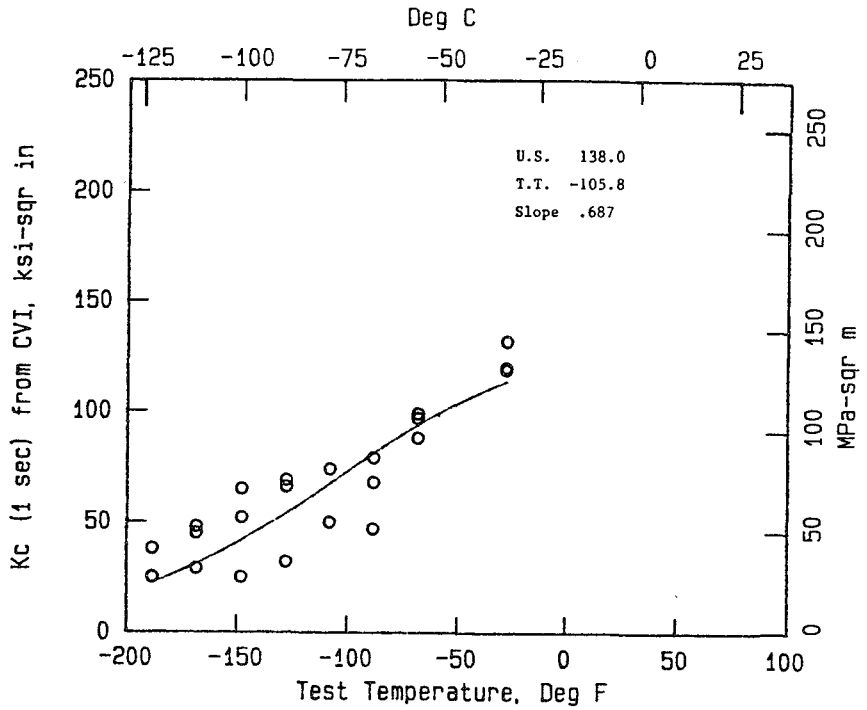
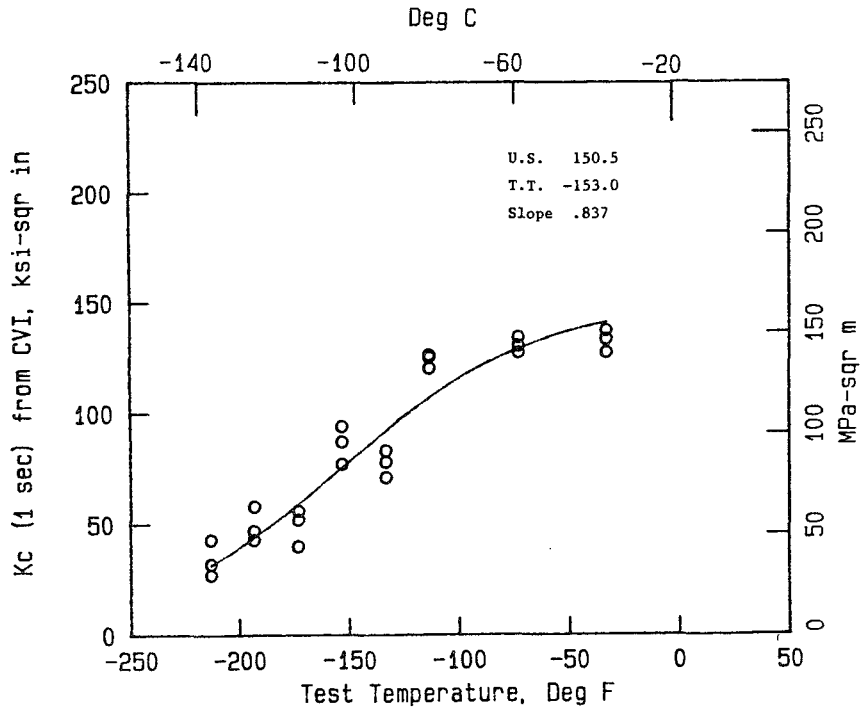


Figure 32.  $K_C$  ( $K_{IC}$ ) calculated from CVI (Barsom-Rolfe correlation) and hyperbolic tangent fit to data (1-in (25 mm) thick A852-85, plate H).

Figure 33.  $K_C$  ( $K_{IC}$ ) calculated from CVI (Barsom-Rolfe correlation) and hyperbolic tangent fit to data (2-in (51 mm) thick A852-85, plate L).

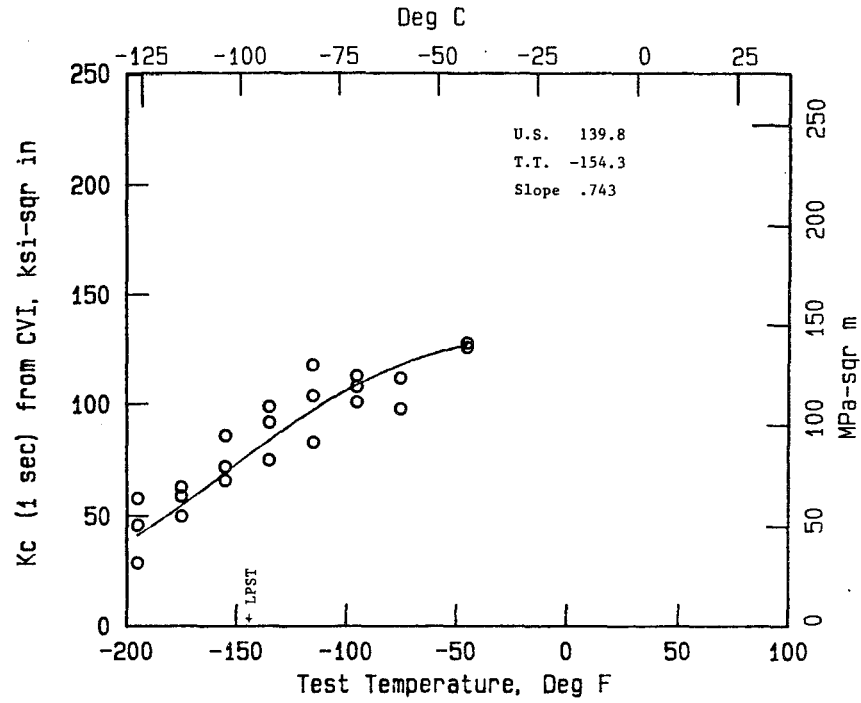


Figure 34.  $K_C$  ( $K_{IC}$ ) calculated from CVI (Barsom-Rolfe correlation) and hyperbolic tangent fit to data (3-in (76 mm) thick A852-85, plate M).

## Procedure for Converting CTOD to K

The CTOD test procedure embraces an unlimited range of possible fracture toughnesses. At the low toughness extreme, the test specimen behaves in a linear elastic plane strain manner as defined in ASTM E399, and the test yields a value of  $K_{Ic}$ . At the other extreme, the specimen may experience plastic deformation across the entire unbroken ligament (see figure 69, appendix A).

This program is concerned with fracture toughness evaluation at temperatures realistic for bridges. This involves fracture toughness levels that are too high to be measured under the plane strain restrictions stipulated in ASTM E399, but low enough that plasticity is confined to a limited region around the leading edge of the crack. Under these conditions, the specimen can be analyzed in a linear elastic manner with corrections made to account for small amounts of plastic flow; the method is referred to as a "small-scale-plasticity" analysis.

The plasticity correction procedure involves calculating the critical K (that is, the fracture toughness) with the appropriate linear elastic formula; but, instead of using the measured crack length,  $a$ , in the formula, the quantity  $a + r_y$  is used, where  $r_y$  is a formally calculated plastic zone size. This procedure has been around for many years and is incorporated in ASTM Standard E561, R-curve Testing. The small-scale-plasticity procedure was extended to use with CTOD specimens in this project. The plastic deformation,  $V_p$ , a quantity which has to be determined in the CTOD test, is used to evaluate  $r_y$ . The details are described in appendix B.

Linear elastic behavior is, of course, an idealization. As soon as a specimen is loaded, a plastic zone forms at the end of a sharp crack. As the plastic zone becomes larger, the linear elastic

characterization, even with a small-scale plasticity correction, becomes increasingly less accurate. ASTM Standard E561, which employs a plasticity correction, imposes the requirement that the uncracked ligament length  $W - a \geq (4/\pi)(K/\sigma_{ys})^2$ . This is much more lenient than ASTM Standard E399 in which a plasticity correction is not used in evaluating  $K_{Ic}$ . The requirement which the contractor uses in this project is  $W - a \geq 4.2(r_y)$ ; that is, specimens which have too high a fracture toughness to meet this restriction are not analyzed by the small-scale plasticity correction procedure to obtain a value of  $K_{Ic}$ . The reason for specifying this requirement, which is less restrictive than that of ASTM E561, is explained in appendix B.

The CTOD data shown in figures 13 to 21 were converted to  $K_{Ic}$  and plotted in figures 35 to 43 along with the hyperbolic tangent best fit to the points. The solid circles indicate valid  $K_{Ic}$  values, and the open circles  $K_{Ic}$  values.

#### $K_{Ic}$ Validity Limit

A curve showing the limit of valid  $K_{Ic}$  measurements as a function of test temperature is also plotted on each  $K_{Ic}$ -from-CTOD chart. The maximum valid value of  $K_{Ic}$  was calculated using the expression:

$$B = 2.5 (K_{Ic}/\sigma_{yd})^2 \quad (5)$$

where

$B$  = plate thickness

$\sigma_{yd}$  = dynamic yield strength



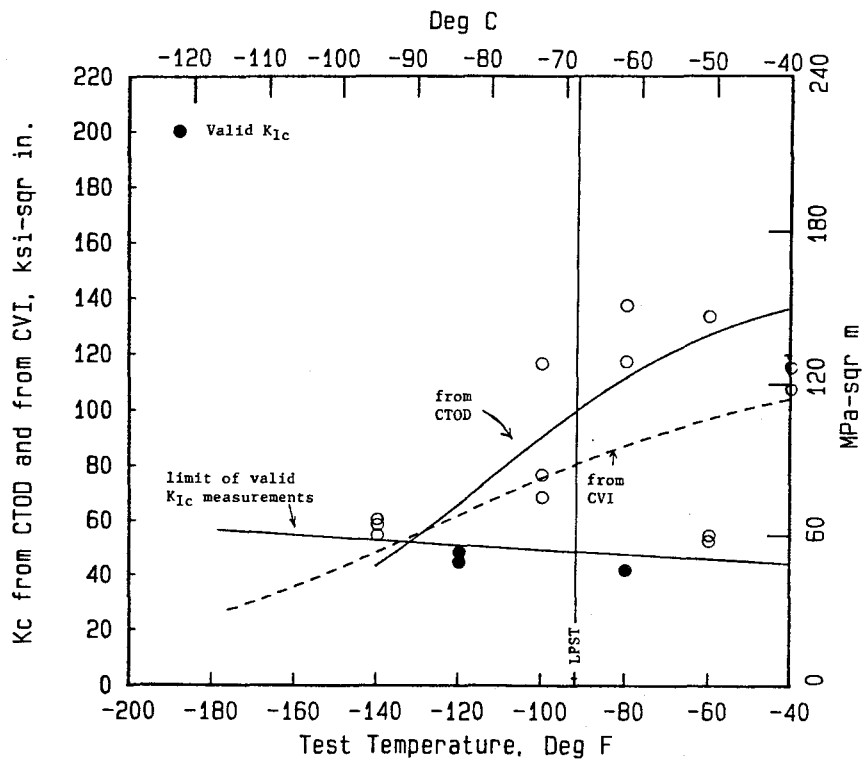


Figure 35. Comparison of  $K_c$  ( $K_{Ic}$ ) obtained from CTOD and CVI. (1-in (25 mm) thick A572-82, grade 50, plate C).

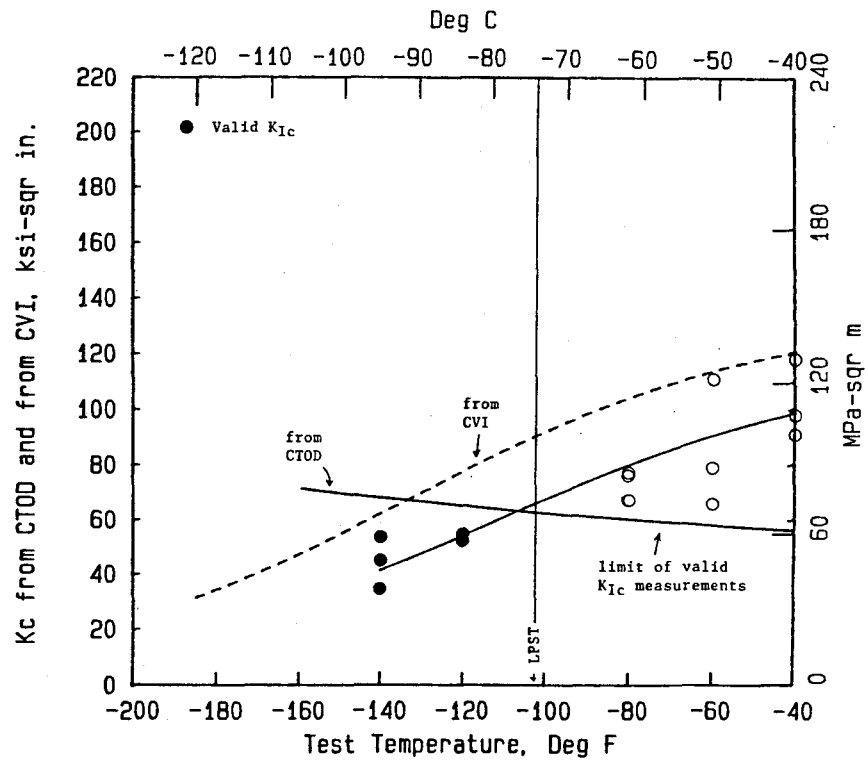


Figure 36. Comparison of  $K_c$  ( $K_{Ic}$ ) obtained from CTOD and CVI. (2-in (51 mm) thick A572-82, grade 50, plate D).

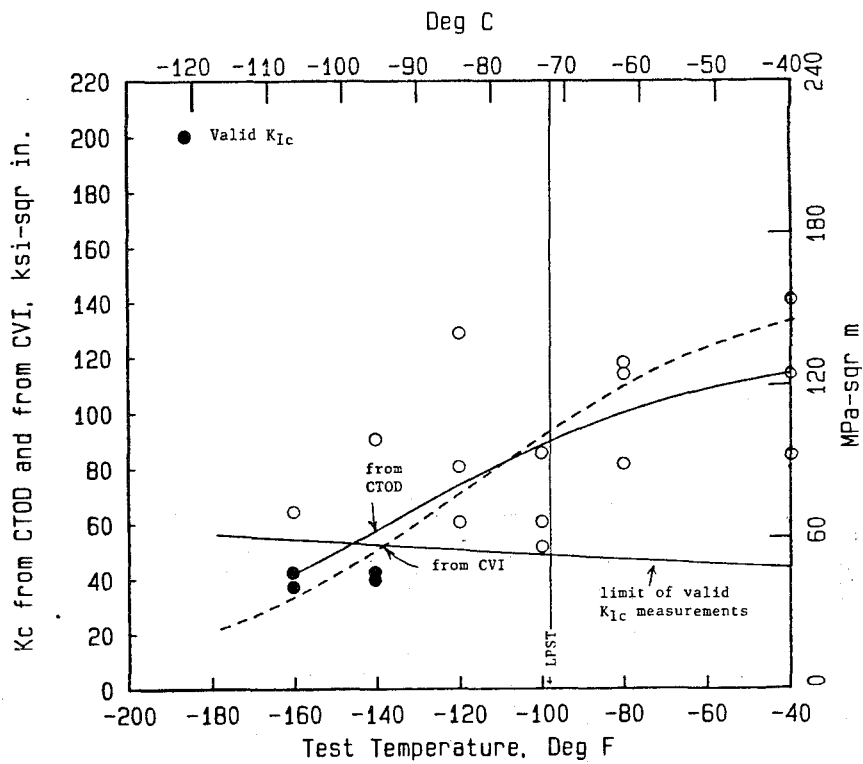


Figure 37. Comparison of  $K_C$  ( $K_{Ic}$ ) obtained from CTOD and CVI. (1-in (25 mm) thick A588-82, grade B, plate E).

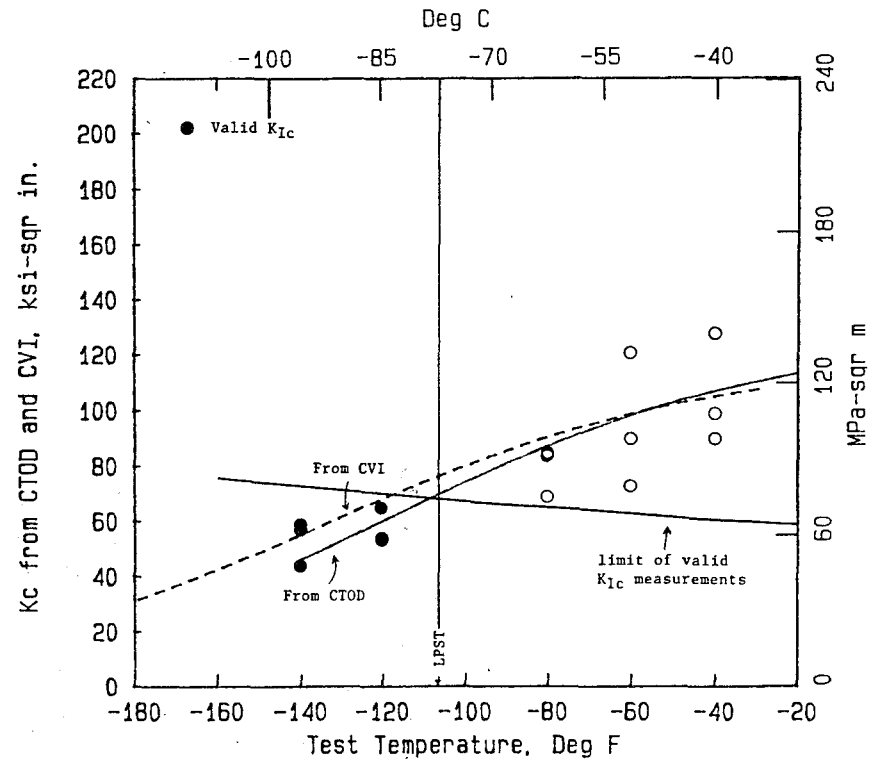


Figure 38. Comparison of  $K_C$  ( $K_{Ic}$ ) obtained from CTOD and CVI. (2-in (51 mm) thick A588-82, grade B, plate F).

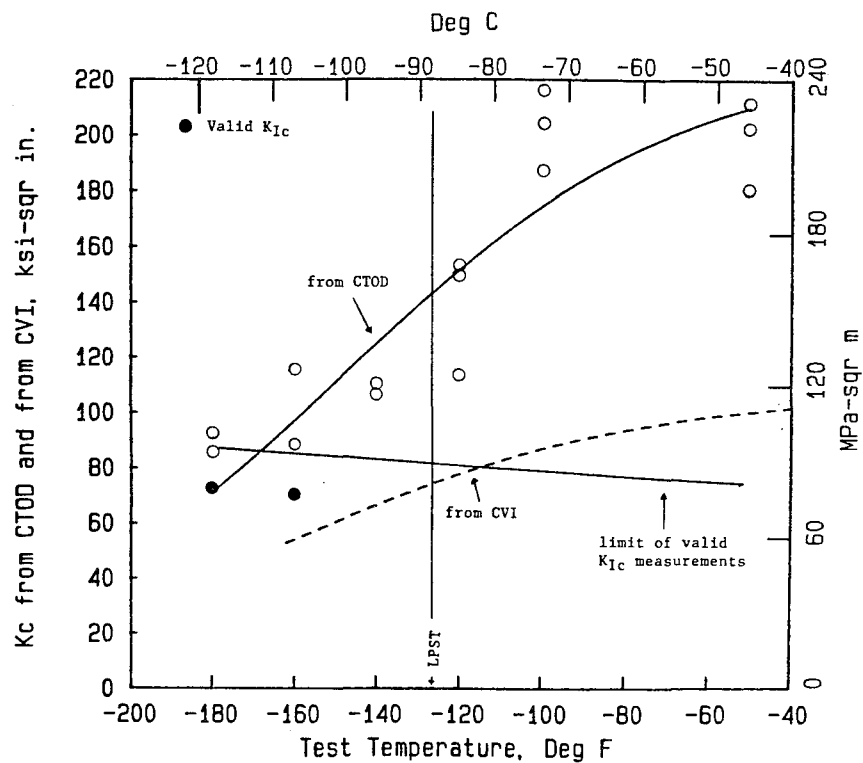


Figure 39. Comparison of  $K_C$  ( $K_{Ic}$ ) obtained from CTOD and CVI. (1-in (25 mm) thick A514, grade B, plate A).

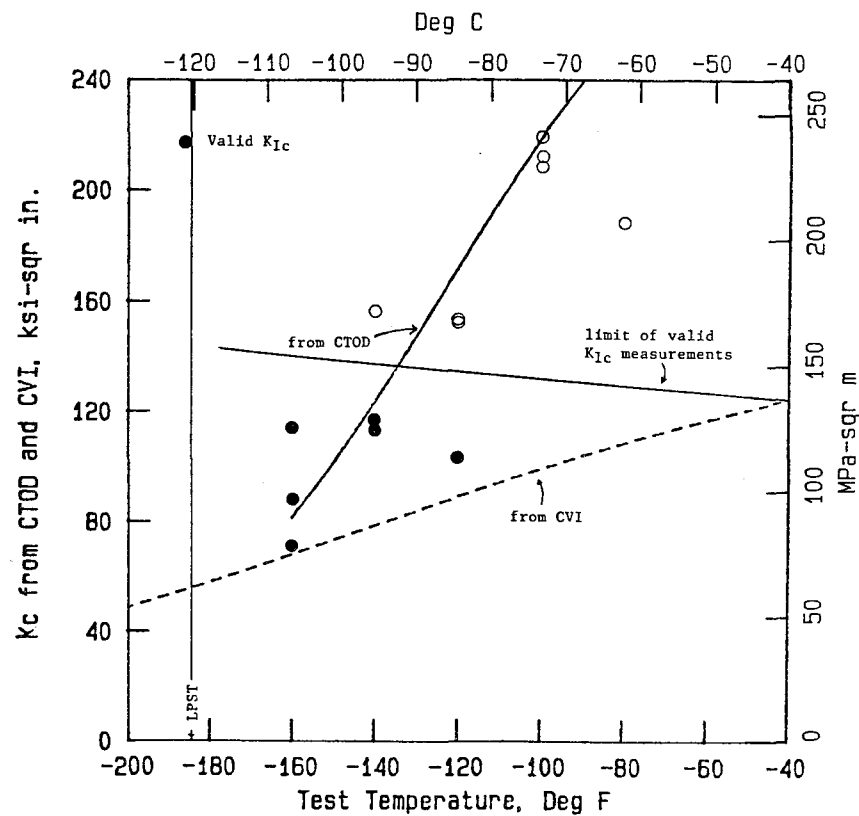


Figure 40. Comparison of  $K_C$  ( $K_{Ic}$ ) obtained from CTOD and CVI. (2-in (51 mm) thick A514-85A, plate B).

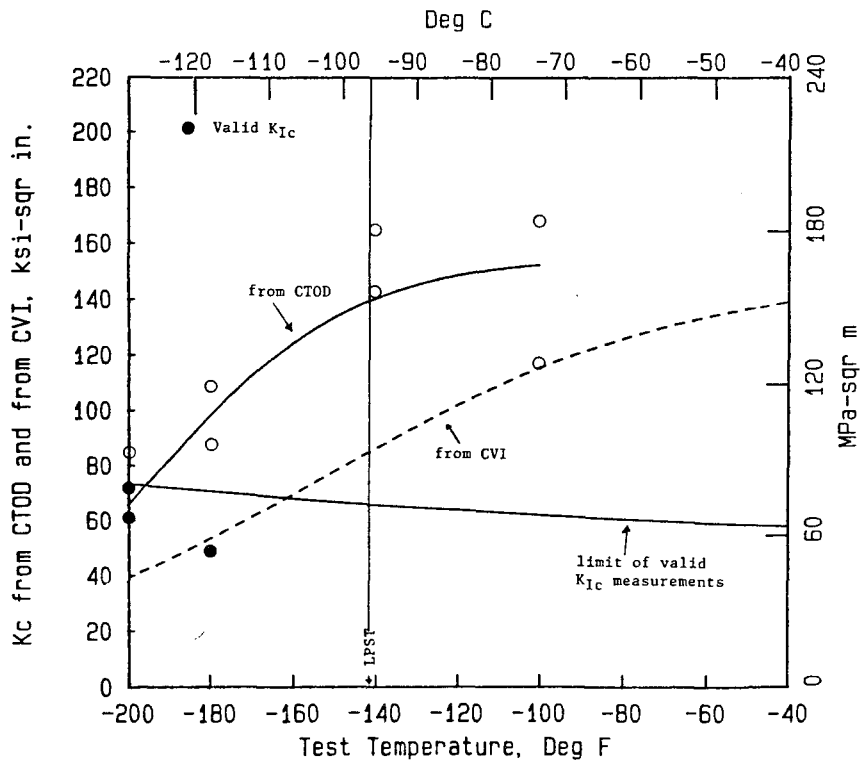


Figure 41. Comparison of  $K_C$  ( $K_{Ic}$ ) obtained from CTOD and CVI. (1-in (25 mm) thick A852-85, plate H).

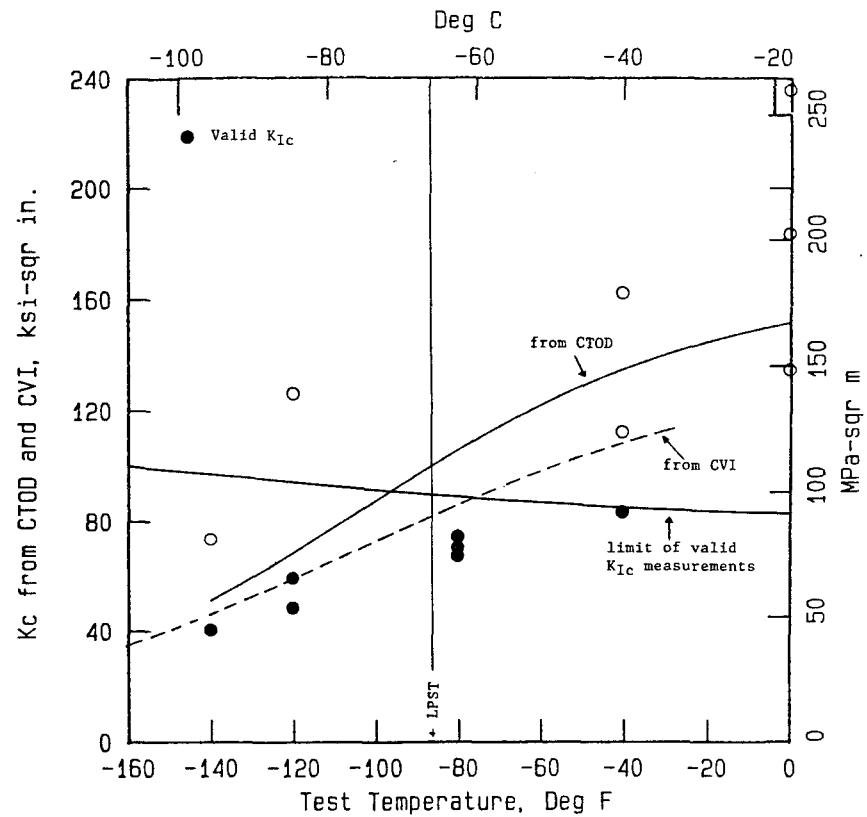


Figure 42. Comparison of  $K_C$  ( $K_{Ic}$ ) obtained from CTOD and CVI. (2-in (51 mm) thick A852-85, plate L).

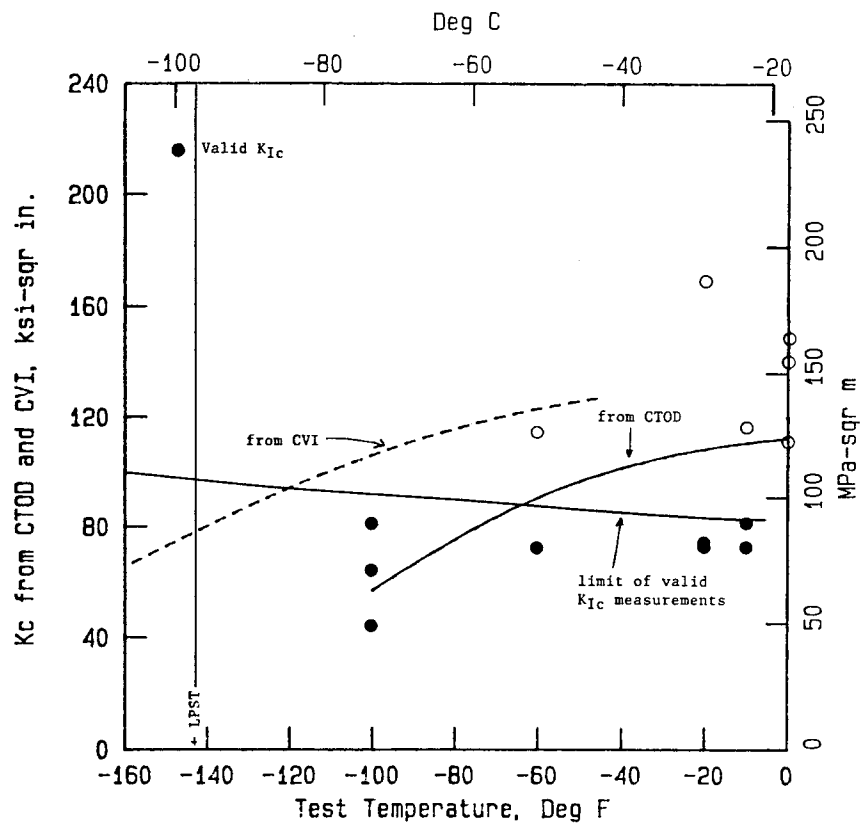


Figure 43. Comparison of  $K_c$  ( $K_{Ic}$ ) obtained from CTOD and CVI. (3-in (76 mm) thick A852-85, plate M).

The dynamic yield strength for some, but not all, of the plates were measured in this project. Hence, calculated values of  $\sigma_{yd}$ , based on an expression proposed by Irwin, rather than measured values were used. The procedure for calculating  $\sigma_{yd}$  and a comparison of calculated and measured values obtained on one plate is shown in appendix C.

## 2.5 Evaluation of the Barsom-Rolfe Steel Selection Criterion

In the earlier referenced project, all data available as of early 1984 in which both a critical K value and CVI were measured on the same plate were examined in order to re-evaluate the Barsom-Rolfe criterion on which the present AASHTO Guide Specifications is based.<sup>[1]</sup> Data collected on the present project increased this earlier data base so that the first kind of analysis carried out on these new data was identical with the one used earlier.

As stated in the Introduction, the Barsom-Rolfe (B-R) criterion is based on the concept that if valid measurement of  $K_{Ic}$  can be made on steel plates at temperatures above the LAST, the steel should not be used in fracture critical, nonredundant bridge members. In the earlier study, data were found for over 70 plates, and it was found that the Barsom-Rolfe temperature shift worked well so that K data collected at static or dynamic loading rates were converted to 1-sec loading time data which increased the size of the data base. A summary of all data that had been collected on A36, and plotted relative to the LPST is shown in figure 44. It is apparent that all valid data lie below LPST, and hence one would expect that valid  $K_{Ic}$  values could not be measured above the LAST for this steel. Similar data were found on A588 steel, figure 45. A few valid points did fall above the LPST for this steel, but these few points do not significantly detract from the use of the Barsom-Rolfe criterion.

Not enough data were found on A572 to evaluate its  $K_{Ic}$  values relative to the LPST in this earlier project, but enough were found for A514 and A517 steels. As shown in figure 46, almost all of the A514 valid data were below the LPST. However, for A517 steel whose toughness requirements are the same as A514, the valid  $K_{Ic}$  vs. temperature data extended through the LPST to the highest test temperatures used on this plate, figure 47. The  $K_{Ic}$  range for these points was quite high: 80 to 130 ksi-in<sup>1/2</sup>. (The highest points were obtained on a 2.25-in (57 mm) thick plate having yield strengths around 120 ksi (827 MPa). It is this combination of thick plates and high yield strength that made it possible to measure valid values of  $K_{Ic}$ .) Nevertheless, the CVI tests failed to show that these measurements could be made.

The data collected on the present project are quite similar to those described in the earlier project, and again support the B-R criterion for plate selection excepting for thick, high strength plates. This is seen by the data plotted in figures 35 to 43, inclusive. The only exception to the B-R criterion for 1-in (25 mm) thick plates was a single data point for A572-82, figure 35, and this point was found at a test temperature where the scatter band was exceptionally wide, and where two of the three data points were quite high, and of course, not valid. Indeed, the only plates in which there were a significant number of valid points above LPST were in the 2-in (51 mm) thick A514 plate, figure 40 and the 3-in (76 mm) thick A852 plate, figure 43. As was the case for the earlier A517 data, passing the validity requirement was a result of the combination of a thick plate with a high yield strength. For the 2-in (51 mm) thick A514,  $\sigma_{ys} = 127$  ksi (876 MPa). The A852 steel in 2-in (51 mm) thickness showed a cluster of points just slightly above the LPST, and another single point that was valid well above LPST, figure 42. The 3-in (76 mm) plate showed valid data over almost the entire test temperature range, however.

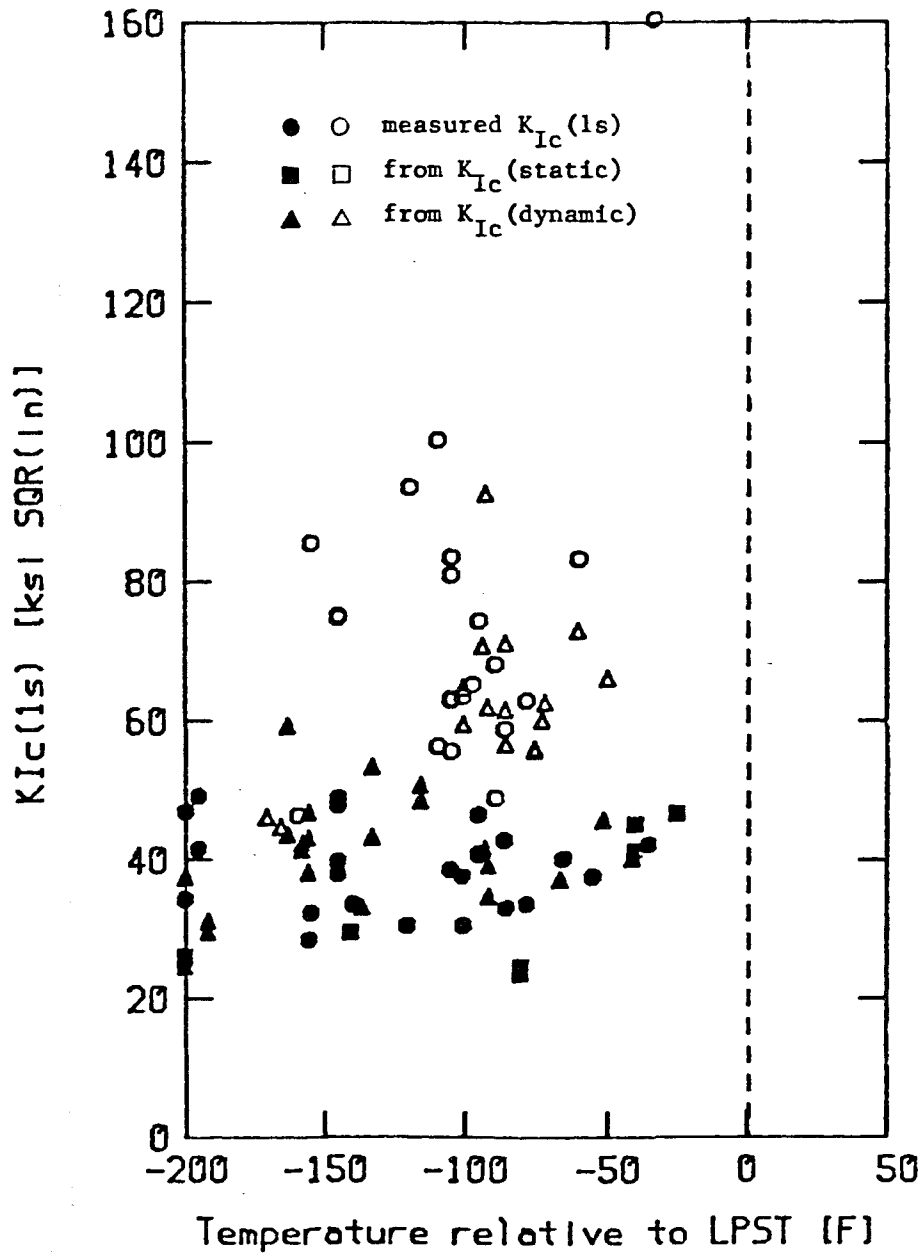


Figure 44.  $K_{Ic}(1s)$  measurements and  $K_{Ic}(1s)$  values derived from  $K_{Ic}(static)$  and  $K_{Ic}(dynamic)$  measurements plotted against temperature measured relative to the LPST. A36 steel, all plates. (Solid symbols are for tests which meet ASTM E399 size requirements; open symbols for undersize specimens. The LPST is 70°F below the 25 ft-lb Charpy temperature for plates up to 1.5 in (38.1 mm) thick, and 50°F below the 25 ft-lb Charpy temperature for thicker plates. 1.0°C = 1.8°F; 1.0 ksi·in<sup>1/2</sup> = 1.099 MPa·m<sup>1/2</sup>.)



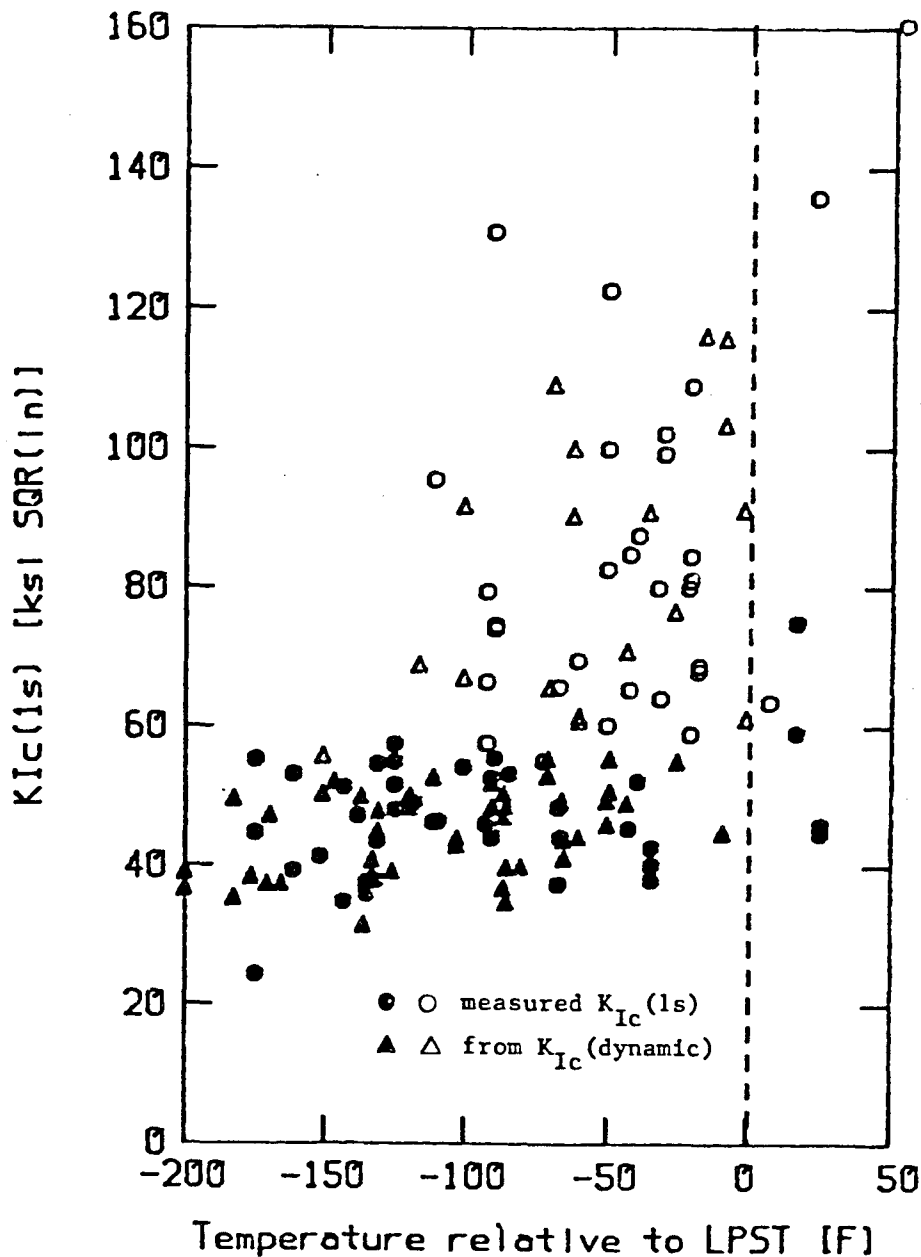


Figure 45.  $K_{Ic}(1s)$  measurements and  $K_{Ic}(1s)$  values derived from  $K_{Ic}(\text{dynamic})$  measurements plotted against temperature measured relative to the LPST. A588 steel, all plates for which 25 or 30 ft-lb (34 or 41J) temperature (as appropriate) as definable. (Solid symbols are for tests which meet ASTM E399 size requirements; open symbols for undersize specimens. The LPST is 70°F below the 25 (or 30) ft-lb Charpy temperature for plates up to 1.5 in (38.1 mm) thick, and 50°F below the 25 (or 30) ft-lb Charpy temperature for thicker plates. 1.0°C = 1.8°F; 1.0  $\text{ksi} \cdot \text{in}^{1/2}$  = 1.099  $\text{MPa} \cdot \text{m}^{1/2}$ .)

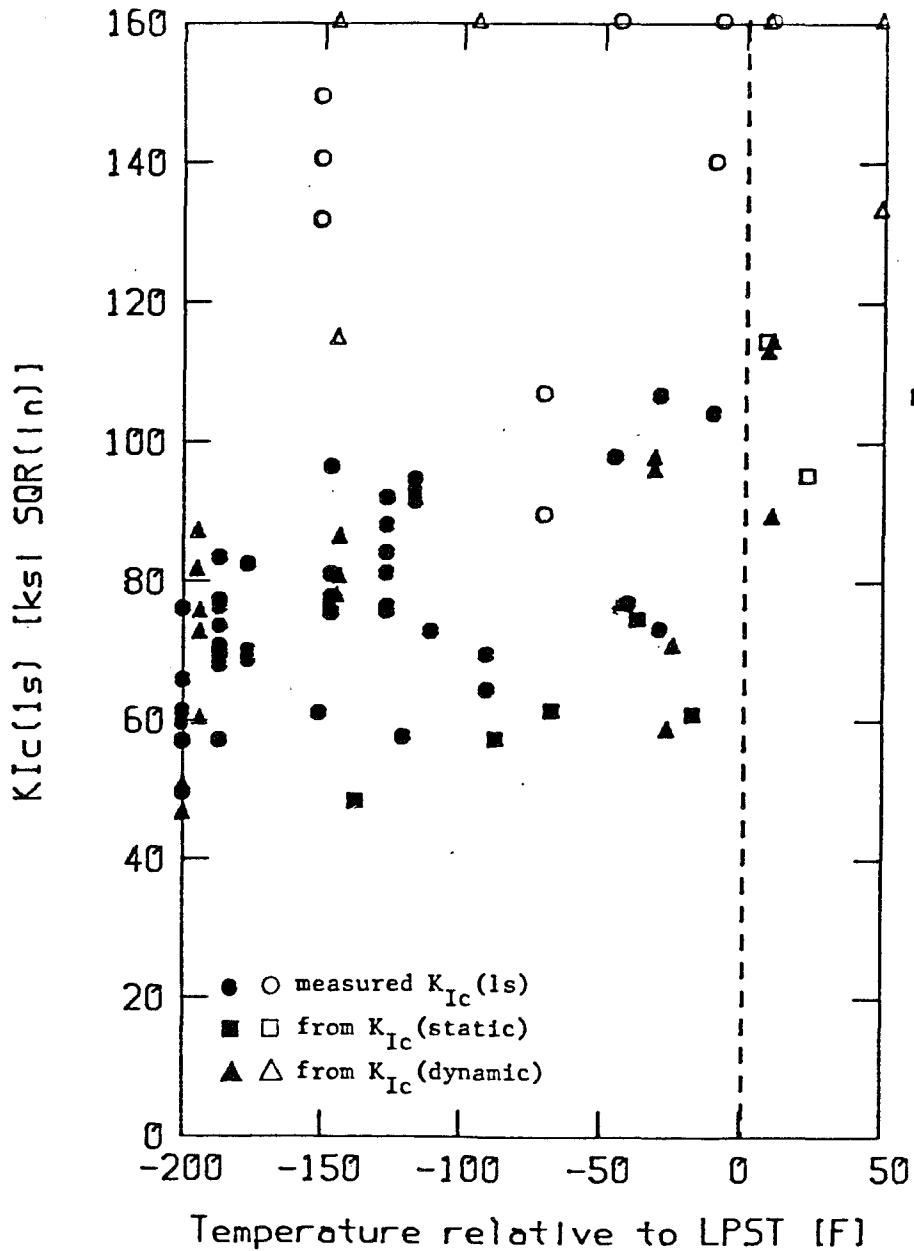


Figure 46.  $K_{Ic}(1s)$  measurements and  $K_{Ic}(1s)$  values derived from  $K_{Ic}(static)$  and  $K_{Ic}(dynamic)$  measurements plotted against temperature measured relative to the LPST. A514 steel, all plates with definable 35 ft-lb (47 J) transition temperature. (Solid symbols are for tests which meet ASTM E399 size requirements; open symbols for undersize specimens. The LPST is 30°F below the 35 ft-lb (47 J) Charpy temperature for plates up to 1.5 in (38.1 mm) thick, and 10°F below the 35 ft-lb (47 J) Charpy temperature for thicker plates. 1.0°C = 1.8°F. 1.0  $\text{ksi} \cdot \text{in}^{1/2} = 1.099 \text{ MPa} \cdot \text{m}^{1/2}$ .)

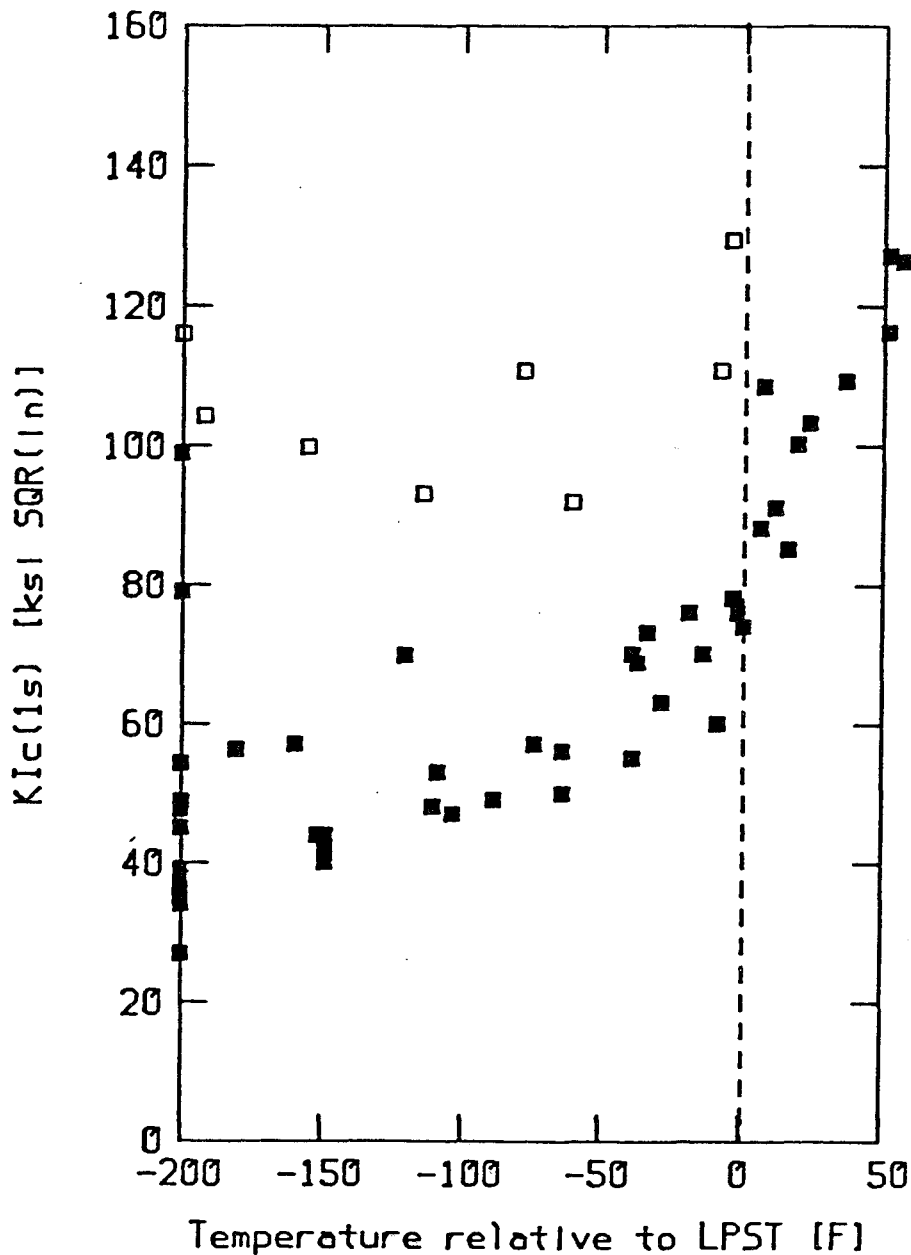


Figure 47.  $K_{Ic}(1s)$  values derived from  $K_{Ic}$  (static) measurements plotted against temperature measured relative to the LPST. A517 steel, all plates with definable 35 ft-lb (47 J) transition temperature. (Solid symbols are for tests which meet ASTM E399 size requirements; open symbols for undersize specimens. The LPST is 30°F below the 35 ft-lb (47 J) Charpy temperature for plates up to 1.5 in (38.1 mm) thick, and 10°F below the 35 ft-lb (47 J) Charpy temperature for thicker plates. 1.0°C = 1.8°F. 1.0 ksi·in<sup>1/2</sup> = 1.099 MPa·m<sup>1/2</sup>.)

In summary, all the data collected on 1-in (25 mm) plates and the data collected on 2-in (51 mm) plates of steels having the intermediate yield strengths, A572 and A588, support the Barsom-Rolfe criterion. For the thicker, high strength plates, A514 and A852, valid  $K_{Ic}$  values were found above the LPST. This was also found in the earlier study with 2 1/4-in (57 mm) plates of A517. These data suggest that the AASHTO requirements for thick, high strength plates should be modified.

## 2.6 Comparison of $K_c$ From CVI and CTOD

In the previous section,  $K_c$  data converted from CTOD and CVI tests were used to ascertain whether or not these new data support the Barsom-Rolfe criterion on which the present AASHTO Guide Specifications are based. In this section, these same data are used to determine the toughness of each of the test plates above the LPST, again in terms of  $K_c$  values calculated from CTOD. In addition, a determination is made of how well these  $K_c$  from CTOD values correspond with  $K_c$  values obtained by the Barsom-Rolfe conversion. Neither of these will have an impact on the AASHTO Guide Specifications, but the data are needed if critical crack sizes are to be calculated at temperatures experienced by bridge members within each of the temperature zones.

Figure 35 shows the  $K_c$  comparisons for the 1-in (25 mm) thick plate of A572. At the LPST and above, the CTOD curve lies well above the CVI curve; i.e. the CVI values are a conservative estimate of full-thickness fracture toughness. The comparison of the two curves for the thicker plate of A572, figure 36, show a behavior opposite to that shown in figure 35. For the thick plate, the CTOD derived curve lies below the CVI one at all temperatures so that  $K_c$  implied from CVI tests is nonconservative.

Both the 1-in (25 mm) and 2-in (51 mm) thick A588 plates, figure 37 and figure 38, respectively, show that  $K_{Ic}$  values calculated from CTOD and CVI are essentially identical.

For the quenched and tempered 1-in (25 mm) thick plates of A514 and A852, figures 39 and 41 respectively, the CTOD curve lies well above the CVI curve so that CVI is a very conservative estimate of  $K_{Ic}$  for these plates. In addition, no valid  $K_{Ic}$  points were found for these steels above LPST.

For the thicker A514 plate, over the temperature range for which  $K_{Ic}$  values were calculated from both CTOD and CVI data, figure 40, the CTOD derived curve lies well above the CVI one. Hence, CVI test data again give a conservative estimate of  $K_{Ic}$ . (Data were not collected as low as the LPST (-185°F) (-121°C) because all the data points at -160°F (-107°C) and two of the three points at -140°F (-96°C) were valid.) For the 2-in (51 mm) thick plate of A852, figure 42, the use of CVI data is certainly not as conservative as it was for the 1-in (25 mm) thick plate. Nevertheless, it is still conservative. On the other hand, the use of CVI data to estimate fracture toughness is nonconservative for the 3-in (76 mm) thick A852 plate, figure 43. Again, as was the case for the 2-in (51 mm) thick A514 plate, CTOD data were not collected at temperatures as low as the LPST because much of the data well above this temperature were valid  $K_{Ic}$  values.

## 2.7 Critical Crack Sizes at LPST

The  $K_{Ic}$  values calculated from the CTOD data make it possible to calculate critical crack sizes at the LPST for the tested plates. The  $K_{Ic}$ -from-CTOD curves in figures 35 to 43 were used to select a  $K_{Ic}$  value at LPST for each steel, and these values are shown in table 12. These

values were used with a design stress of half the yield strength to calculate critical crack sizes. If a lower bound value of  $K_c$  had been selected,  $K_c$  and hence the critical crack lengths would have been lower. Nevertheless, the critical crack sizes for 2-in (51 mm) thick A514 and 3-in (76 mm) thick A852 are less than 1/2-in (13 mm).

Table 12.

Critical crack sizes at LPST for plates for design stress equal to one-half the yield strength.

<u>Plate</u>	<u>Thickness</u> <u>in (mm)</u>	<u>Assumed</u> <u>Design</u> <u>Stress</u> <u>ksi (MPa)</u>	<u>K<sub>c</sub> at</u> <u>LPST</u> <u>ksi√in</u> <u>(MPa√m)</u>	<u>Critical Crack Size</u>	
				<u>Edge</u> <u>Crack</u> <u>in (mm)</u>	<u>Non-Edge</u> <u>Crack</u> <u>in (mm)</u>
A572	1 (25)	25.0 (172)	99 (109)	5.0 (127)	10.0 (254.0)
	2 (51)	25.0 (172)	66 (72)	2.2 (55.9)	4.4 (111.8)
A588	1 (25)	25.0 (172)	89 (98)	4.0 (102)	8.0 (203.2)
	2 (51)	25.0 (172)	69 (76)	2.4 (61.0)	4.8 (122.0)
A514	1 (25)	50.0 (345)	139 (153)	2.5 (63.5)	5.0 (127.0)
	2 (51)	50.0 (345)	40* (44)	0.2 (5.1)	0.4 (102.0)
A852	1 (25)	32.5 (224)	140 (154)	5.9 (149.9)	11.8 (299.7)
	2 (51)	32.5 (224)	100 (110)	3.0 (76)	6.0 (152.4)
	3 (76)	32.5 (224)	20* (22)	0.1 (2.5)	0.2 (5.1)

\*Estimated

## CHAPTER 3: TEST RESULTS, WELDMENTS

In addition to the base plate tests, tests were also made on Submerged Arc Weldments. Unlike base plates, the CVI requirements given in the AASHTO Guide Specifications for welds do not depend on temperature zone. For all three zones, the requirements are as follows:

The Charpy test requirements for weld metal connecting AASHTO M183, M222, M223 (ASTM A36, A588, A572) steels shall be 25-ft-lb (33.9 Nm) at -20F (-28.9C). The Charpy test requirements for weld metal connecting AASHTO M244 (ASTM A514) and ASTM A517 steels shall be 35 ft-lb (47.5 Nm) at -30F (-34.4C), except for fillet welds made with filler metal normally used for welding AASHTO M183, M223 and M222 (ASTM A36, A572 and A588) steels. The toughness for these fillet welds shall be 25 ft-lb (33.9 Nm) at -20F (-28.9C).

Specifying requirements this way makes it impossible to analyze the data in terms of a reference temperature such as LAST or LPST. Hence, the data are analyzed in this section by comparing weld metal (WM) and heat-affected zone (HAZ), Charpy and CTOD toughness, to those of the base plate on which the welds were made.

### 3.1 Material

Six plates were selected for submerged arc welding: 1-in (25 mm) thick plates of all test materials, A572, A588, A514 and A852, and 2-in (51 mm) thick plates of the two non-heat-treated steels, A572 and A588. All weldments were produced by a local bridge fabricator. The plate preparation and welding requirements that were supplied to



the fabricator are shown in table 13. A complete Welding Procedure Qualification was only carried out on the 2-in (51 mm) thick weldment of A588, table 14. Charpy Impact and tensile tests were made on most of the welds as shown in the following sections; and even though complete qualifications were not made, it is apparent that the welds are of high quality.

### 3.2 Test Results

Tensile tests were conducted on weld metal of all 1-in (25 mm) thick plates, and 2-in (51 mm) thick plates of the non-heat-treated steels, table 15.

Charpy V-notch Impact tests were made on the weld metal and heat-affected zone of the 1-in (25 mm) thick plates of all test materials, A572, A588, A514 and A852, and on 2-in (51 mm) thick weldments of A572. The results are plotted in figures 48 to 57.

CTOD tests were also conducted on the WM and HAZ of four selected plate weldments: 2-in (51 mm) thick A572, 1- and 2-in (25 and 51 mm) thick A588, and 1-in (25 mm) thick A852. The CTOD data are plotted in figures 63 to 66.

### 3.3 Analysis of Weldment Data

In the base plate study, a comparison was made of  $K_{IC}$  values calculated from CVI data and from CTOD. The calculations made use of the Lowest Permissible Service Temperature (LPST) which is based on the use of the Barsom-Rolfe temperature shift as given in the AASHTO Guide Specifications. The CVI requirements for weld metal are independent of temperature zones, and hence these are not fixed

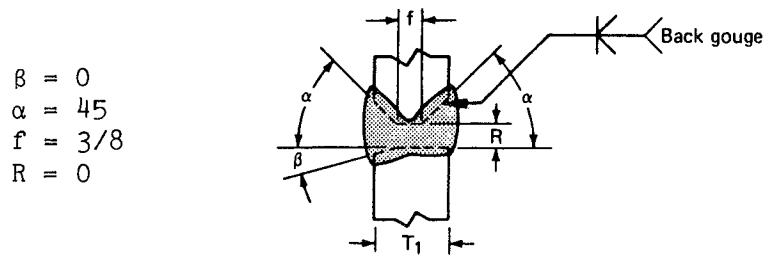
Table 13.

Plate preparation and welding requirements.

1. Procedure Qual Tests to be run on 2-in (51 mm) plate of A588 only.
2. Preheats and Interpass Temperature limits for:
  - a) A572 and A588 are given in table 8.1A of AASHTO Guide Specifications for Fracture Critical Non-Redundant Steel Bridge Members.
  - b) A514 - table 8.1B - same reference
  - c) A852 - min. preheat

Up to 3/4 in (19 mm) thickness	50°F (10°C)
Over 3/4 in (19 mm) to 1 1/2 in (38 mm)	125°F (52°C)
1 1/2 in (38 mm) to 2 1/2 in (64 mm)	175°F (79°C)
Over 2 1/2 in (64 mm)	225°F (107°C)

3. Weld Details of Double Bevel-Groove  
Weld (5) Butt Joint (B)  
AWS D1.1-86 p. 17 top with following requirements:



Materials: A572, grade 50; A588, A514 and A852  
 Thickness: 1 in (25 mm) and 2 in (51 mm)

Filler Metals: Table 4.1.1 of AWS01.1-86 for SAW  
 A852 A5.23 F9AX-EXX-X  
 A572 Gr. 50 F72-EM12K (LINCOLN L61)  
 A588 F72-EM12K (LINCOLN L61)  
 A514 F11-ECM2

Table 14.

Subcontractor's welding procedure qualification form.

GROOVE WELD  
 FILLET WELD


PROCEDURE SPECIFICATION	PROCESS SAW		BASE METAL SPECIFICATION A588		WELDING POSITION FLAT					
	MATERIAL THICKNESS TWO INCH		ELECTRODE E612K (LINCOLN L61)		PREHEAT & INTERPASS TEMP. 200°F ± 100					
	SHIELDING E7A2 (LINCOLN 860)		TYPE OF CURRENT DC +							
	OTHER A.A.S.H.T.O. FRACTURE CRITICAL PLAN									
AIR ARC AND GRIND SIDE 2 BEFORE WELDING										
WELDERS NAME			SYMBOL & NO. LL							
WELD SEQUENCE										
Pass No.	Electrode Diameter	Amperes	Volts	Speed						
1 - 18	3/32	420	33	17						
SUMMARY OF TEST RESULTS	CVN at -20°F	WELD		WELD		HAZ		HAZ		
		76	47	102			84	70	92	
		41	73	3 Ave. 65			92	80	3 Ave. 85	
	GROOVE WELD	All Weld Metal Tensile	YIELD POINT		ELONGATION		ULTIMATE STRENGTH		REDUCTION IN AREA	
			57,600		63,200		70,300		74,600	
		Reduced Section Tensile	ULTIMATE STRENGTH		WELD		DUCTILE			
			1. 75,800	78,600		WELD		DUCTILE		
			2. 76,300		81,400		WELD		DUCTILE	
	GUIDED BEND		PASS / PASS		PASS / PASS		PASS / PASS		PASS / PASS	
			PASS / PASS		PASS / PASS		PASS / PASS		PASS / PASS	
WELDING WITNESSED BY			DATE		TESTING		DATE			
<p>The undersigned certifies that the above data are correct and that the test welds were prepared, welded and tested in accordance with the requirements of <u>AASHTO FRACTURE CRITICAL CONTROL PLAN</u> TEST PROCEDURE.</p>										
INSPECTION AGENCY										
BY					BY					
TITLE			DATE		TITLE			DATE		
								6-2-88		
REVISION			REVISION			PROCEDURE NO.				

Table 15.

Room temperature tensile properties of  
weld metal - longitudinal direction.

	<u>Tensile Strength ksi (MPa)</u>	<u>Yield Strength ksi (MPa)</u>	<u>Elong. (2 in G.L.) Percent</u>	<u>Red. in Area Percent</u>
1-in (25 mm) thick A572-82, grade 50 (plate C)				
	82.6 (569.5)	58.3 (402.0)	23.0	68.0
	82.6 (569.5)	60.0 (413.7)	22.0	68.2
2-in (51 mm) thick A572-82, grade 50 (plate D)				
	80.0 (551.6)	53.4 (368.2)	23.0	65.0*
	75.2 (518.5)	53.6 (369.6)	23.0	70.0
*Failed in Base Plate				
1-in (25 mm) thick A588-82, grade B (plate E)				
	78.6 (542.0)	57.2 (394.4)	23.0	69.9
	79.6 (548.8)	56.9 (392.3)	22.0	68.0
2-in (51 mm) thick A588-82, grade B (plate F)				
	70.3 (484.7)	57.6 (397.2)	34.0	72.0
	74.6 (514.4)	63.2 (435.8)	30.0	71.0
1-in (25 mm) thick A514, grade B (plate A)				
	111.0 (765.4)	97.8 (674.3)	21.0	62.0
	111.8 (770.9)	99.2 (684.0)	18.0	60.0
1-in (25 mm) thick A852-85 (plate H)				
	91.0 (627.5)	73.3 (505.4)	21.0	75.3
	89.9 (619.9)	73.1 (504.0)	21.0	74.4

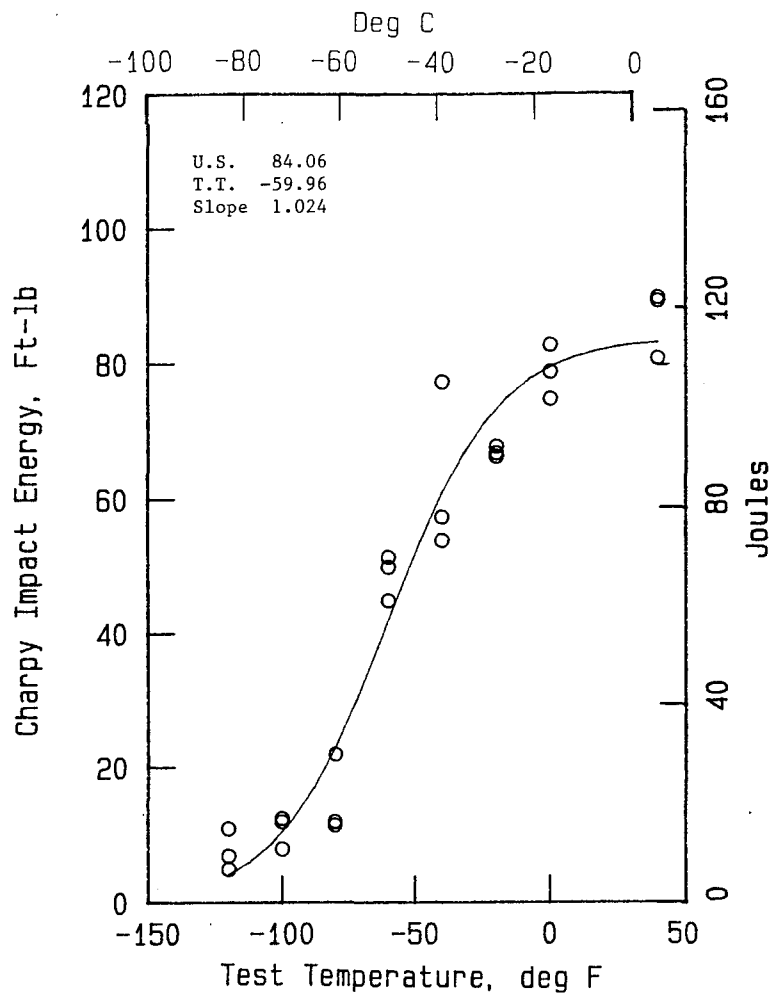


Figure 48. Charpy impact energy vs test temperature (1-in (25 mm) thick A572-82, grade 50, plate C, weld metal).

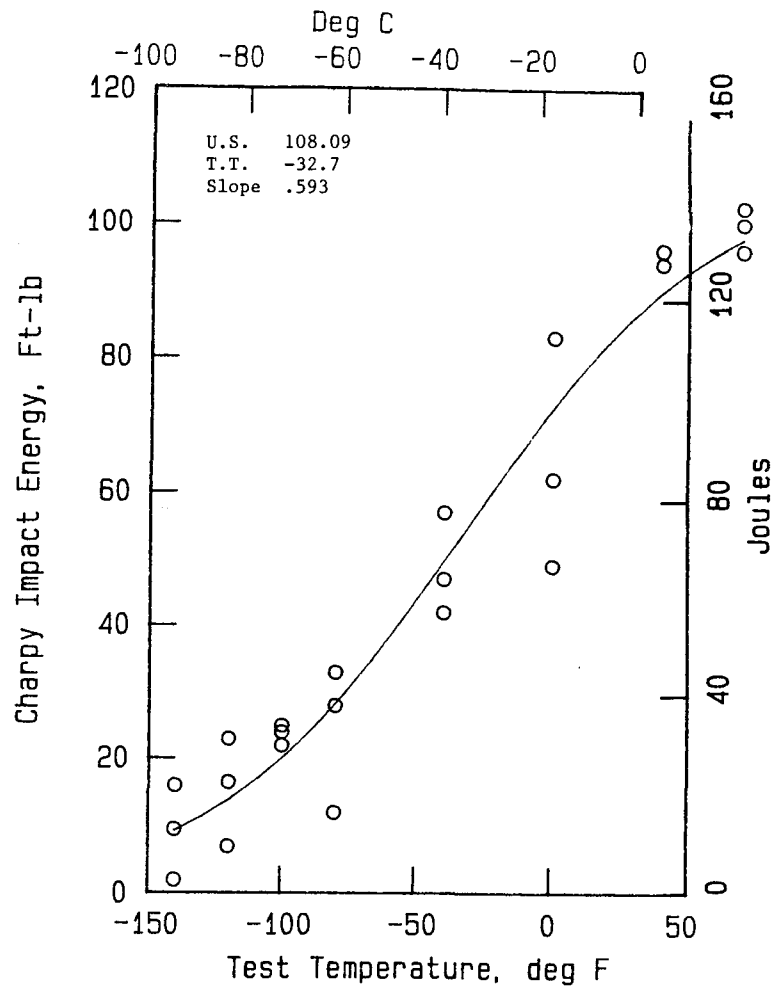


Figure 49. Charpy impact energy vs test temperature (1-in (25 mm) thick A572-82, grade 50, plate C, HAZ).

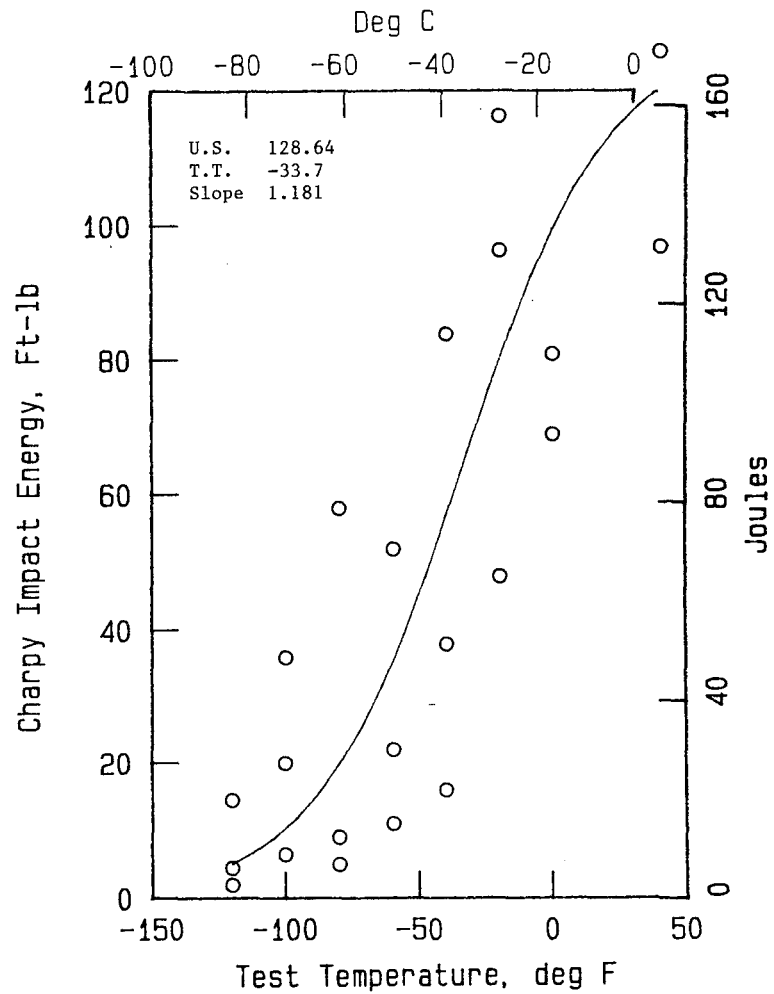


Figure 50. Charpy impact energy vs test temperature (2-in (51 mm) thick A572-82, grade 50, plate D, weld metal).

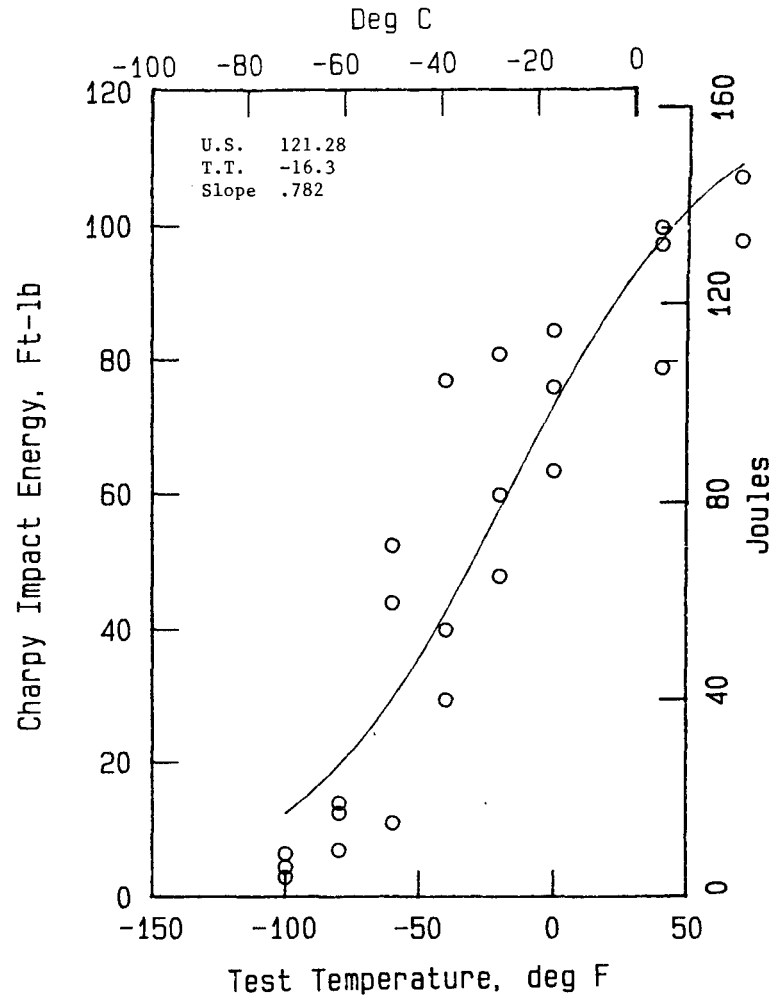


Figure 51. Charpy impact energy vs test temperature (2-in (51 mm) thick A572-82, grade 50, plate D, HAZ).

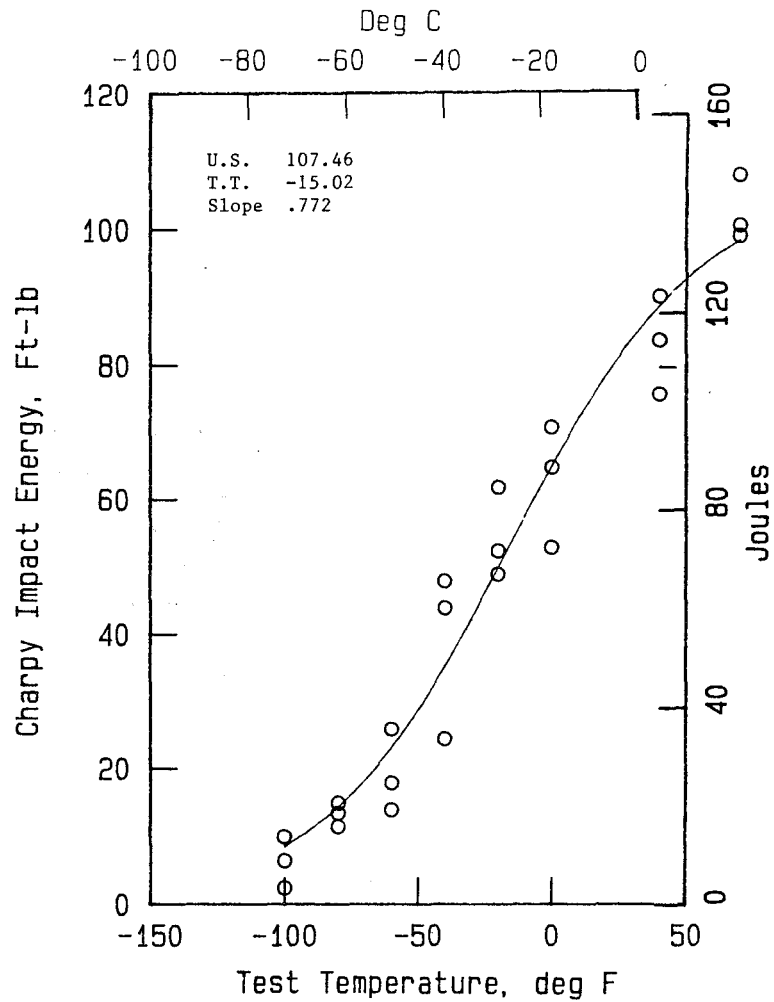


Figure 52. Charpy impact energy vs test temperature (1-in (25 mm) thick A588-82, grade B, plate E, weld metal).

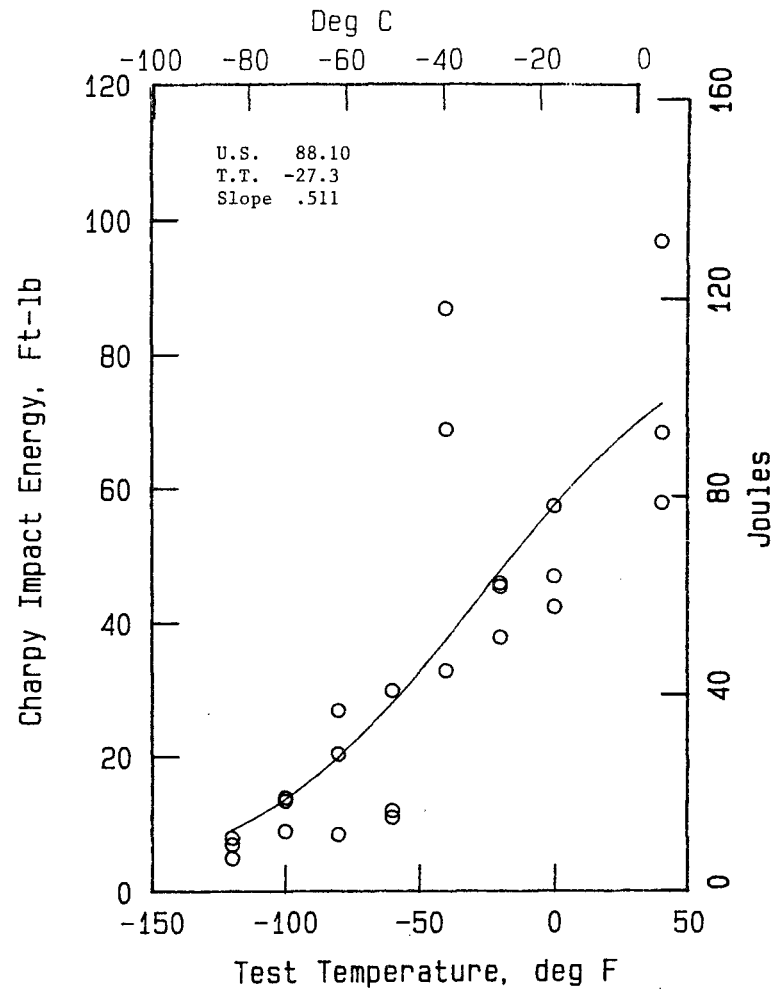


Figure 53. Charpy impact energy vs test temperature (1-in (25 mm) thick A588-82, grade B, plate E, HAZ).

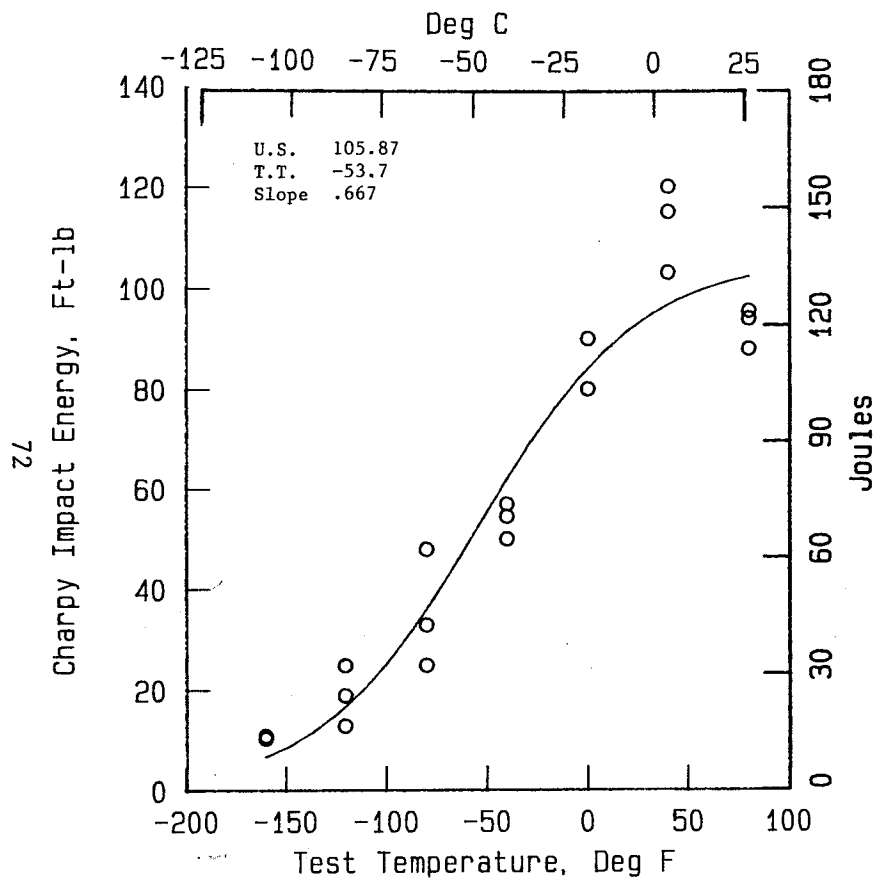


Figure 54. Charpy impact energy vs test temperature (1-in (25 mm) thick A514, grade B, plate A, weld metal).

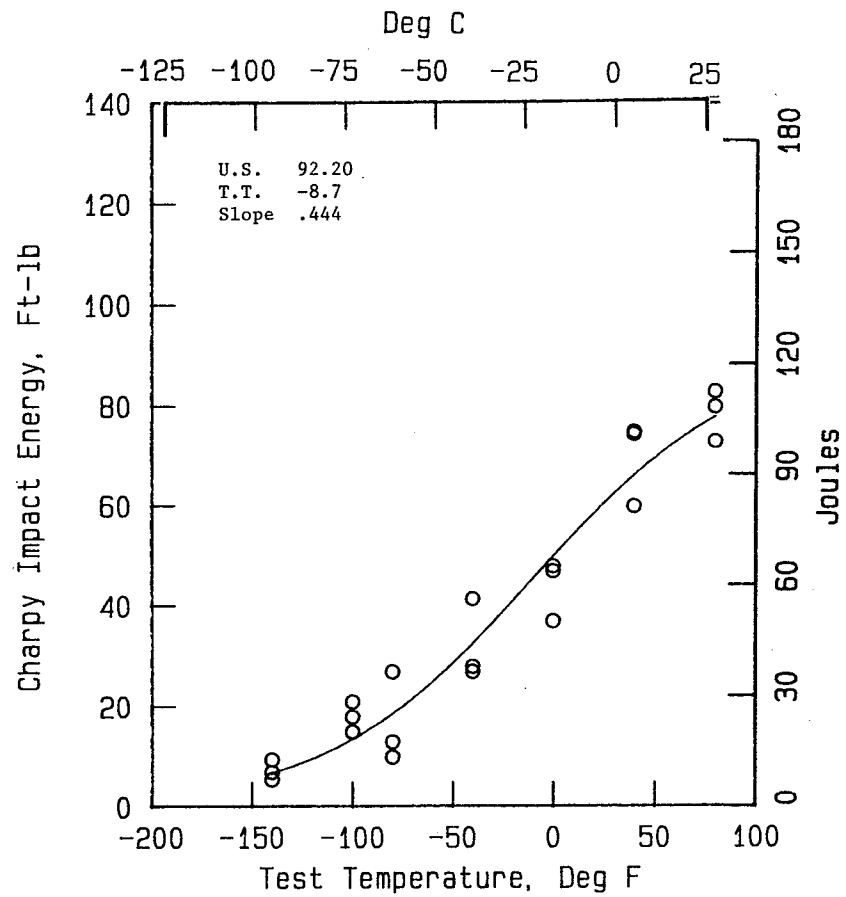


Figure 55. Charpy impact energy vs test temperature (1-in (25 mm) thick A514, grade B, plate A, HAZ).



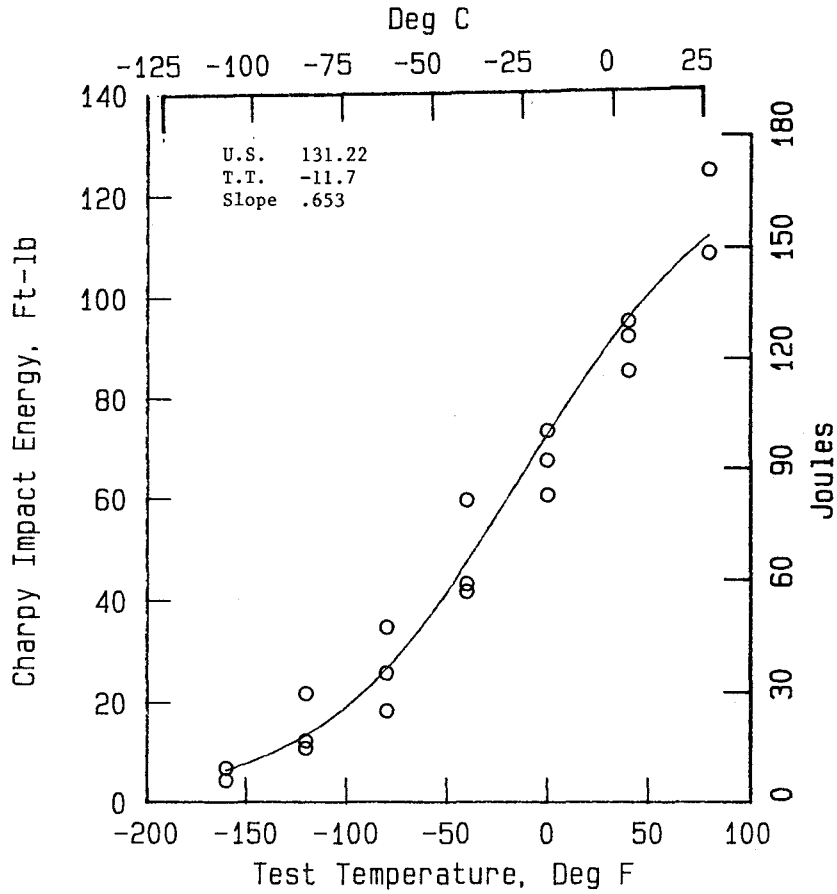


Figure 56. Charpy impact energy vs test temperature (1-in (25 mm) thick A852-85, plate H, weld metal).

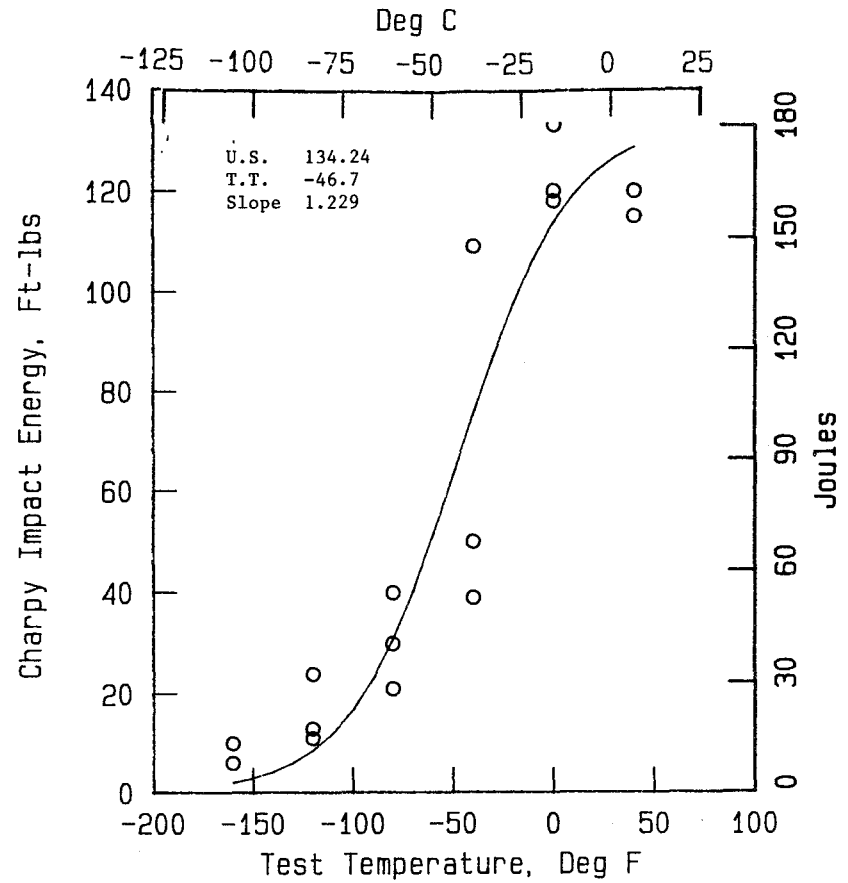


Figure 57. Charpy impact energy vs test temperature (1-in (25 mm) thick A852-85, plate H, HAZ).

differences between zone temperatures and CVI tests so that this analysis method cannot be used on weldments. Instead, as stated above, the CVI and CTOD values obtained on weld metal and heat-affected zone are compared with base plate data.

These comparisons are shown in figures 58 to 62 for the CVI data. For the two non-heat-treated steels, both the WM and HAZ generally have higher CVI values than the base plate (BP). For the 1-in (25 mm) thick A514 steel (figure 60), the HAZ has moderately lower CVI than the BP, but the weld metal for this steel as well as the WM and HAZ of the A852 (figure 61) are similar to the base plate. For the 2-in (51 mm) thick A572 (figure 62), both the WM and HAZ have higher CVI values than the BP.

In all cases, the CVI values measured on the weld metal exceed the requirements that were quoted earlier.

The CTOD comparisons of the WM, HAZ and BP's are shown in figures 63 to 66. The most striking feature of these figures is that the scatter band of the BP, WM and HAZ data are almost the same for a particular plate. This suggests that the critical K values, and critical crack lengths of the entire weldment can be assumed to have the values shown in table 12.

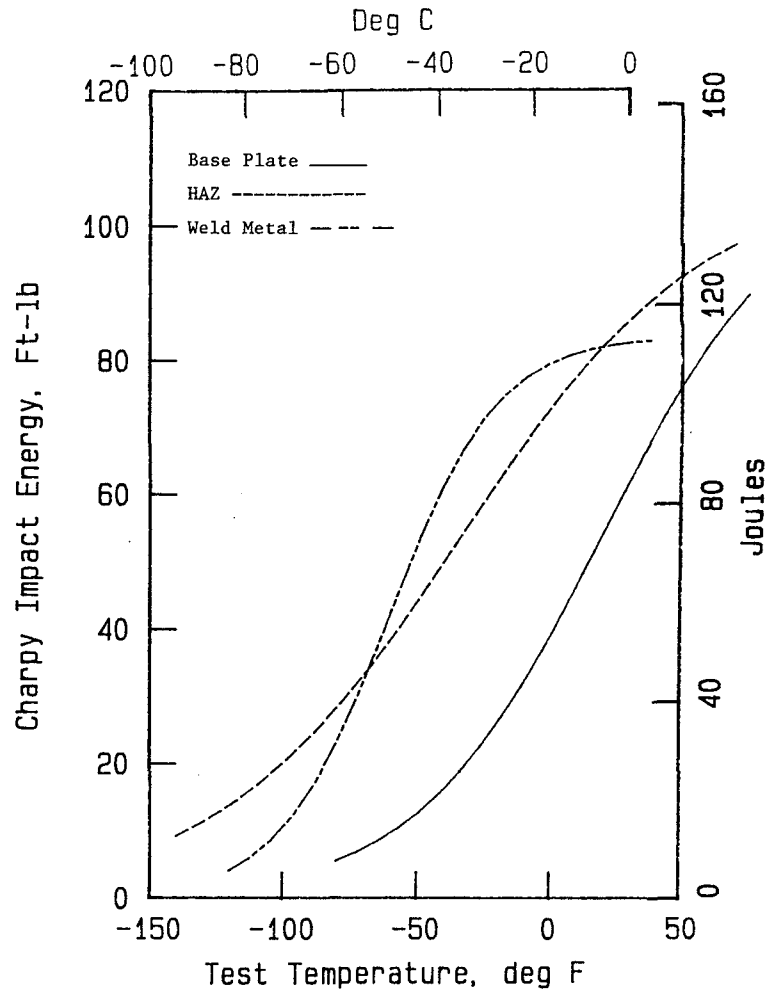


Figure 58. Comparison of base plate, weld metal and heat-affected zone Charpy impact energy vs test temperature (1-in (25 mm) thick A572-82, grade 50, plate C).

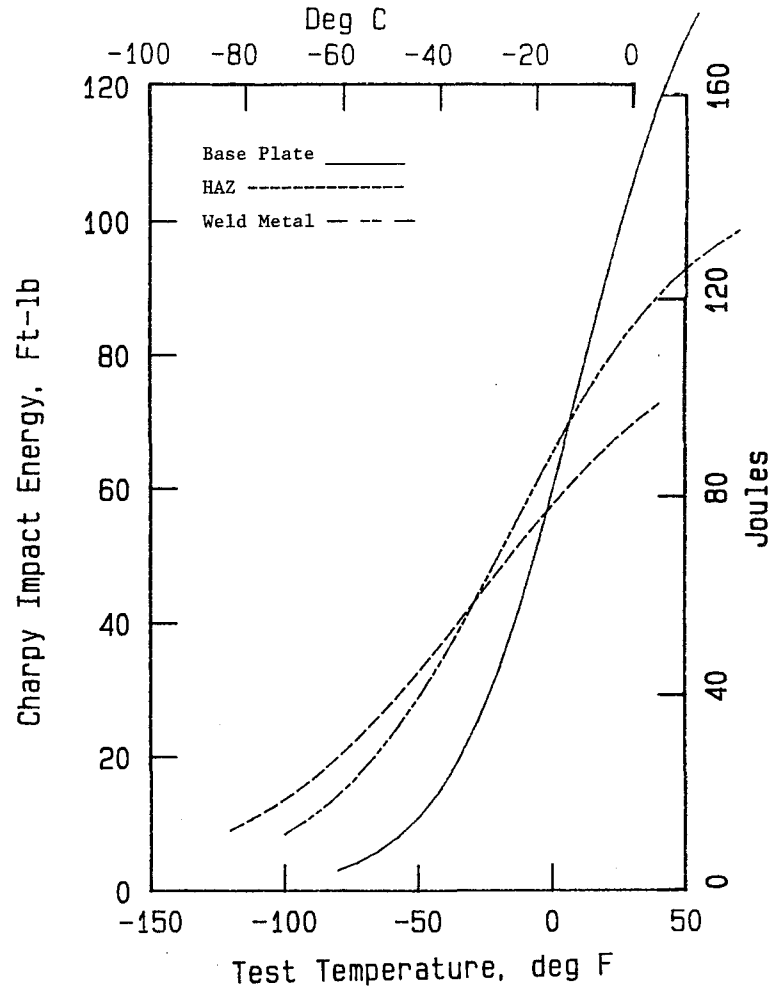


Figure 59. Comparison of base plate, weld metal and heat-affected zone Charpy impact energy vs test temperature (1-in (25 mm) thick A588-82, grade B, plate E).

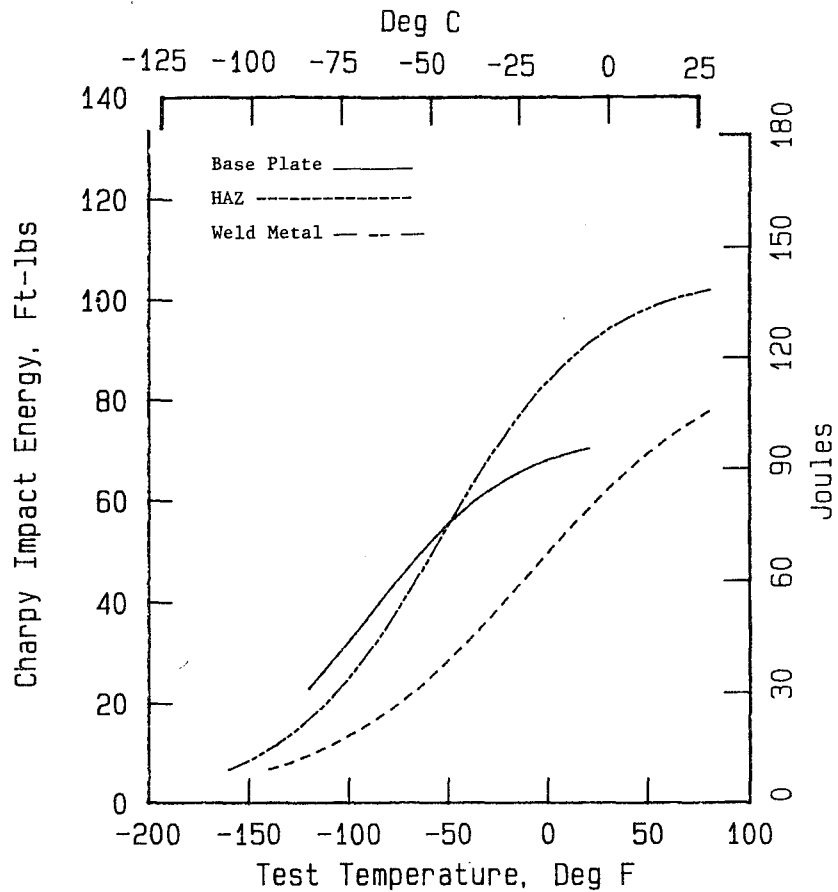


Figure 60. Comparison of base plate, weld metal and heat-affected zone Charpy impact energy vs test temperature (1-in (25 mm) thick A514, grade B, plate A).

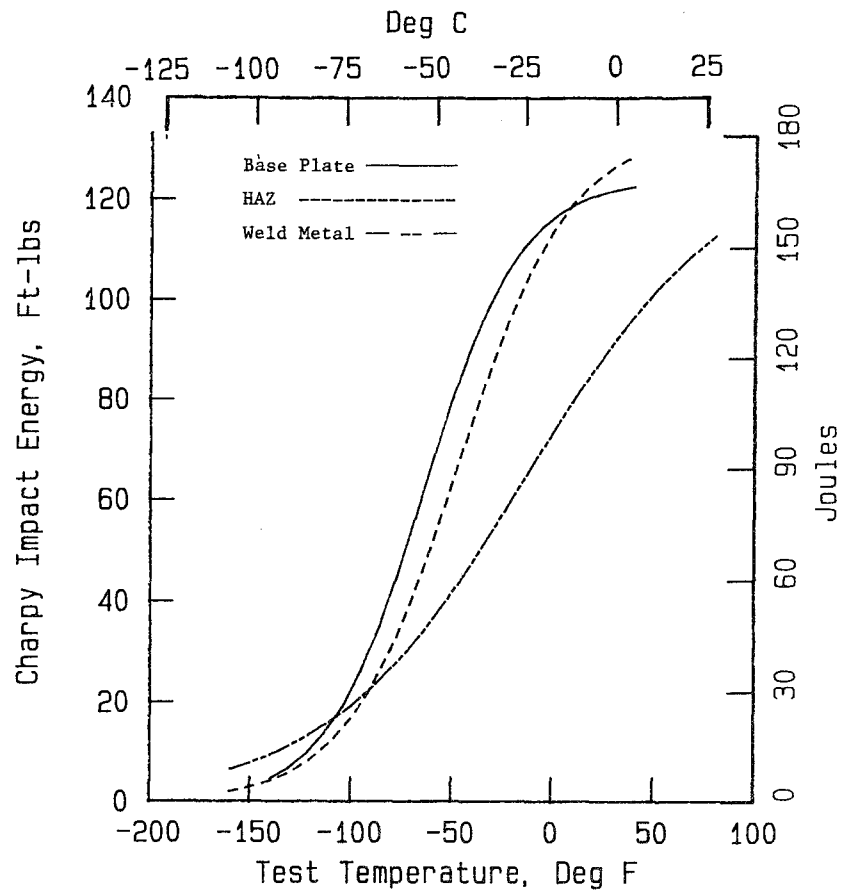


Figure 61. Comparison of base plate, weld metal and heat-affected zone Charpy impact energy vs test temperature (1-in (25 mm) thick A852-85, plate H).

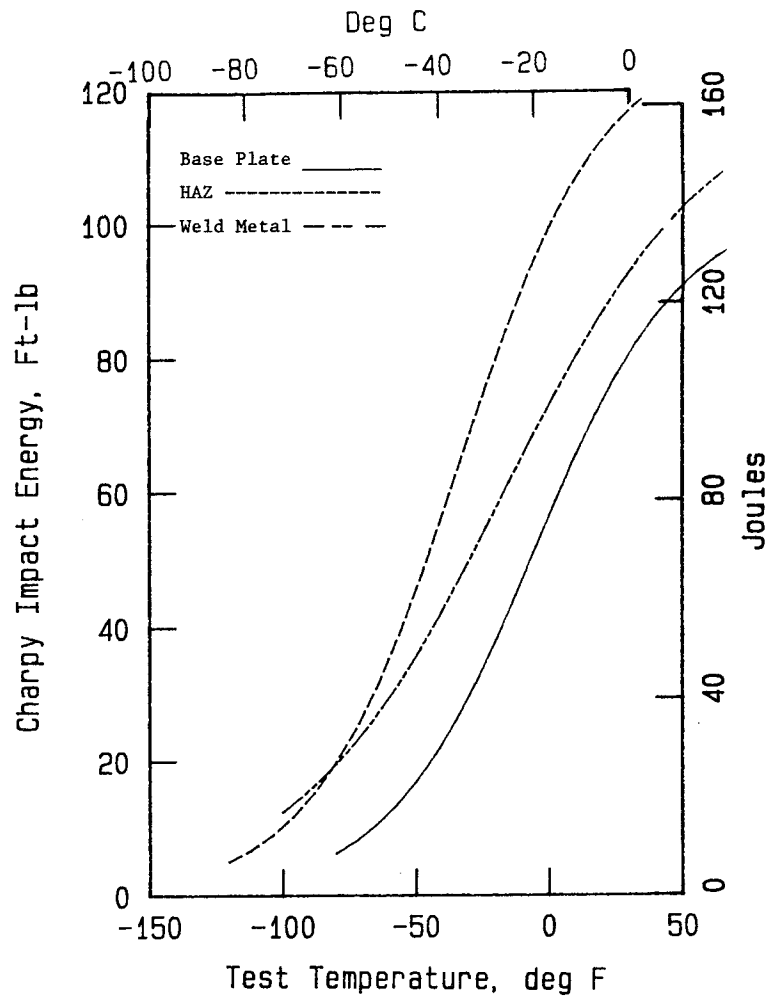


Figure 62. Comparison of base plate, weld metal and heat-affected zone Charpy impact energy vs test temperature (2-in (51 mm) thick A572-82, grade 50, plate D).

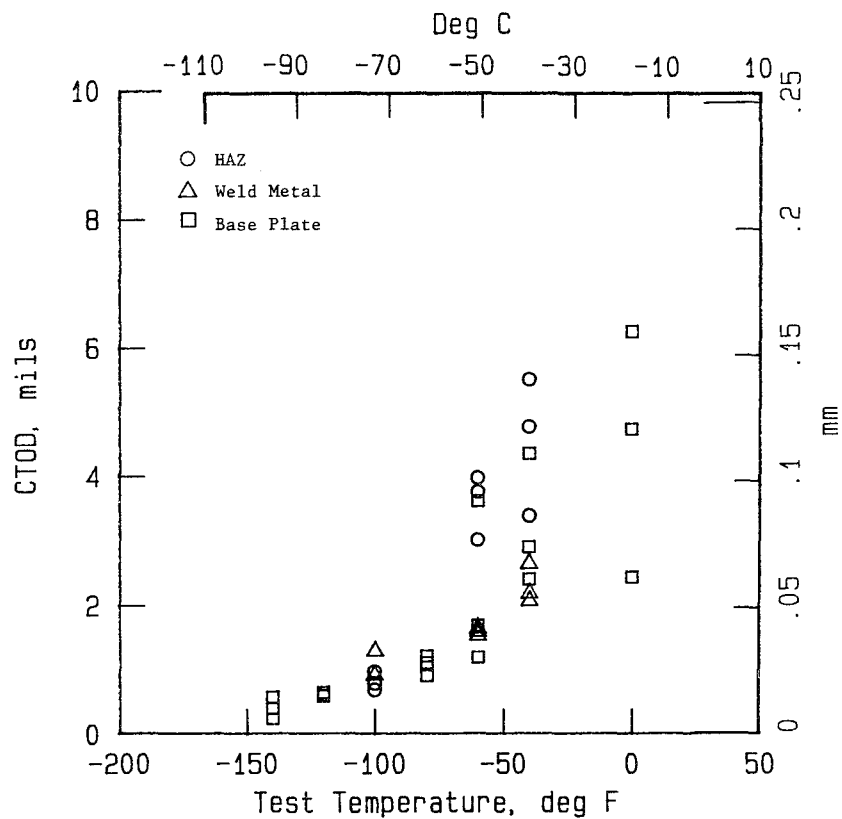


Figure 63. CTOD values as a function of test temperature for the 2-in (51 mm) thick A572-82, grade 50 steel plate (plate D).

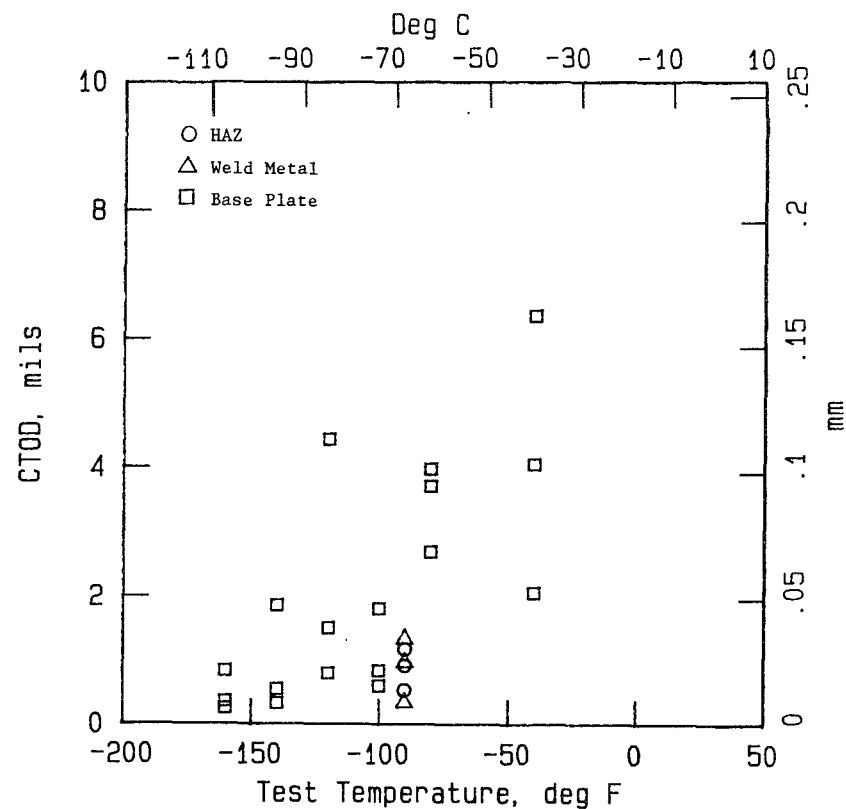


Figure 64. CTOD values as a function of test temperature for the 1-in (25 mm) thick A588-82, grade B steel plate (plate E).

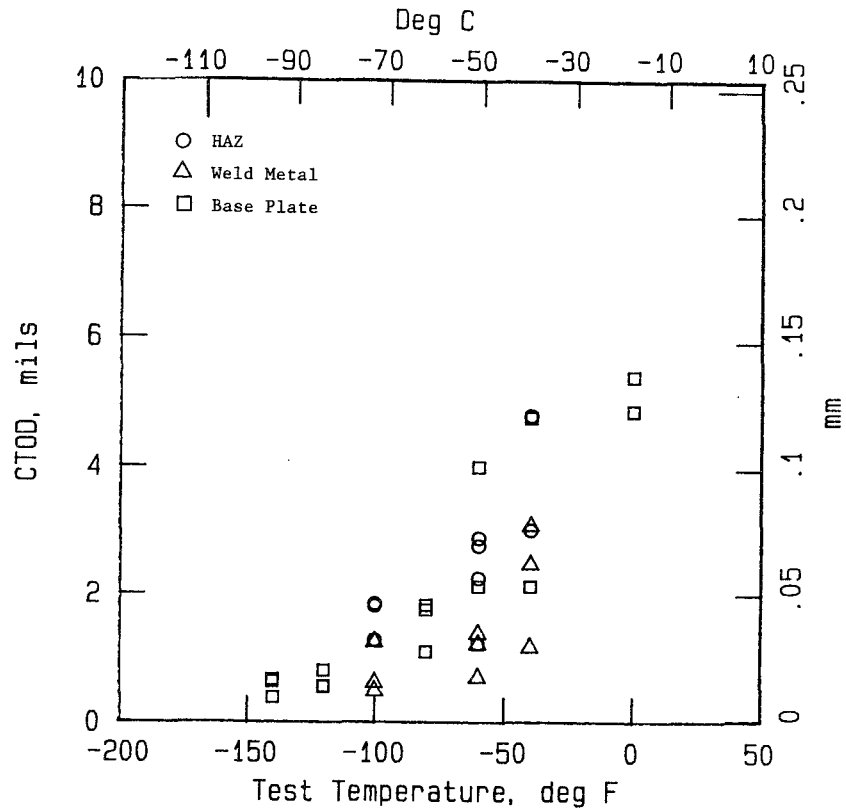


Figure 65. CTOD values as a function of test temperature for the 2-in (51 mm) thick A588-82, grade B steel plate (plate F).

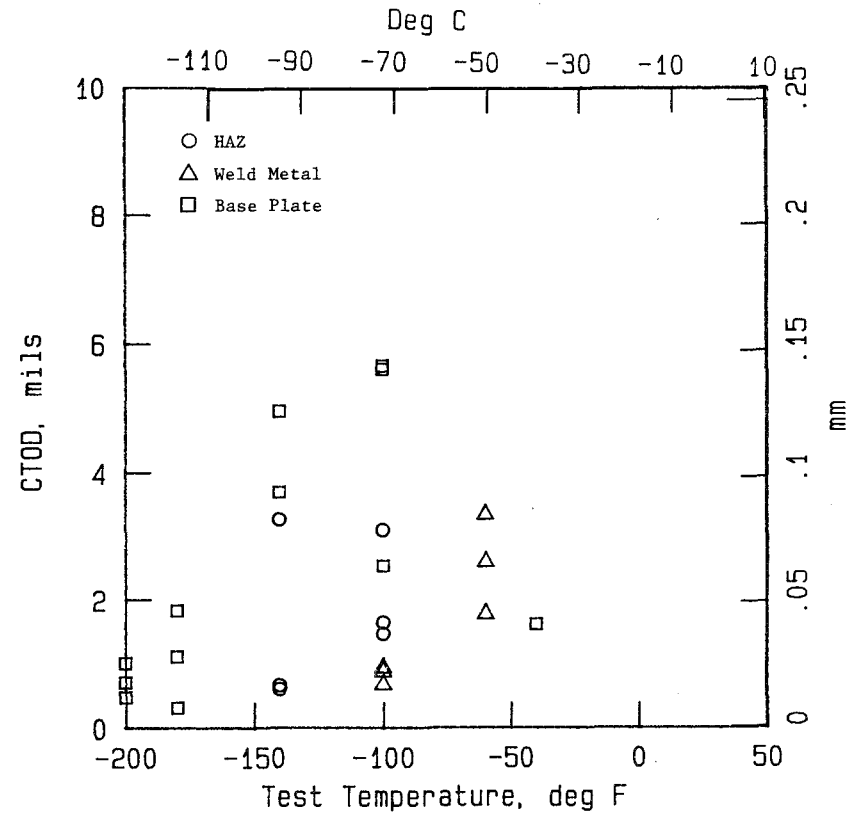


Figure 66. CTOD values as a function of test temperature for the 1-in (25 mm) thick A852-85 steel plate (plate H).

## CHAPTER 4: DISCUSSION

Two observations were made on the toughness behavior of the test plates that are important to the AASHTO Guide Specifications for Fracture Critical Non-Redundant Bridge Steels. First is the fact that CTOD test data scatter far more than CVI data. Second, for the non-heat-treated steels, A572 and A588,  $K_C$  (or  $K_{IC}$ ) values implied from CVI tests are generally conservative for both 1- and 2-in (25 and 51 mm) thicknesses. That is, if CVI values are converted to  $K_C$  values by use of the Barsom-Rolfe procedure for these steels, the actual  $K_C$  values are generally at least as high as those implied from CVI tests.

The two heat-treated steels, A514 and A852, behaved quite differently. For 1-in (25 mm) thick plates,  $K_C$  converted from CVI was lower than directly measured values of  $K_C$ , especially for the A514 plate. On the other hand, as plate thickness increased, toughness implied from CVI tests became increasingly nonconservative. Indeed, for the A514, 2-in (51 mm) thick plate,  $K_{IC}$  values could be measured as high as 60°F (33°C) above LPST (see figure 40). For the A852 plate,  $K_{IC}$  could be measured at moderately high temperatures above LPST for the 2-in (51 mm) thick plate, but for the 3-in (76 mm) thick plate,  $K_{IC}$  could be measured up to 130°F (72°C) above LPST (see figure 43).

Both the apparent excessive scatter in CTOD compared to CVI test results and the plate thickness effect may be a result of the manner in which Charpy test bars are sampled. CVI tests are sampled at the quarter-points of plates, but crack extension in full-thickness plates starts at the plate's midplane. For all plates, the micro-structure on the midplane may vary more than at the quarter-points,



which might explain the difference in scatter. The nonconservative fracture toughness predictions of thick plates of the heat-treated steels would also be consistent with this difference in sampling locations. As plate thickness increases, the difference between microstructure at the quarter-point and center also increases, especially for heat-treated steels having moderate hardenability. The CTOD tests may be measuring crack toughness for the microstructure on the plate center-plane while the CVI are measuring it on the quarter-thickness plane. If, indeed both the scatter differences and thickness effect are a result of different sampling locations for the two tests, both the differences in amount of scatter between the two tests and the thickness effect would be eliminated by changing the CVI sampling location.

The procedure used for converting CVI to  $K_{Ic}$  values is based on the Barsom-Rolfe criterion. Inherent to their criterion is the need for a temperature shift to account for the difference in loading time between CTOD or  $K_{Ic}$  testing and the much higher loading rate used in Charpy testing. Analyzing CVI data required the introduction of a reference temperature, the Lowest Permissible Service Temperature (LPST) which is a material property related to the Lowest Anticipated Service Temperature (LAST). In the steels tested in this project, LPST was much lower than LAST, and the shape of transition curves that occurred at lower temperatures may be different from the shape of curves found at higher temperatures. This might influence the analysis used in this report. Nevertheless, the analysis worked well for all 1-in (25 mm) thick plates and the non-heat-treated thicker plates so that this possible difference in transition temperature shape is thought to have only a minor effect in the analysis.

Critical crack size,  $a_{Ic}$ , was also calculated for each of the plates at the LPST, assuming a design stress equal to one-half the

yield strength. Most of the plates had high critical crack lengths, but the 2-in (51 mm) thick plate of A514, and the 3-in (76 mm) thick plate of A852 had estimated critical crack lengths of less than 1/2-in (12 mm).

Calculating critical K values from CVI tests for weldments is not possible because the temperature shift procedure that is basic to the Barsom-Rolfe criterion can not be used since the CVI toughness requirements are not dependent on temperature zones. In order to analyze the weld metal and heat-affected zone data, they were compared with the properties of the base plate from which the weld was fabricated. For the welds made in these plates, both WM and HAZ are generally no poorer than the base plate in terms of both CVI and CTOD toughness. Hence the BP, WM and HAZ all have approximately the same crack resistance and critical crack sizes for design loads.

In calculating critical crack sizes in this project, only design stresses were considered. When cracks are near or in non-stress-relieved welds, large local as well as long range residual stresses may be present. The presence of these stresses, of course, will reduce critical crack sizes.

## CHAPTER 5: RECOMMENDATIONS

As stated above, the difference in scatter between CTOD and CVI tests and the thickness effects found in heat-treated plates may result from the fact that CVI test specimens are cut from the quarter-positions in the plates, while full-thickness cracks initiate at the midplane. If this is the case, then both scatter differences and thickness effects might be minimized by sampling Charpy specimens from the midplane.

Determining whether or not Charpy sampling procedures should be changed should not be based on single plate data, however. Hence, it is recommended that additional testing be carried out to ascertain whether the failure of the Barsom-Rolfe criterion for thick heat-treated plates is, indeed, a result of the manner in which Charpy specimens are sampled. Whether or not CVI testing reflects the toughnesses of heat-treated thick plates, it may be found that it is not uncommon for directly measured fracture toughnesses of thick heat-treated plates to be as low as found in this program. If such is the case, it would be advisable to re-examine the AASHTO Guide Specifications for these materials.

## APPENDIX A

### Analysis on Which CTOD is Based and Description of CTOD Test Method

The definition of CTOD for small-scale yielding based on the Dugdale-Barenblatt strip yield model shown in figure 67 is:

$$\delta = (8\sigma_Y a / \pi E) (1 - \nu^2) (\ln \sec(\pi\sigma / 2\sigma_Y)) \quad (6)$$

where

- $\delta$  = CTOD
- $\sigma_Y$  = Flow Stress governing the development of crack tip plasticity (in this case the strip yield zone)
- $a$  = Crack Length
- $E$  = Young's Modulus
- $\nu$  = Poisson's ratio

For stress less than about  $3\sigma_{ys}/4$ , a reasonable approximation to  $\ln \sec(\pi\sigma/2\sigma_Y)$  can be made by using the first term of its series expansion which gives:

$$\delta = (\pi\sigma^2 a) (1 - \nu^2) / E\sigma_Y$$

For the specimen shown in figure 67,  $K^2 = \sigma^2 \pi a$  from which

$$\delta = K^2 (1 - \nu^2) / E\sigma_Y, \text{ and the} \quad (7)$$

strain-energy-release rate,  $G$ , is:

$$G = K^2 (1 - \nu^2) / E = \delta / \sigma_Y \quad (8)$$

The practical utility of the CTOD approach is, of course, that it can be applied under conditions of general yielding. In cases of extensive plastic deformation, analysis based on plasticity must, of course, be used to define the CTOD.

The particular case of interest here is the three-point bend specimen used in the British Standard, BS5762-1979. The calculation procedure specified in the standard suggests a very simple dependence of the CTOD on the plastic displacement measured near the edge of the specimen. The formula given in BS5762-1979 is:

$$\delta = [K^2(1-\nu^2)]/[2\sigma_{ys}E] + [0.4(W-a)V_p]/[0.4W+0.6a+z] \quad (9)$$

where  $V_p$  is the plastic component of displacement, figure 68, measured at a small distance  $z$  from the specimen edge, and the other quantities are as defined previously. (The measuring point is assumed not to be at the mouth of the specimen, but on knife-edges having a thickness =  $z$ .) The first term on the right in eq. (9) represents an elastic contribution to the CTOD; it is based on eq. (7) with the flow stress  $\sigma_Y$  taken to be  $2\sigma_{ys}$ . The second term is the plastic contribution and it indicates that, so far as plastic straining is concerned, the specimen behaves as if there were a hinge-point at a position ahead of the crack a distance of 0.4 of the way to the back edge of the specimen. (The ratio of the CTOD [ $\delta$ ] to the front edge displacement [ $V_p$ ] is the ratio of the distance from the crack tip to the hinge-point [ $0.4(W-a)$ ] to the distance from the measurement point to the hinge-point [ $0.4(W-a)+a+z$ ].)

The CTOD test is meant to be applied to plate materials in their full-thickness. To the extent that CTOD is a meaningful crack

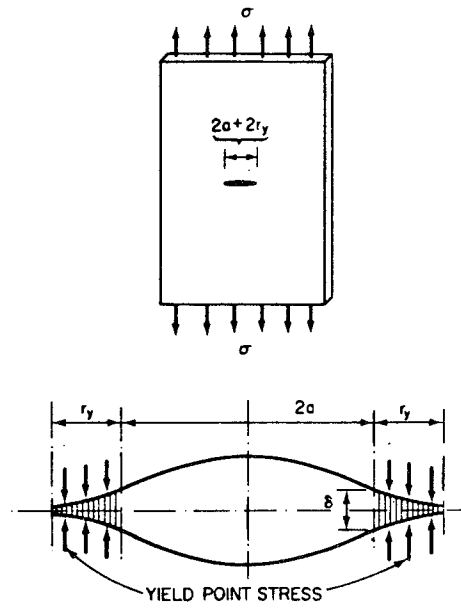


Figure 67. Dugdale strip yield model.

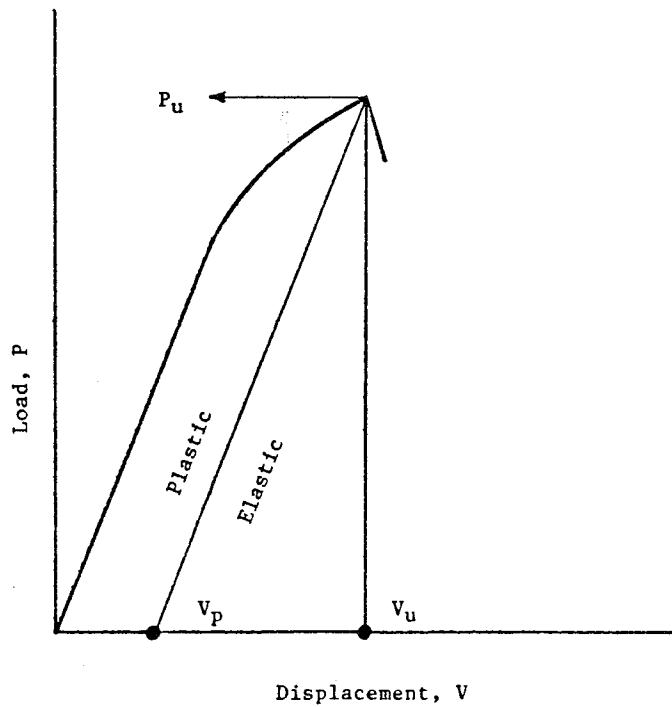


Figure 68. Schematic load-clip gauge displacement showing plastic ( $V_p$ ) and elastic component of total displacement ( $V_u$ ).

tip characterization parameter accurately evaluated by eq. (7) for a three-point bend specimen or another suitable formula for a different configuration, the fracture toughness measured in terms of CTOD should be independent of in-plane dimensions. A specimen with large in-plane dimensions might fail in an essentially linear elastic manner such that the only contribution to CTOD would come from the first term of eq. (9); in other words, the test would yield an elastic measurement of CTOD which could be converted to K by the small-scale yielding relationship. A small specimen of the same material in the same thickness and tested at the same temperature and strain rate could undergo general yielding prior to the onset of crack extension, and the critical CTOD would be determined mainly by the second term of eq. (9). This fracture toughness should agree with that measured on the larger specimen. The degree of confidence that can be placed in the CTOD methodology will ultimately be determined by the degree to which such an invariance of CTOD is established experimentally. Indeed, this is one purpose of collecting the test data on this project.

It may be pointed out, however, that the standard BS5762-1979 makes no claim for size independence of CTOD. A preferred test specimen with  $W = 2B$  is said to provide a lower bound result. A subsidiary test piece with  $W = B$  is permitted, but the standard points out that it is less constrained than the preferred test piece and, therefore, presumably likely to give a somewhat different result. Thus, while the method is based on a parameter,  $\delta$ , which in concept is a unique crack tip characterization parameter in the elastic-plastic regime as is K in the linear elastic regime; the measurement practice specified a preferred test piece the size of which is uniquely tied to plate thickness.

## CTOD Test Method

The test method that was followed in conducting the CTOD tests for this project is the British Standard Method For Crack Opening Displacement (COD) Testing, BS5762:1979. An American Standard has also been written and is now available as Draft ASTM Test Method For Crack Tip Opening Displacement (CTOD) Testing: March, 1987. Both methods are based on the use of full-thickness plates, and both allow for the use of the two types of 3-point bend specimens:  $W = 2B$ , and  $W = B$ . The former specimen, having the greater restraint, is a better model of cracking in bridge materials and was used in the present project. The smaller specimen is especially useful for evaluating microstructures that occur in relatively small layers such as those found in heat-affected zones. However, because the specimen may give a nonconservative toughness value, it was not used in this project.

The Draft American Standard, unlike the British one, allows the use of a compact specimen whose shape and dimensions are much like the specimen described in ASTM E813-81, Standard Test for  $J_{IC}$ , a MEASURE OF FRACTURE TOUGHNESS. Because so much CTOD data has been collected on the bend specimen, it was used for all CTOD testing on this project other than for the 3-in (76 mm) thick plate.

CTOD values are obtained from load-crack mouth opening displacement (P- $\Delta$ ) records. As stated earlier, CTOD ( $\delta$ ) measures different events depending on the material tested and the test temperature. Five types of P- $\Delta$  records are shown in both the British Standard and Draft of the American Standard, figure 69. Barsom and Rolfe described these as follows:<sup>[4]</sup>

Type a: Unstable (brittle) fracture with no prior crack growth.



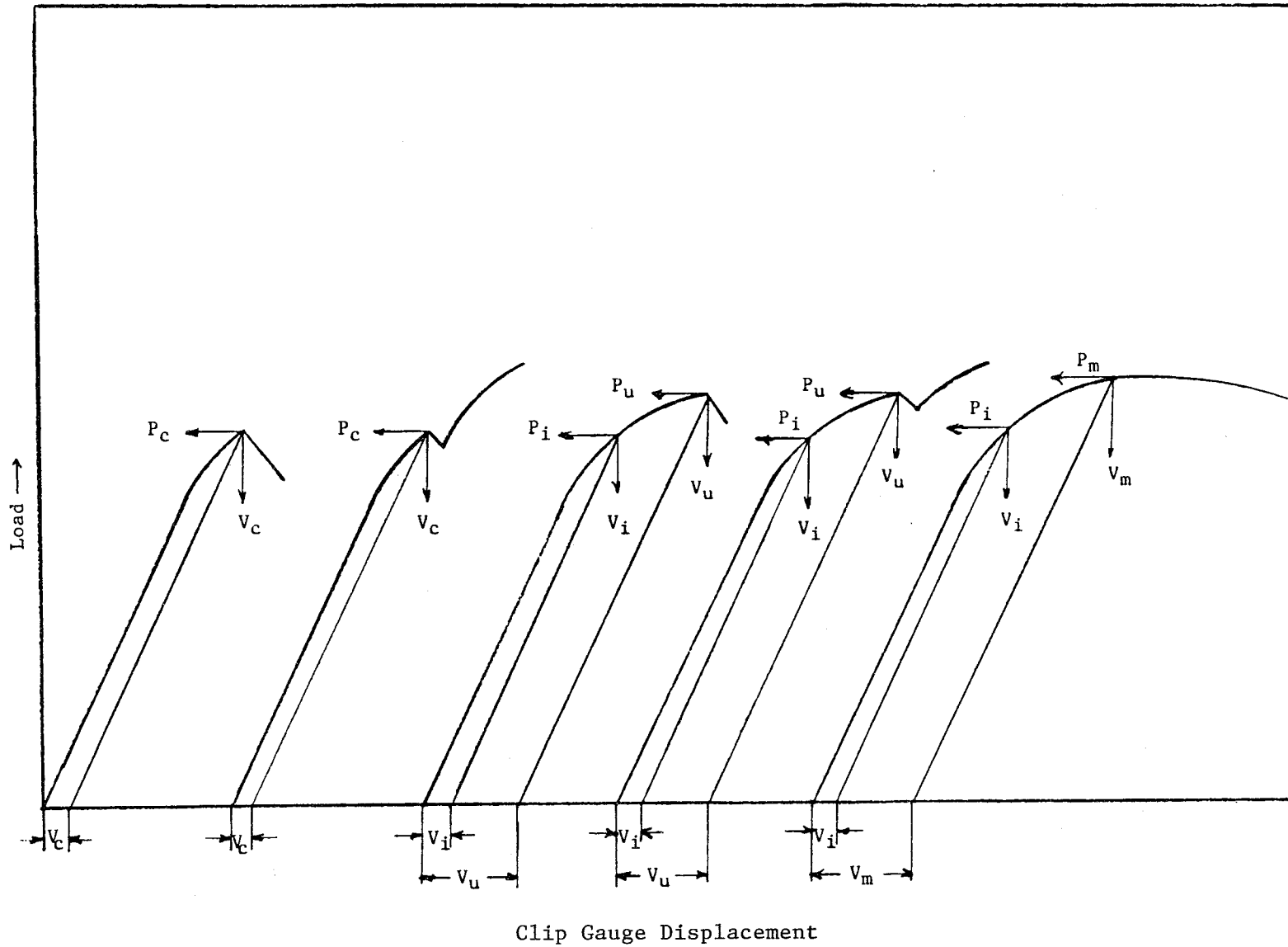


Figure 69. Types of load (P) vs clip gauge displacement (V) records.

- Type b: Brittle crack initiation or pop-in ( $V_{ic}$ ) which is arrested followed by subsequent increase in load. Final failure is by cleavage,  $V_c$ .
- Type c: Stable crack extension (ductile fibrous thumbnail, ( $V_i$ ) followed by unstable cleavage fracture at  $V_u$ . Stable crack extension starts at  $P_i$ . To determine  $P_i$ , special techniques are required such as multiple specimens or unloading compliance. Thus, use of  $P_i$  to determine  $V_i$  is not widely used.
- Type d: Stable crack extension starting at  $P_i$ , followed by subsequent increase in load and cleavage failure at  $V_u$ . Cleavage pop-in ( $V_{ic}$ ) may also occur, but not necessarily.
- Type e: Generally stable ductile fibrous tearing resulting in a roundhouse curve. Failure is by stable ductile tearing at  $P_m$ . The value of  $V_m$  nominally is selected at the first attainment of maximum load.

Four different clip-gauge, or mouth opening displacement values, can be obtained from these five types of P- $\Delta$  records and used to calculate CTOD ( $\delta$ ) values as follows:

$\delta_c$  (from  $V_c$ ). A critical value of CTOD at the onset of unstable brittle crack extension or pop-in. The use of this value implies that there is no evidence of slow crack growth (ductile tearing). Indeed, the American Standard restricts this term to fractures in  $\Delta a_p < 0.2$  mm (0.0079 in).

$\delta_i$  (from use of  $V_i$ ). An engineering estimate of CTOD near the onset of slow stable crack growth.

$\delta_u$  (from  $V_u$ ). A critical value of CTOD at unstable cleavage fracture after some slow crack growth.

$\delta_m$  (from  $V_m$ ). A value of CTOD at the first attainment of a maximum load plateau for full plastic behavior.

For bridge steels at operating temperatures, thicknesses and loading rates,  $\delta_m$  values are not expected and, indeed, if they do occur would indicate that the steel is extremely flaw tolerant. Evaluating  $\delta_i$  requires the use of an R-curve technique and would be only useful in structures where very small cracks could not be tolerated. This is not the case for bridge members and, hence,  $\delta_i$  was not evaluated. Most of the data were  $\delta_u$  type, but for the higher thickness and strengths, and for the lower temperatures  $\delta_c$  types also occurred.

## APPENDIX B

### Analytical Basis for Converting CTOD Data to $K_c$

Figure 70 shows a load deflection curve that might be obtained in a fracture toughness test. The specimen is loaded up to point A where fracture is initiated. In a linear elastic fracture toughness test, the fracture toughness,  $K$ , is calculated from an expression of the type

$$K = P/(B\sqrt{W}) f(a/W) \quad (10)$$

where  $P$  is the load,  $B$  is the specimen thickness,  $W$  is the specimen width, and  $a$  is the crack length. Linear elastic behavior is assumed. Linear elastic behavior is, of course, an idealization; when the specimen is loaded a plastic zone forms at the leading edge of the crack; and the higher the load, the larger is the plastic zone, and the greater is the departure from linear elasticity. An increasing deviation from linear elasticity is evident in the load-displacement curve depicted in figure 70.

A time-honored method for taking into account limited crack tip plasticity is to use an  $r_y$  correction to the crack length. The factor  $f(a/W)$  in eq. (10) is replaced by  $f([a+r_y]/W)$  where  $r_y$  is given by:

$$r_y = (1/[2\pi]) (K/\sigma_Y)^2 \quad (11)$$

where  $\sigma_Y$  is an effective flow stress which governs the development of the crack tip plastic zone. In making the plasticity correction, eq. (10), with  $(a + r_y)$  substituted for  $a$ , and eq. (11) must be solved

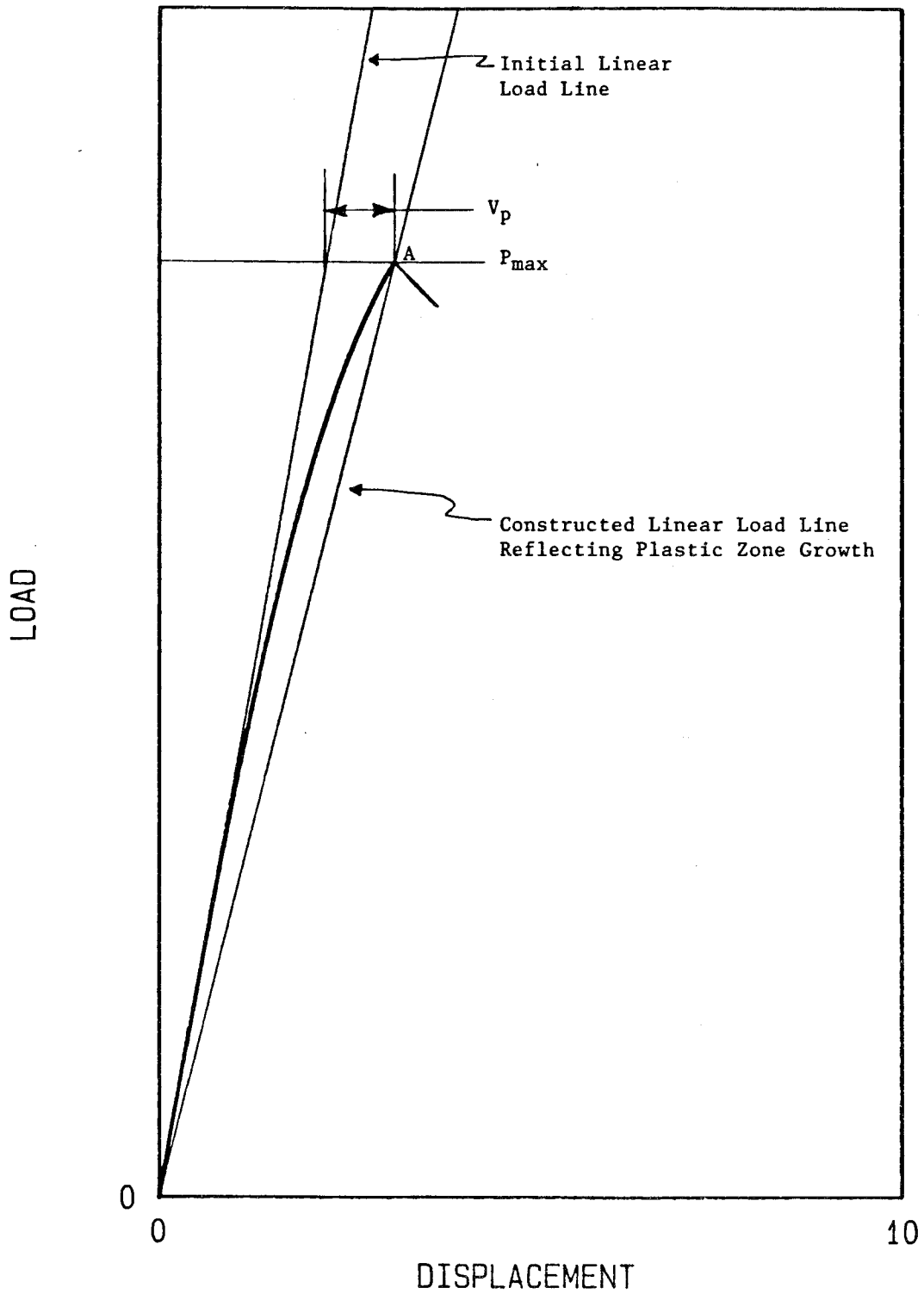


Figure 70. Schematic load-displacement curve for a specimen exhibiting measurable plastic deformation prior to fracture.

simultaneously for the same value of  $K$ . This is generally done in an iterative fashion starting with an initial calculation of  $K$  for  $r_y = 0$ , using eq. (11) to calculate an updated  $r_y$ , using eq. (10) to calculate an updated  $K$ , and so forth, until the desired closeness of convergence is attained. If the uncorrected  $K$  is too large (relative to  $\sigma_Y \sqrt{W}$ ) a plasticity correction cannot be made; a simultaneous solution of eqs. (10) and (11) does not exist, and the iterative procedure fails to converge.

A practical difficulty encountered in carrying out this plasticity correction procedure is arriving at the appropriate value of  $\sigma_Y$  to use. The uniaxial yield stress would be the lowest meaningful value, but through-thickness constraint and strain hardening could conceivably result in values twice as high as the uniaxial yield stress. As  $r_y$  is inversely proportional to the square of the flow stress, the predicted extent of plastic deformation is highly dependent on the choice of  $\sigma_Y$ .

The procedure which we use in this report takes advantage of the fact that the load-displacement curve itself furnishes the necessary information about the extent of plastic deformation. Indeed, the evaluation of fracture toughness in terms of CTOD is based on a measurement of  $V_p$ , the plastic component of displacement at the measurement point which, in this work, is the point of maximum load. The procedure utilizes the fact that the slope of the linear elastic loading line is uniquely dependent on the crack size. Specifically,

$$EBV/P = g(a/W) \quad (12)$$

where  $E$  is Young's modulus and  $V$  is the displacement, and the left-hand term, therefore, is a nondimensional measure of the inverse

of the slope of the load-displacement curve. All the equation says is that this slope depends uniquely on the normalized crack length,  $a/W$ . Given a value of the load-displacement curve slope, a value of  $a/W$  can be obtained:

$$a/W = G(EBV/P) \quad (13)$$

where the function  $G$  is the inverse of the function  $g$ . The procedure for carrying out the plasticity correction is as follows:

1. Using the measured crack length,  $a_0$ , use eq. (12) to calculate an initial elastic compliance,  $(EBV/P)_0$ .
2. Using the measured  $V_p$  and  $P_{max}$  form the quantity  $(EBV/P)_0 + (EBV_p/P_{max})$  and use this quantity in eq. (13) to calculate a value of  $a/W$ . This is, in fact,  $(a_0 + r_y)/W$ .
3. Use  $(a_0 + r_y)/W$  in eq. (10) to calculate the plasticity corrected  $K$ .
4. The quantity  $(a_0 + r_y)/W$  implies, of course, the value of  $r_y$ ; and this value along with the  $K$  calculated in step 3 can be used in eq. (11) to calculate  $\sigma_Y$ .

What this procedure does, in effect, is to use the measured plastic displacement,  $V_p$ , to infer the value of  $\sigma_Y$  rather than to guess ahead of time what value of the flow stress might be appropriate. Although the foregoing description is somewhat involved, carrying out the procedure is, in practice, quite simple given expressions for the functions  $f$ ,  $g$ , and  $G$  in eqs. (10), (12), and (13), respectively.

These functions describe linear elastic behavior, and they are available for common test specimens. For example, for the three-point bend specimen with span (S) to width (W) ratio of  $S/W = 4$ , the required expressions are:

$$f(x) = \{6x[1.99 - x(1 - x)(2.15 - 3.93x + 2.7x^2)]\} / (1 + 2x)(1 - x)^{3/2} \quad (14)$$

$$g(G) = 24G[0.76 - 2.28G + 3.87G^2 - 2.04G^3 + 0.66/(1-G)^2] \quad (15)$$

$$G(g) = 0.994 - 3.9g^{-1/2} + 6.23g^{-1} - 3.97g^{-3/2} \quad (16)$$

Equations (14) and (15) are taken from Tada and eq. (16) is simply an expression developed by the contractor for the inverse of eq. (15).<sup>[5]</sup> These equations can be easily put into a computer, and the plasticity correction routinely made. No iterative solution is required.

Mathematically, the correction procedure can be used up to  $(a+r_y)/W = 1$ ; but, physically, this would correspond to a fully plastic ligament and is, therefore, clearly beyond the range where a small-scale plasticity model is meaningful. A more stringent restriction is needed, and one way to select a criterion is to examine the shape of the load-displacement curve predicted by the small-scale plasticity model. The curve for a three-point bend specimen at  $a_0/W = 0.5$  is shown in figure 71; the abscissa is a non-dimensional displacement  $(VE)/(\sigma_y W)$  and the ordinate is a non-dimensional load  $P/(A_y BW)$ . The curve goes through a maximum at point A which is, in effect, a predicted plastic instability point. Up to point A the curve is a reasonable approximation to an actual load-displacement curve; beyond this point it is not. Moreover, convergence of the customary iterative procedure for evaluating a plasticity corrected K



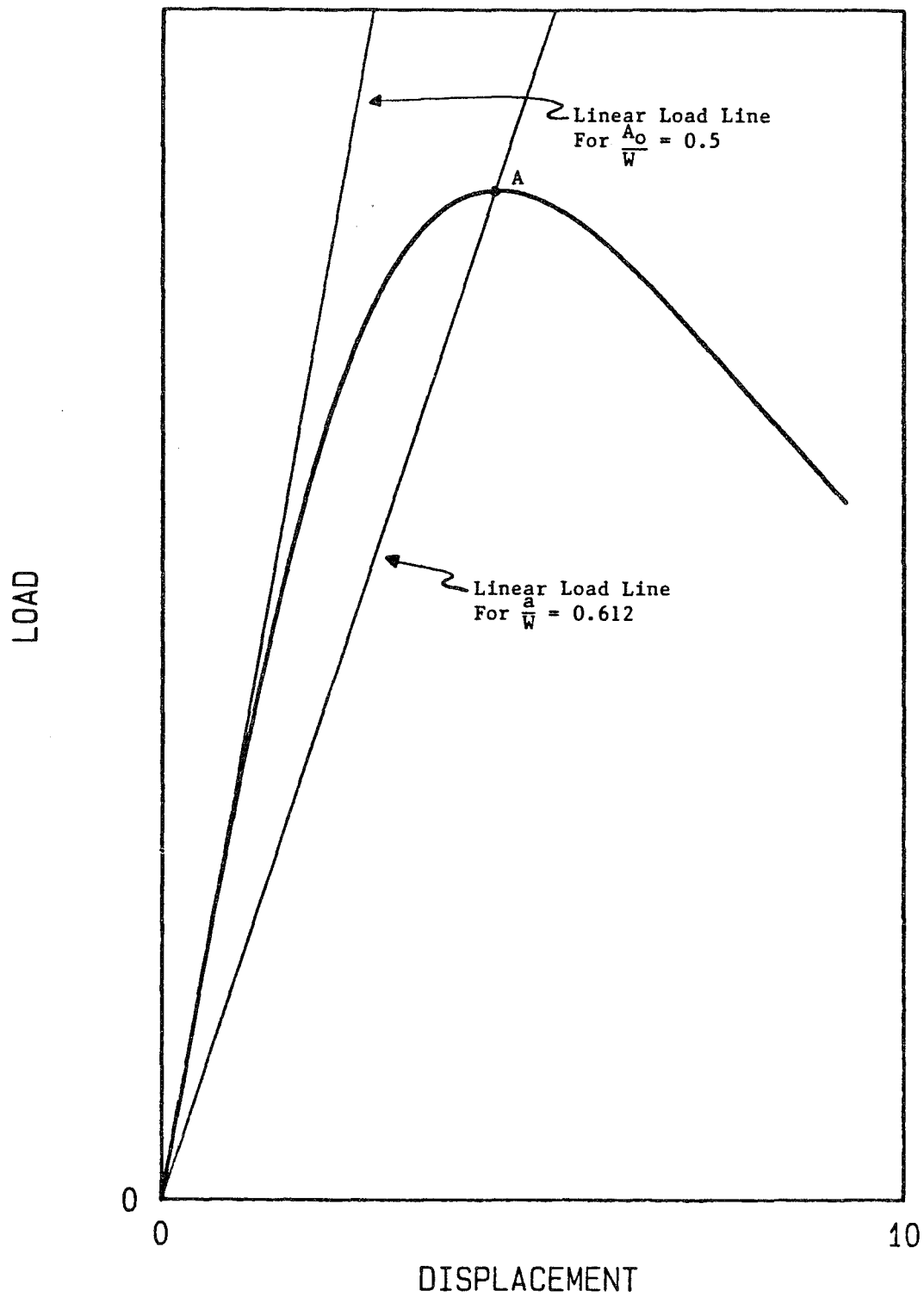


Figure 71. Non-dimensional load-displacement curve for a 3-point bend specimen with  $a_0/W = 0.5$  based on small-scale plasticity model.

is restricted to the rising portion of the curve. At the value  $a_0/W = .5$ , the point A occurs at  $(W - a_0)/r_y = 4.10$ . Applying the restriction  $W - a \leq 4.2 r_y$  ensures that the plasticity correction is applied only on the rising portion of the predicted load-displacement curve not only for  $a_0/W = 0.5$  but for any value greater than 0.3. Thus, this restriction on  $r_y$  has been selected as defining the maximum allowable plasticity for obtaining a plasticity corrected K for the three-point bend specimen.

## APPENDIX C

### Calculation of Dynamic Yield Strengths

The Irwin expression for calculating the dynamic yield strength as a function of test temperature and loading time eq. (17) is shown below:<sup>[6]</sup>

$$\sigma_{yd} = \sigma_{ys} - 27.2 + \{174,000 / [(T + 459) \times \log (2 \times 10^{10} t)]\} \quad (17)$$

where  $\sigma_{yd}$  = 0.2 percent yield stress corrected for temperature and strain rate,

$t$  = loading time in seconds to yield load.

$\sigma_{ys}$  = yield stress (ksi) in a static test at 75°F (24°C).

$T$  = testing temperature (F).

One-sec loading time tensile tests were made on specimens cut from the 1-in (25 mm) thick A514, grade B, steel plate (plate A), over a range of temperatures from 70°F to -180°F (21°C to -118°C). The measured yield strength is plotted as a function of test temperature in figure 72 and these are compared with the calculated curve based on eq. (17). Except for the very lowest temperature where the measured yield strength is surprisingly low, the fit is quite good.

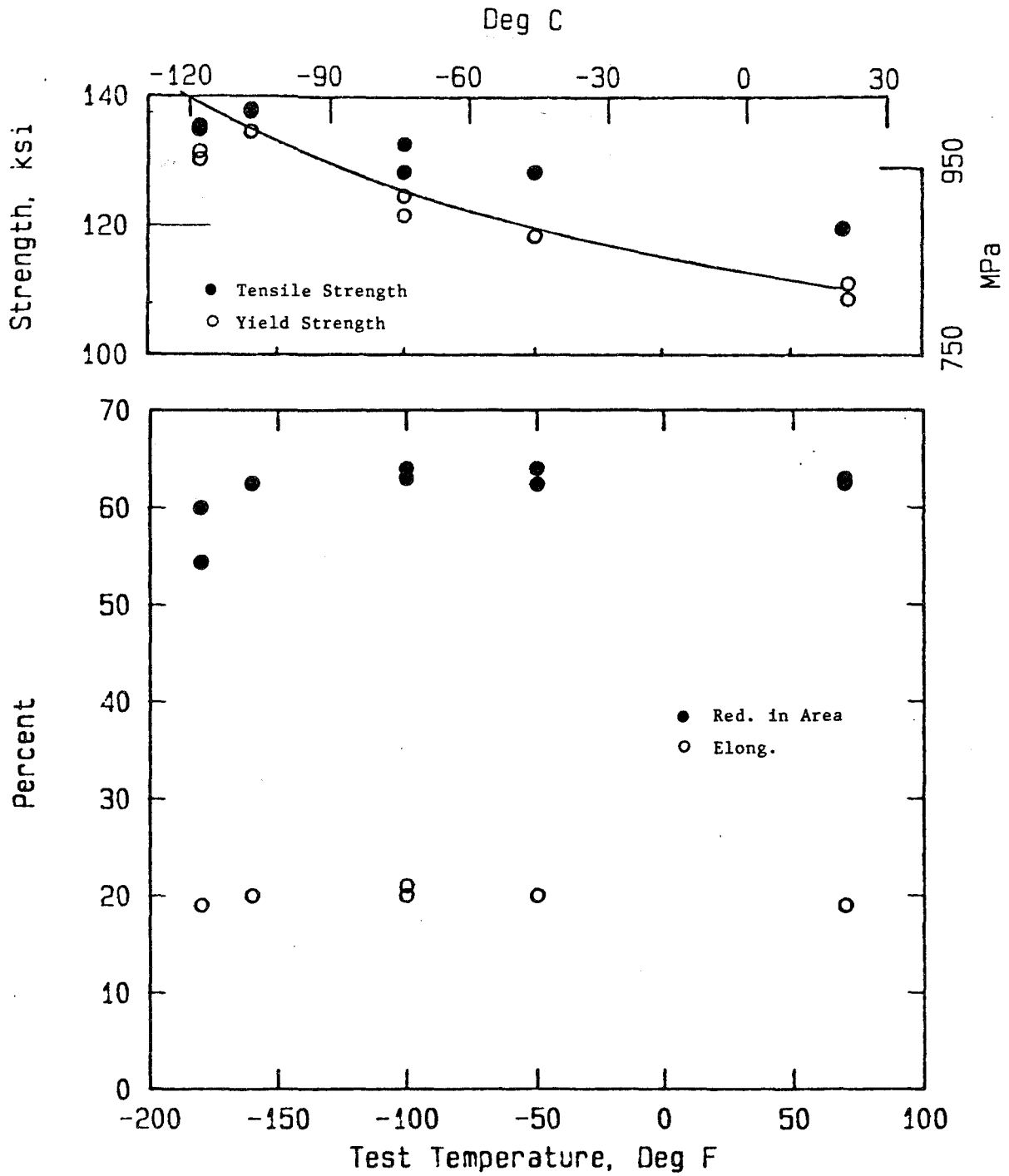


Figure 72. 1-sec loading time tensile properties vs test temperature.

## REFERENCES

1. E.J. Ripling and P.B. Crosley, "Fracture Control in Relation to Bridge Design--Toughness Requirements," Final Report, Materials Research Laboratory, Inc., MRL No. 7008, Federal Highway Administration, Contract No. DTFH61-82-C-000111, April 1984.
2. G.W. Wellman, S.T. Rolfe, and R.H. Dodds, "Three-Dimensional Elastic-Plastic Finite Element Analysis of Three-Point Bend Specimens," Welding Research Council Bulletin, #299, November 1984.
3. F.M. Burdekin and M.G. Dawes, "Practical Use of Linear Elastic and Yielding Fracture Mechanics with Particular Reference to Pressure Vessels," Practical Application of Fracture Mechanics to Pressure-Vessel Technology, Institute of Mechanical Engineering, London, May 1971.
4. J.M. Barsom and S.T. Rolfe, Fracture & Fatigue Control In Structures, Applications of Fracture Mechanics, Second Edition, Prentice-Hall, 1987.
5. H. Tada, P.C. Paris, and G.R. Irwin, "The Stress Analysis of Cracks Handbook, Second Edition," Paris Productions Incorporated, 226 Woodbourne Drive, St. Louis, Missouri 63105, (1985).
6. G.R. Irwin, "Linear Fracture Mechanics, Fracture Transition and Fracture Control," Engineering Fracture Mechanics, Vol. 1, pp. 241-257, 1968.





FHWA TFHRC Tech Reference Center



1000007592

HNR-10/7-90(250)QE